CRUISE REPORT: P03W

Downloaded: March 2024 Created: April 2024

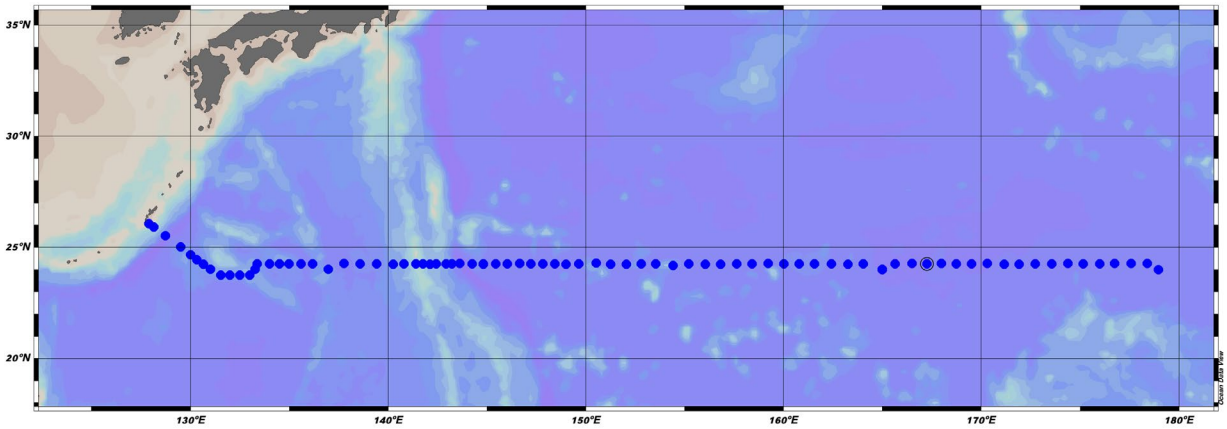

Highlights

Cruise Summary Information

Section Designation	P03W , RF21-06
Expedition Designation (ExpoCode)	**49UP20210719**
Chief Scientist	**NAGAI Naoki**
Dates	Leg 1: 19 July – 24 July, 2021 Leg 2: 28 July – 17 August, 2021
Ship	*R/V* Ryofu Maru
Ports of Call	Leg 1: Tokyo, Japan – Shimizu, Japan Leg 2: Shimizu, Japan – Tokyo, Japan
Geographic Boundaries	26° 6”N 127°9”E 179° 96”E 23° 76”N
Stations	89
Floats and Drifters Deployed	5 ARVOR floats (JMA) 2 APEX floats (JAMSTEC)
Moorings Deployed and Recovered	0

Contact Information:

SASANO Daisuke

Atmospheric Environment and Ocean Division – Atmosphere and Ocean Department– Japan Meteorological Agency (JMA)

3-6-9, Toranomon, Minato-ku, Tokyo 105-8431, JAPAN

Phone: +81-3-6758-3900 Ext. 4678 • Fax: +81-3-3434-9125 • Email: seadata@met.kishou.go.jp

Report assembled by Savannah Lewis

Contents

A. Cruise narrative

1. Highlights

Cruise designation: RF21-06, RF21-07, RF21-08 (WHP-P03 revisit)

a. EXPOCODE: RF21-06 49UP20210719

RF21-07 49UP20210827

RF21-08 49UP20210920

b. Chief scientist: NAGAI Naoki

Atmospheric Environment and Ocean Division

Atmosphere and Ocean Department

Japan Meteorological Agency (JMA)

c. Ship name: R/V Ryofu Maru

d. Ports of call: RF21-06: Leg 1: Tokyo (Japan) – Shimizu (Japan)

Leg 2: Shimizu (Japan) – Tokyo (Japan)

RF21-07: Tokyo (Japan) –Tokyo (Japan)

RF21-08: Tokyo (Japan) – Tokyo (Japan)

e. Cruise dates (JST): RF21-06: Leg 1: 19 July 2021 – 24 July 2021

Leg 2: 28 July 2021 – 17 August 2021

RF21-07: 27 August 2021 – 16 September 2021

RF21-08: 20 September 2021 – 14 October 2021

f. Principal Investigator (Contact person):

SASANO Daisuke

Atmospheric Environment and Ocean Division

Atmosphere and Ocean Department

Japan Meteorological Agency (JMA)

3-6-9, Toranomon, Minato-ku, Tokyo 105-8431, JAPAN

Phone: +81-3-6758-3900 Ext. 4678

FAX: +81-3-3434-9125

E-mail: seadata@met.kishou.go.jp

2. Cruise Summary

RF21-06, RF21-07 and RF21-08 cruises were carried out during the period from July 19 to October 14, 2021. The cruises started from the east of Okinawa Island, Japan, and sailed eastern, thereafter to 179° E along approximately 24° N. This line (WHP-P03) was observed by JMA in 2013 as CLIVER (Climate Variability and Predictability Project) / GO-SHIP (Global Ocean Ship-based Hydrographic Investigations Program). In the cruises, we also conducted hydrographic observation along other sections (see Figure A.1). For some parameters, we included these data to determine coefficients to calculate data and to evaluate data quality. These data were not reported here, but available from the JMA (https://www.data.jma.go.jp/gmd/kaiyou/db/vessel_obs/data-report/html/ship/ship_e.php?year
=2021&season=summer).

A total of 89 stations were occupied using a Sea-Bird Electronics (SBE) 36 position carousel equipped with 10-liter Niskin water sample bottles, a CTD system (SBE911plus) equipped with SBE35 deep ocean standards thermometer, JFE Advantech oxygen sensor (RINKO III), Teledyne Benthos altimeter (PSA-916D), and Teledyne RD Instruments L-ADCP (300kHz). To examine consistency of data, we carried out the observation repeatedly twice at stations of 24° 15'N, 144° 50'E (Stns.42 and 43) and 24° 00'N, 165° 00'E (Stns.70 and 71) at the cross points of each cruise. Station location and cruise track are shown in Figure A.1.

At almost all station, full-depth CTDO_2 (temperature, conductivity (salinity) and dissolved oxygen) profile were taken, and up to 36 water samples were taken and

analyzed. Water samples were obtained from 10 dbar to approximately 10 m above the bottom. In addition, surface water was sampled by a stainless steel bucket at each station. Sampling layer is designed as so-called staggered mesh as shown in Table A.1 (*Swift*, 2010). The bottle depth diagram is shown in Figure A.2.

Water samples were analyzed for salinity, dissolved oxygen, nutrients, dissolved inorganic carbon (DIC), total alkalinity (TA), pH, CFCs (CFC-11, CFC-12, and CFC-113), SF_6 and phytopigments (chlorophyll-a and phaeopigment). Underway measurements of partial pressure of carbon dioxide (pCO_2), temperature, salinity, chlorophyll-*a*, subsurface current, bathymetry and meteorological parameters were conducted along the cruise track.

At RF21-06, R/V Ryofu Maru departed from Tokyo (Japan) on July 19, 2021. We deployed an underwater glider of Meteorological Research Institute (MRI) in the south of Honshu, thereafter she called for Shimizu (Japan) on July 24 (Leg 1). She left Shimizu on July 28. After X-BT observation was conducted along Tokara Channel (JMA-Line), the hydrographic cast of $CTDO_2$ was started at the first station (Stn.1 (26° 04'N, 127° 54'E; RF6860)) in the east of Okinawa Island on July 31. RF21-06 consisted of 42 stations from Stn.1 to Stn.42 (24° 15'N, 144° 50'E; RF6901). Observation at Stn.42 was finished on August 13. She returned at Tokyo on August 17 (Leg 2).

At RF21-07, she departed from Tokyo on August 27. After the hydrographic cast of $CTDO_2$ was observed in north of 32° N along 137° E meridian (JMA-Line), restarted

at the same station (Stn.43 (24° 15'N, 144° 50'E; RF6910)) with the RF21-06 last station on August 31. RF21-07 consisted of 28 stations from Stn.43 to Stn.70 (40° 00'N, 165° 00'E; RF6937). Observation at Stn.70 was finished on September 10. She returned at Tokyo on September 16.

At RF21-08, she departed from Tokyo on September 20. After the hydrographic cast of $CTDO_2$ was observed off the Boso Peninsula (JMA-Line), restarted at same station (Stn.71 (24° 00'N, 165° 00'E; RF6956)) with the RF21-07 last station on September 28. RF21-08 consisted of 19 stations from Stn.71 to Stn.89 (24° 00'N, 179° 00'E; RF6974). Observation at Stn.89 was finished on October 5. She returned at Tokyo on October 14. Location data of stations is shown in Table A.2.

Seven Argo floats were deployed along the cruise track. The information of deployed the float is listed in Table A.3.

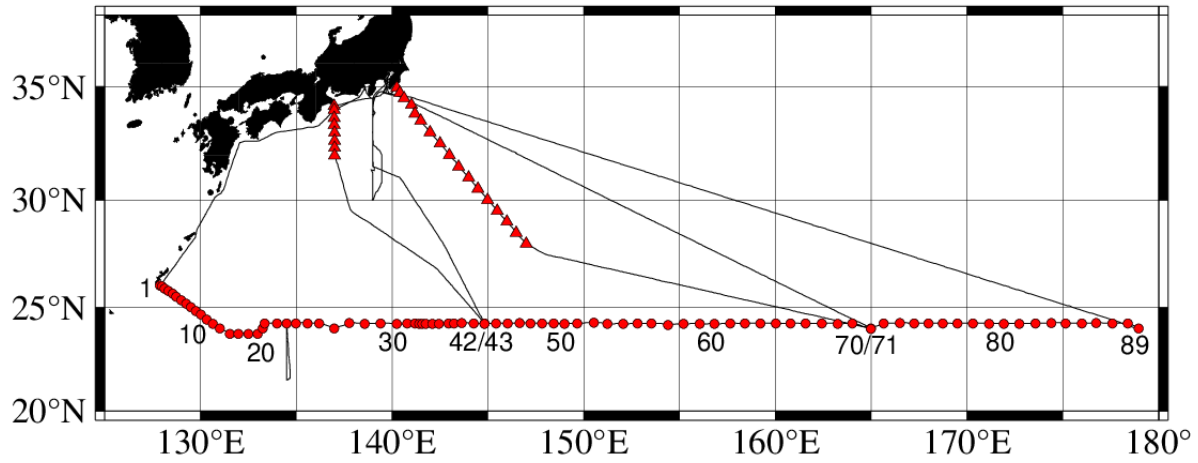

Figure A.1. Location of hydrographic stations and cruise track of RF21-06, RF21-07 and RF21-08. Circles indicate stations along WHP-03. Triangles show stations along other sections. These data are available from the JMA (https://www.data.jma.go.jp/gmd/kaiyou/db/vessel_obs/data-report/html/ship/ship_e.php?year=2021&season=summer).

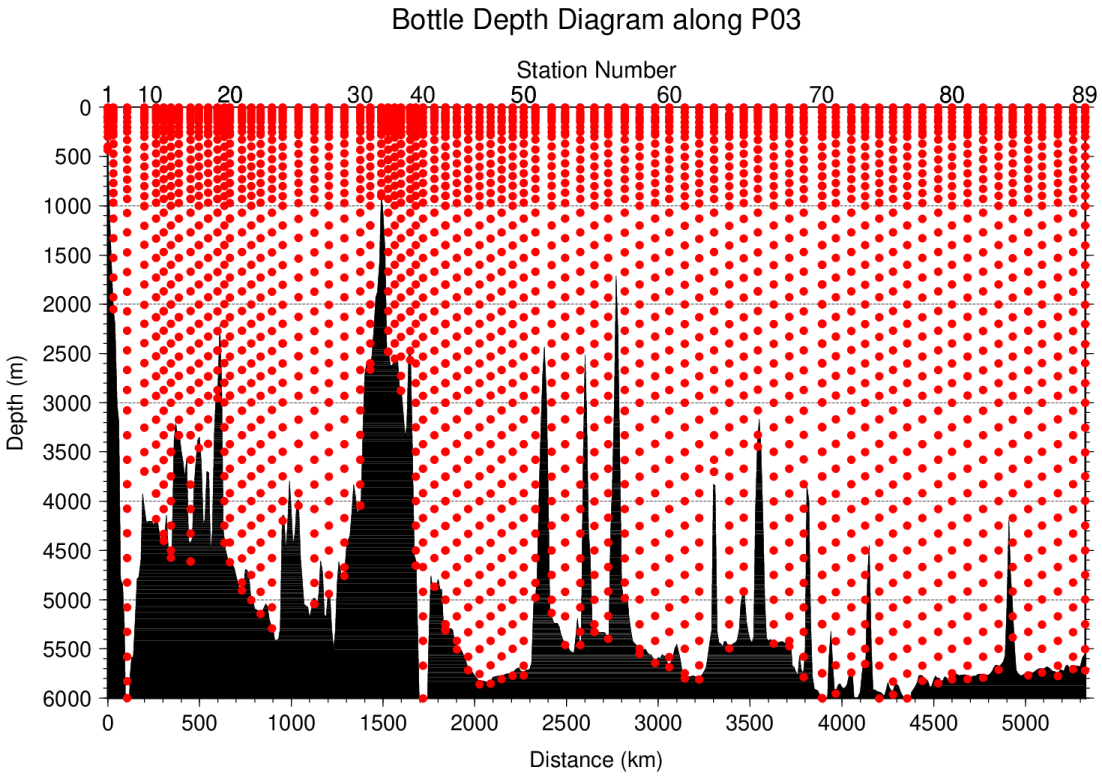

Figure A.2. The bottle depth diagram for WHP-P03 revisit.

Table A.1. The scheme of sampling layer in meters.

Bottle count	*Scheme 1*	*Scheme 2*	*Scheme 3*

Table A.2(a). Station lists of RF21-06 cruise. The 'RF' column indicates the JMA station identification number.

Station		*Location*		*Station*		*Location*	
Stn.	*RF*	*Latitude*	*Longitude*	*Stn.*	*RF*	*Latitude*	*Longitude*
1	6860	26-03.90 N	127-53.90 E	22	6881	24-15.17 N	134-30.04 E
2	6861	25-59.98 N	127-59.72 E	23	6882	24-14.75 N	135-00.08 E
3	6862	25-54.10 N	128-08.83 E	24	6883	24-15.01 N	135-36.90 E
4	6863	25-46.45 N	128-20.85 E	25	6884	24-15.10 N	136-11.81 E
5	6864	25-38.14 N	128-32.74 E	26	6885	24-00.04 N	136-59.82 E
6	6865	25-30.20 N	128-44.77 E	27	6886	24-15.07 N	137-47.76 E
7	6866	25-20.14 N	128-59.86 E	28	6887	24-14.83 N	138-34.74 E
8	6867	25-10.18 N	129-15.11 E	29	6888	24-14.85 N	139-24.96 E

9	6868	25-00.13 N	129-29.84 E	30	6889	24-14.76 N	140-16.00 E
10	6869	24-50.19 N	129-45.10 E	31	6890	24-14.97 N	140-47.95 E
11	6870	24-39.93 N	130-00.22 E	32	6891	24-15.00 N	141-11.78 E
12	6871	24-26.92 N	130-19.88 E	33	6892	24-14.92 N	141-24.02 E
13	6872	24-15.01 N	130-39.86 E	34	6893	24-14.90 N	141-34.13 E
14	6873	23-59.90 N	131-00.01 E	35	6894	24-14.86 N	141-46.03 E
15	6874	23-45.01 N	131-32.94 E	36	6895	24-14.98 N	142-06.96 E
16	6875	23-45.10 N	131-59.84 E	37	6896	24-14.88 N	142-26.86 E
17	6876	23-44.95 N	132-29.96 E	38	6897	24-14.89 N	142-57.16 E
18	6877	23-45.08 N	133-00.07 E	39	6898	24-15.11 N	143-14.01 E
19	6878	24-00.15 N	133-15.02	40	6899	24-15.19 N	143-37.94

			E				E
20	6879	24-15.08 N	133-21.93 E	41	6900	24-14.99 N	144-15.03 E
21	6880	24-15.14 N	134-00.02 E	42	6901	24-14.98 N	144-50.05 E

Table A.2(b). Same as Table A.2(a) but for RF21-07 cruise.

Station		*Location*		*Station*		*Location*	
Stn.	*RF*	*Latitude*	*Longitude*	*Stn.*	*RF*	*Latitude*	*Longitude*
43	6910	24-14.78 N	144-50.00 E	57	6924	24-10.81 N	154-26.73 E
44	6911	24-15.11 N	145-26.81 E	58	6925	24-15.09 N	155-13.86 E
45	6912	24-14.81 N	146-02.93 E	59	6926	24-14.92 N	156-03.88 E
46	6913	24-15.03 N	146-40.09 E	60	6927	24-14.81 N	156-49.67 E
47	6914	24-15.14 N	147-14.89 E	61	6928	24-14.88 N	157-39.82 E
48	6915	24-14.87 N	147-50.69 E	62	6929	24-15.11 N	158-26.83 E
49	6916	24-15.01 N	148-26.77 E	63	6930	24-15.48 N	159-13.96 E
50	6917	24-14.68 N	149-01.31 E	64	6931	24-14.87 N	160-02.89 E
51	6918	24-15.60 N	149-39.81	65	693	24-15.23 N	160-49.31

			E		2		E
52	6919	24-17.72 N	150-31.21 E	66	693 3	24-15.18 N	161-35.27 E
53	6920	24-14.88 N	151-15.01 E	67	693 4	24-15.07 N	162-26.71 E
54	6921	24-14.87 N	152-03.97 E	68	693 5	24-14.75 N	163-15.97 E
55	6922	24-14.84 N	152-49.86 E	69	693 6	24-15.16 N	164-02.68 E
56	6923	24-14.96 N	153-33.80 E	70	693 7	24-00.15 N	164-59.83 E

Table A.2(c). Same as Table A.2(a) but for RF21-08 cruise.

Station		*Location*		*Station*		*Location*	
Stn.	*RF*	*Latitude*	*Longitude*	*Stn.*	*RF*	*Latitude*	*Longitude*
71	6956	23-59.86 N	164-59.97 E	81	696 6	24-14.81 N	172-44.88 E
72	6957	24-14.86 N	165-39.84 E	82	696 7	24-15.01 N	173-34.91 E

73	6958	24-14.90 N	166-29.97 E	83	6968	24-15.05 N	174-24.87 E
74	6959	24-15.07 N	167-14.91 E	84	6969	24-14.94 N	175-10.02 E
75	6960	24-15.06 N	167-59.83 E	85	6970	24-15.06 N	175-59.99 E
76	6961	24-14.86 N	168-44.95 E	86	6971	24-14.98 N	176-44.72 E
77	6962	24-15.06 N	169-30.04 E	87	6972	24-14.74 N	177-34.95 E
78	6963	24-15.19 N	170-19.50 E	88	6973	24-15.03 N	178-24.76 E
79	6964	24-14.78 N	171-10.02 E	89	6974	23-59.83 N	178-59.81 E
80	6965	24-14.89 N	171-55.00 E				

Table A.3. Information of deployed float and buoy.

Float	*Date and Time*	*Position of deployment*		*PI*	*Manufacturer*
WMO number	*of Deployment (UTC)*	*Latitude*	*Longitude*		
2903684	July 21, 2021 02:30	30-00.12 N	138-58.76 E	JMA	ARVOR
2903686	August 1, 2021 18:50	25-00.07 N	129-29.98 E	JMA	ARVOR
2903687	August 9, 2021 03:40	24-01.10 N	136-57.35 E	JMA	ARVOR
2903688	August 11, 2021 07:35	24-14.46 N	141-43.86 E	JMA	ARVOR
2903691	August 28, 2021 22:53	31-59.28 N	137-00.83 E	JMA	ARVOR
2903664	October 1, 2021 00:32	24-17.32 N	170-17.53 E	JAMSTEC	APEX
2903665	October 3, 2021 03:59	24-16.74 N	175-06.94 E	JAMSTEC	APEX

ARVOR: NKE Instrumentation (France)

APEX: Teledyne Webb Research (USA)

3. List of Principal Investigators for Measurements

The principal investigators for each parameter are listed in Table A.4.

Table A.4. List of principal investigators for each parameter.

Hydrography	$CTDO_2$	CHIBA Yasuomi
	Salinity	WADA Koichi
	Dissolve oxygen	KAKUYA Keita
	Nutrients	KAKUYA Keita
	Phytopigments	KAKUYA Keita
	DIC	ENYO Kazutaka
	TA	ENYO Kazutaka
	pH	ENYO Kazutaka
	CFCs	ENYO Kazutaka
	SF_6	ENYO Kazutaka
	LADCP	CHIBA Yasuomi
Underway	Meteorology	NAGAI Naoki
	Thermo-Salinograph	ENYO Kazutaka
	pCO_2	ENYO Kazutaka
	Chlorophyll *a*	KAKUYA Keita
	ADCP	CHIBA Yasuomi
	Bathymetry	CHIBA Yasuomi
Float	JMA	NAKAMURA Tetsuya
	JAMSTEC	HOSODA Shigeki

Reference

Swift, J. H. (2010): Reference-quality water sample data: Notes on acquisition, record keeping, and evaluation. *IOCCP Report No.**14**, ICPO Pub. 134, 2010 ver.1*

B. Underway measurements

1. Navigation

25 November 2021

(1) Personnel

NAGAI Naoki (JMA)
CHIBA Yasuomi (JMA)

(2) Overview of the equipment

The ship's position was measured by navigation system manufactured by FURUNO ELECTRIC CO., LTD., Japan. The system has three 12-channels GPS receivers (GP-150, GP-170, JLR-7800). GPS antennas were installed on the compass deck. We switched the receivers to choose better receiving state if the number of received GPS satellites was small or HDOP was large. The GPS data, gyro heading data and log speed data were integrated and delivered to two workstations. These workstations work as the primary and secondary NTP (Network Time Protocol) servers.

The navigation data were obtained approximately every one second and one minute data were extracted from one second data. These one minute data were recorded as "LOG data (GPS data)".

(3) Data Period

05:00, 19 Jul. 2021 to 01:00, 24 Jul. 2021 (UTC).

05:00, 28 Jul. 2021 to 01:00, 17 Aug. 2021 (UTC).

05:00, 27 Aug. 2021 to 00:00, 16 Sep. 2021 (UTC).

05:00, 20 Sep. 2021 to 00:00, 14 Oct. 2021 (UTC).

2. Bathymetry

25 November 2021

(1) Personnel

CHIBA Yasuomi (JMA)

WADA Koichi (JMA)

(2) Overview of the equipment

R/V Ryofu Maru equipped a single beam echo sounder, EA 600 (Kongsberg Maritime, Norway).

The main objective of the survey is to collect continuous bathymetry data along the ship's track.

The sound speed to correct depth data was set to 1500 m/s during the cruise. Data interval was about 10 seconds in the measurement for 7500 m depth.

(3) System Configuration and Performance

System:	Kongsberg EA 600
Frequency:	12 kHz
Transmit power:	2 kW
Transmit pulse interval:	Within 20 seconds
Depth range:	5–15,000 m
Depth resolution:	1 cm
Depth accuracy (Assuming correct sound velocity, transducer depth and	Within 20 cm

shortest pulse length):

(4) Data Period

05:00, 19 Jul. 2021 to 01:00, 24 Jul. 2021 (UTC).

05:00, 28 Jul. 2021 to 01:00, 17 Aug. 2021 (UTC).

05:00, 27 Aug. 2021 to 00:00, 16 Sep. 2021 (UTC).

05:00, 20 Sep. 2021 to 00:00, 14 Oct. 2021 (UTC).

3. Maritime Meteorological Observations

25 November 2021

(1) Personnel

NAGAI Naoki (JMA)
CHIBA Yasuomi (JMA)

(2) Data Period

05:00, 19 Jul. 2021 to 01:00, 24 Jul. 2021 (UTC).

05:00, 28 Jul. 2021 to 01:00, 17 Aug. 2021 (UTC).

05:00, 27 Aug. 2021 to 00:00, 16 Sep. 2021 (UTC).

05:00, 20 Sep. 2021 to 00:00, 14 Oct. 2021 (UTC).

(3) Methods

The maritime meteorological observation system on R/V Ryofu Maru is Ryofu Maru maritime meteorological measurement station (RMET). Instruments of RMET are listed in Table B.3.1. All RMET data were collected and processed by KOAC-7800 weather data processor made by KOSHIN DENKI KOGYO CO., LTD., Japan. The result of Maritime meteorological observation data were shown in Figures B.3.1 and B.3.2.

Table B.3.1. Instruments and locations of RMET.

Sensor	Parameter	Type (Manufacture)	Location (Height from

maximum load line)

Thermometer	Air Temperature	R005-341 (CHINO CORPORATION)	Compass deck (13.3 m)
Hygrometer	Relative humidity	HMT3303JM (Vaisala)	Compass deck (13.3 m)
Thermometer	Sea surface temperature	RFN1-0 (CHINO CORPORATION)	Engine Room (−4.7 m)
Aerovane	Wind Speed Wind Direction	KVS-400-J (KOSHIN DENKI KOGYO CO., LTD.)	Mast top (19.8 m)
Wave gauge	Wave Height Wave period	Micro Wave WM-2 (Tsrumi-Seiki Co., Ltd.)	Ship front (6.5 m)
Barometer	Air pressure	PTB-220 (Vaisala)	Observation room (2.8 m)

Note that there are two sets of a thermometer and a hygrometer at the starboard and the port sides.

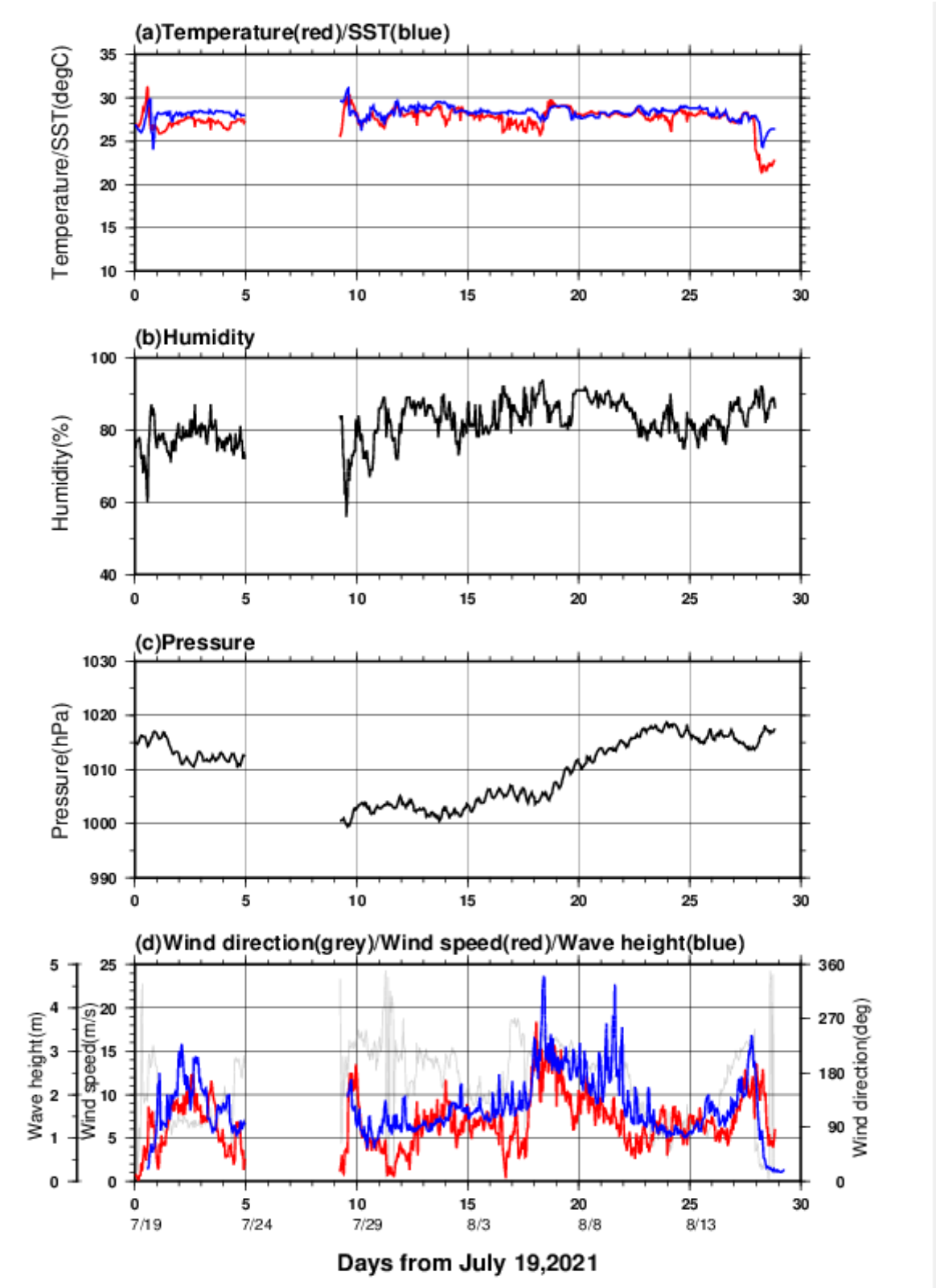

Figure B.3.1.1 Time series of (a) air temperature and sea surface temperature (SST), (b) relative

humidity, (c) sea-level pressure, and (d) wind direction, wind speed and wave height. The light blue line in (d) panel shows the instrumental observation of wave height. Day 0 corresponds to July 19, 2021 (JST).

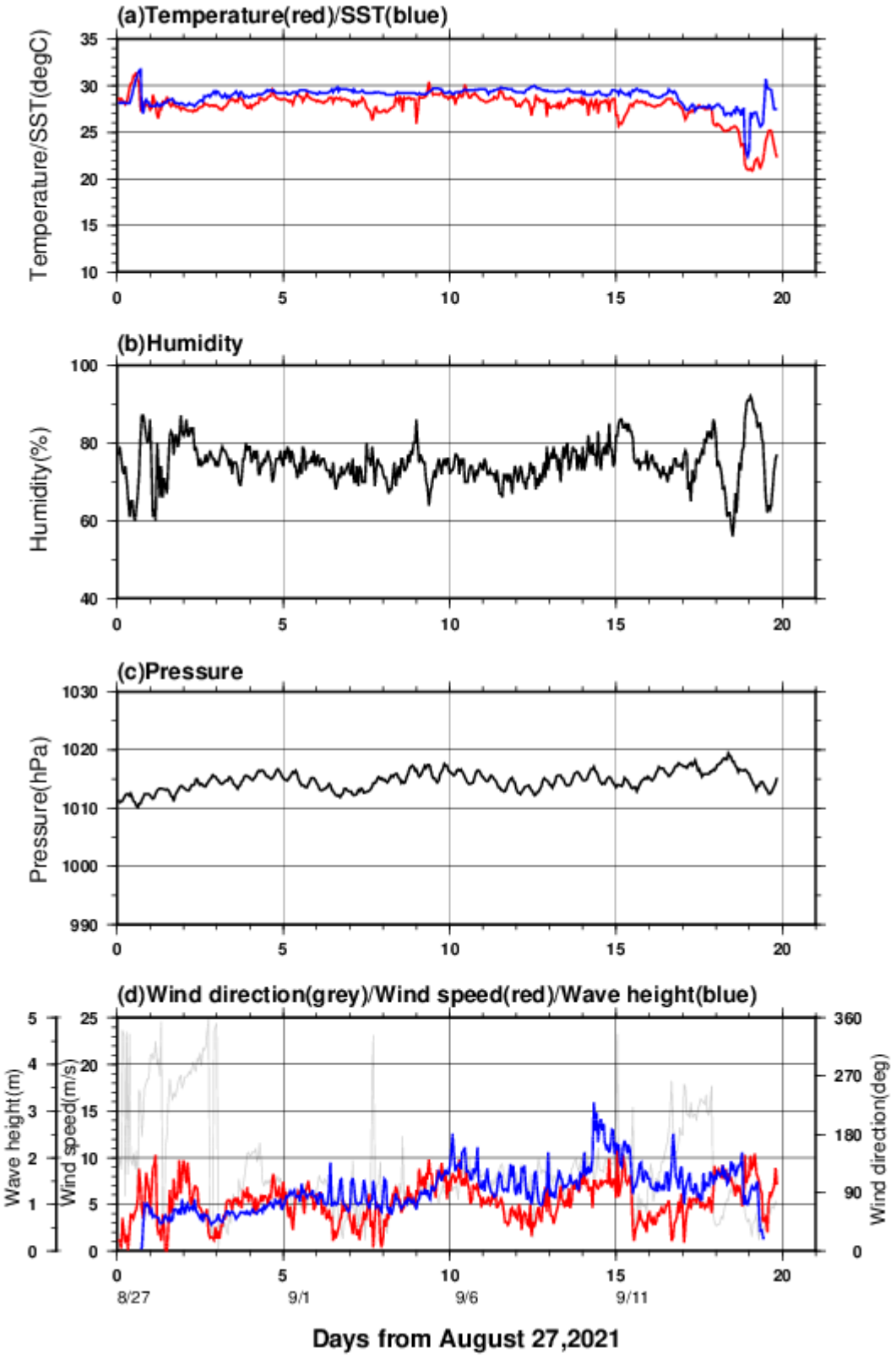

Figure B.3.1.2 Same as Fig. B.3.1.1, but day 0 corresponds to August 27, 2021 (JST).

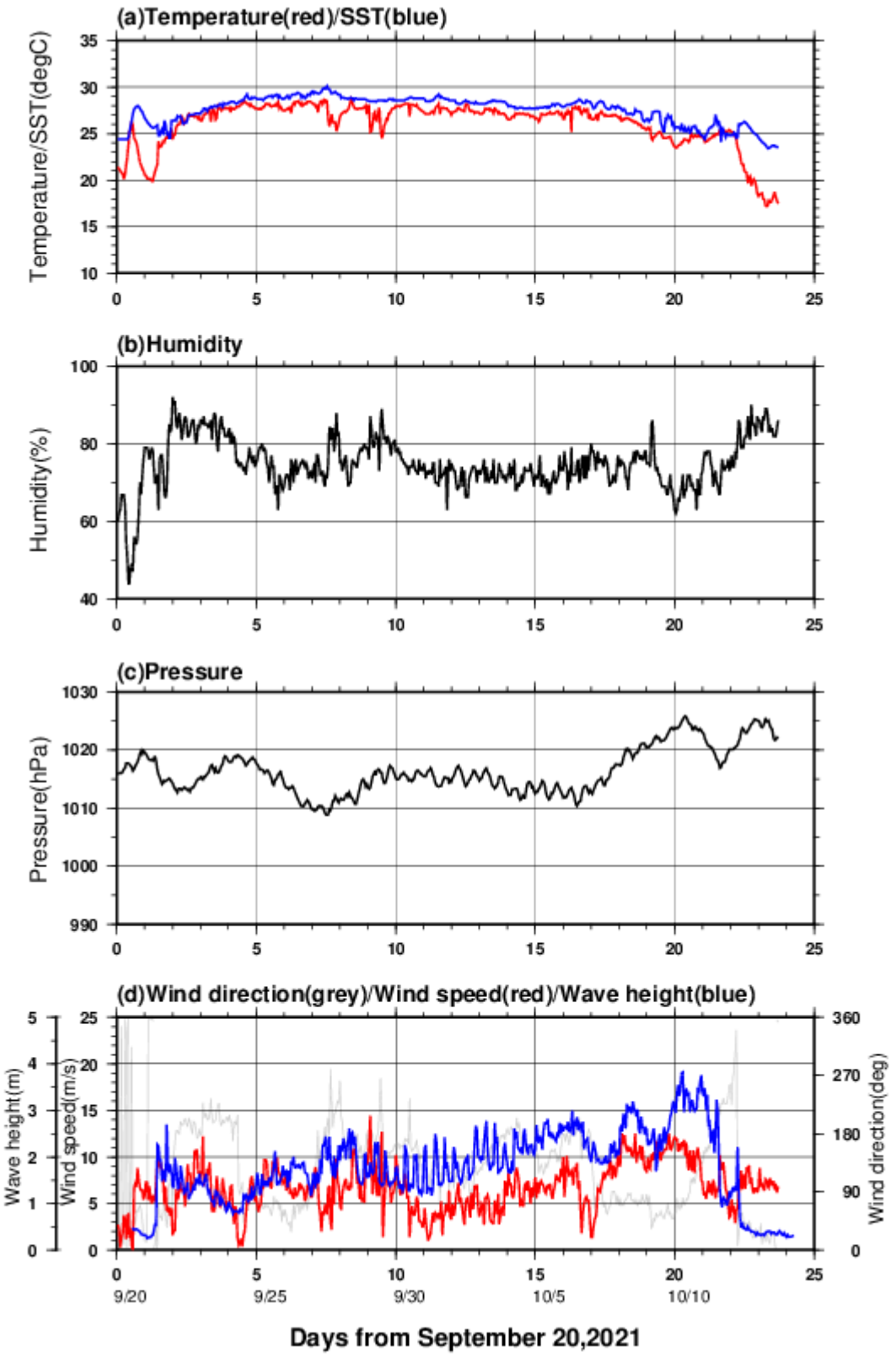
(a)Temperature(red)/SST(blue)
Temperature/SST(degC)
(b)Humidity
Humidity(%)
(c)Pressure
Pressure(hPa)
(d)Wind direction(grey)/Wind speed(red)/Wave height(blue)
Wave height(m)
Wind speed(m/s)
Wind direction(deg)
9/20
9/25
9/30
10/5
10/10
Days from September 20,2021

Figure B.3.1.3. Same as Fig. B3.1.1, but day 0 corresponds to September 20, 2021 (JST).

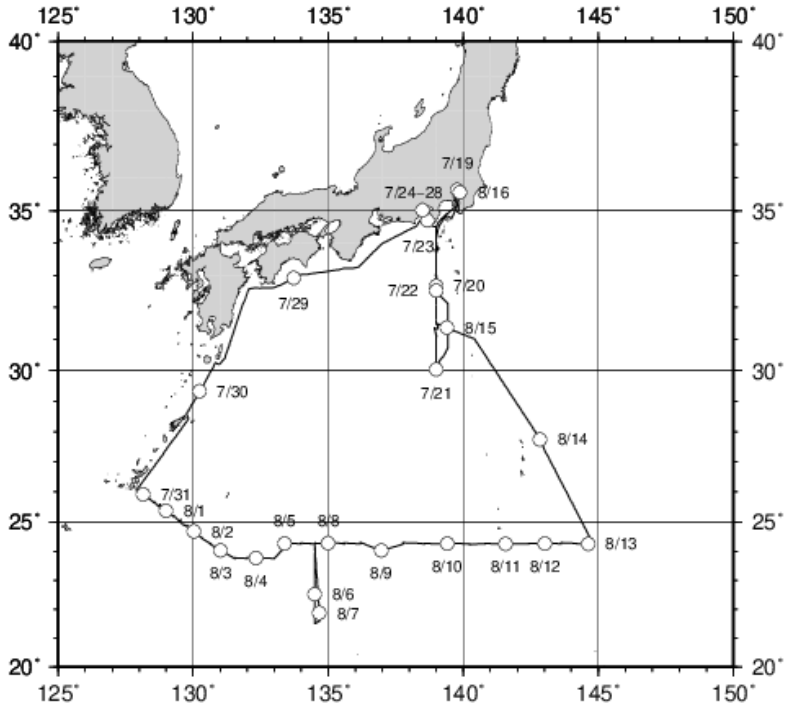

Figure B.3.2.1 Cruise track from July 19, 2021 to August 17, 2021 (UTC). Circles indicate all noon positions (JST) along the cruise track.

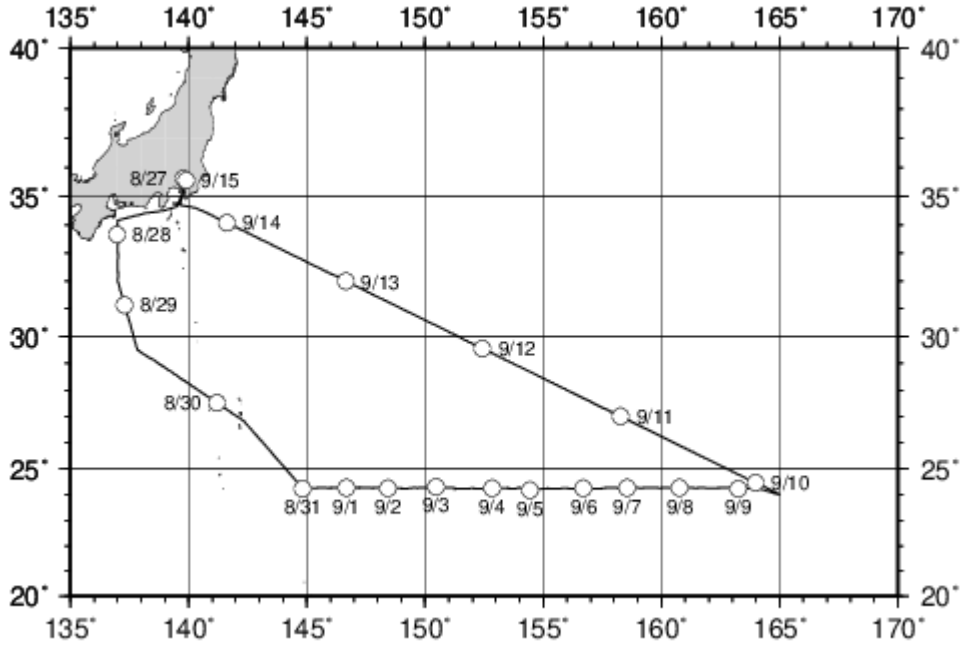

Figure B.3.2.2 Cruise track from August 27, 2021 to September 16, 2021 (UTC). Circles indicate all noon positions (JST) along the cruise track.

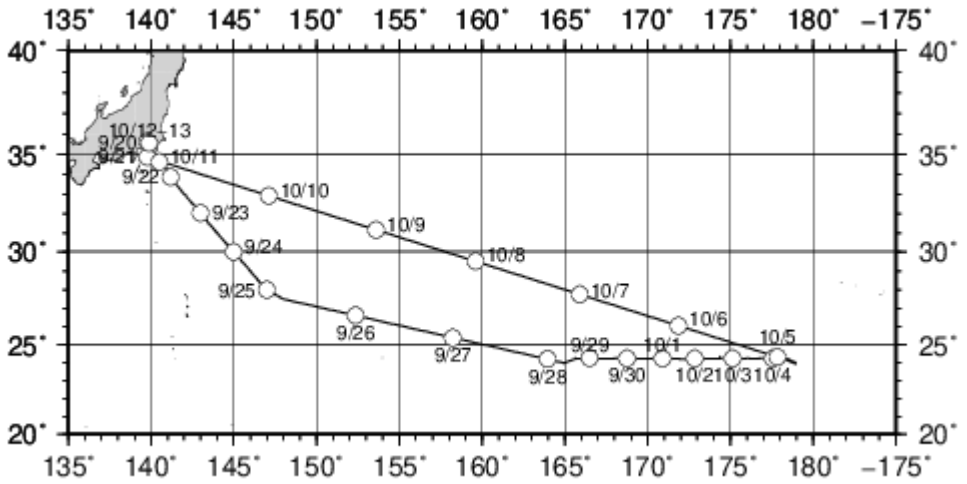

Figure B.3.2.3 Cruise track from September 20, 2021 to October 14, 2021 (UTC). Circles indicate all noon positions (JST) along the cruise track.

(4) Data processing and Data format

All raw data were recorded in every 6-seconds. The values of 1-minute and 10-minute data were averaged from 6-seconds raw data. The 10-minute data in every three hours are available from JMA web site (https://www.data.jma.go.jp/kaiyou/db/vessel_obs/data-report/html/ship/cruisedata_e.php?id=RF2106).

(https://www.data.jma.go.jp/kaiyou/db/vessel_obs/data-report/html/ship/cruisedata_e.php?id=RF2107).

(https://www.data.jma.go.jp/kaiyou/db/vessel_obs/data-

report/html/ship/cruisedata_e.php?id=RF2108).

Because the thermometers and the hygrometers are equipped on the both starboard/port sides on the compass deck, we used air temperature/relative humidity data taken at upwind side at difference time. Dew point temperature was calculated from relative humidity and air temperature.

Pressure data was corrected to sea level pressure. During the cruise, fixed value +0.5 hPa (for the height of the observation room) was used for the correction. Data were stored in ASCII format and representative parameters are as follows; time in UTC, longitude (E), latitude (N), ship speed (knot), ship direction (degrees), sea-level pressure (hPa), air temperature (degrees Celsius), dew point temperature (degrees Celsius), relative humidity (%), sea surface temperature (degrees Celsius), wind direction (degree) and wind speed (m/sec).

Wave height and period were observed twice in an hour. The measurement period was 20 minutes and each measurement started at 5 minutes and 35 minutes after the hour. In addition to those data, ship's position and observation time were recorded in ASCII format.

(5) Data quality

To confirm the data quality, each sensor was checked as follows.

Temperature/Relative humidity sensor:

The temperature and relative humidity (T/RH) sensors on the both sides of the ship were checked

by the manufacturer before delivering and, they were also checked by the calibrated Assmann psychrometer before and after the cruise. The discrepancy between T/RH sensors and Assmann psychrometer were within ± 0.4 degrees Celsius and ± 4 %, respectively.

Thermometer (Sea surface temperature):

The sea temperature sensor was calibrated once a year by the manufacturer. Certificated accuracy of the sensor is better than ± 0.4 degrees Celsius. At the start of the cruise, the values are also compared with temperature of water, taken from sea surface using a bucket, which was measured by a calibrated mercury thermometer (Yoshino Keisoku S-441, accuracy is better than ± 0.1 degrees Celsius).

Pressure sensor:

Using calibrated portable barometer (Vaisala 765-16B, certificated accuracy is better than ± 0.1 hPa), pressure sensor was checked before the cruise. Mean difference of RMET pressure sensor and portable sensor is less than 0.7 hPa.

Aerovane:

Aerovane was checked once per year by the manufacturer, and once per five years by the Meteorological Instrument Center, JMA.

(6) Ship's weather observation

Non-instrumental observations such as weather, cloud, visibility, wave direction and wave height

were made by the ship crews every three hours. We sent those data together with the RMET data to the Global Collecting Centre for Marine Climatological Data in IMMT (International Maritime Meteorological Tape) -V format. The RMET data are available from JMA web site.

(https://www.data.jma.go.jp/kaiyou/db/vessel_obs/data-report/html/ship/cruisedata_e.php?id=RF2106).

(https://www.data.jma.go.jp/kaiyou/db/vessel_obs/data-report/html/ship/cruisedata_e.php?id=RF2107).

(https://www.data.jma.go.jp/kaiyou/db/vessel_obs/data-report/html/ship/cruisedata_e.php?id=RF2108).

4. Thermosalinograph (to be submitted in the next update)

5. Underway chlorophyll-a

31 March 2022

(1) Personnel

SHINODA Yoshihiro

HASHIMOTO Susumu

SASAKI Takuya

OKAJIMA Shingo (RF21-06)

FUJII Takuya (RF21-06, RF21-08)

IMAI Yoichi (RF21-07)

KAKUYA Keita (RF21-07, RF21-08)

(2) Method

The Continuous Sea Surface Water Monitoring System of fluorescence (NIPPON KAIYO CO., LTD., Japan) automatically had been continuously measured seawater which is pumped from a depth of about 4.5 m below the maximum load line to the laboratory. The flow rate of the surface seawater was controlled by several valves and adjusted to about 0.6 L min^{-1}. The sensor in this system is a fluorometer 10-AU (S/N: 7062, Turner Designs, United States).

(3) Observation log

The chlorophyll-*a* continuous measurements were conducted during the entire cruise;

from 19 Jul. to 23 Jul., 2021 in RF21-06 Leg 1, from 28 Jul. to 16 Aug., 2021 in RF21-06 Leg2, from 27 Aug. to 14 Sep., 2021 in RF21-07, and from 21 Sep. to 11 Oct., 2021 in RF21-08.

(4) Water sampling

Surface seawater was corrected from outlet of water line of the system at nominally 1 day intervals. The seawater sample was measured in the same procedure as hydrographic samples of chlorophyll-*a* (see Chapter C9 "Phytopigments").

(5) Calibration

At the beginning and the end of legs, a raw fluorescence value of sensor was adjusted in sensitivity of the sensor using deionized water and a rhodamine 0.1ppm solution measured.

After the cruise, the fluorescence value was converted to chlorophyll-*a* concentration by programs in the system based on nearby water sampling data (chlorophyll-*a* concentration and distance from location of sensor data).

(6) Data

Underway fluorescence and chlorophyll-*a* data is distributed in JMA format in "49UP20210719_P03W_underway_chl.csv". The record structure of the format is as follows;

Column1 DATE: Date (YYYYMMDD) [JST]

Column2 TIME: Time (HHMM) [JST] (= UTC + 9h)

Column3 LATITUDE: Latitude

Column4 LONGITUDE: Longitude

Column5 FLUOR: Fluorescence value (RFU)

Column6 CHLORA: Chlorophyll-*a* concentration (μg L^{-1})

Column7 BTLCHL: Chlorophyll-*a* concentration of water sampling (μg L^{-1}).

6. Partial Pressure of Carbon Dioxide (to be submitted in the next update)

7. Acoustic Doppler Current Profiler

25 November 2021

(1) Personnel

CHIBA Yasuomi (JMA)

WADA Koichi (JMA)

(2) Instruments and Methods

Current direction and speed were measured by the hull-mounted 38 kHz Ocean Surveyor ADCP (Teledyne RD Instruments, Inc., USA; hereafter TRDI). The transducer of the system was installed in a dome at 3 m left of center and 13 m aft of the bow at the water line. The firmware version was 23.17 and the data acquisition software was TRDI/VMDAS Version. 1.49. The instrument was used in water-tracking mode during the operations, and was recording each ping raw data in 20 m × 60 bin from about 36 m to 1200 m in depth. Sampling interval was variable as short as possible and typically 6.4 seconds. GPS navigation data and ship's gyrocompass data were recorded with the ADCP data. In addition to the raw data, 60 seconds and 300 seconds averaged data were stored as short term average (STA) and long term average (LTA) data, respectively. Current field based on the gyrocompass was used to check the operation and the performance on board.

(3) Performance and quick view of the ADCP data on board

The performance of the ADCP instrument was almost good throughout the cruise, and current profiles were usually reached about 1000 m. We monitored the current profiles based on LTA data in this cruise on board.

(4) Data Processing

LTA data were processed by CODAS (Common Oceanographic Data Access System) software, developed at the University of Hawaii (https://currents.soest.hawaii.edu/docs/adcp_doc/index.html). We used a standard CODAS processing including a PC time correction, a sound-speed correction based on the thermistor temperature at the transducers, and an amplitude and phase calibration constant applied to the measured velocities.

Calibration constants to be applied were evaluated for each leg using the water track data. The values of amplitude and phase applied to each leg are listed in Table B.7.1. Figure B.7.1 shows surface current at the depth of 36 m during the cruise.

Table B.7.1. The values of amplitude and phase applied to each leg (cruise).

	Amplitude	Phase
RF2106 Leg2	1.0039	0.3015
RF2107	1.0054	-0.2846
RF2108	1.0050	-0.3587

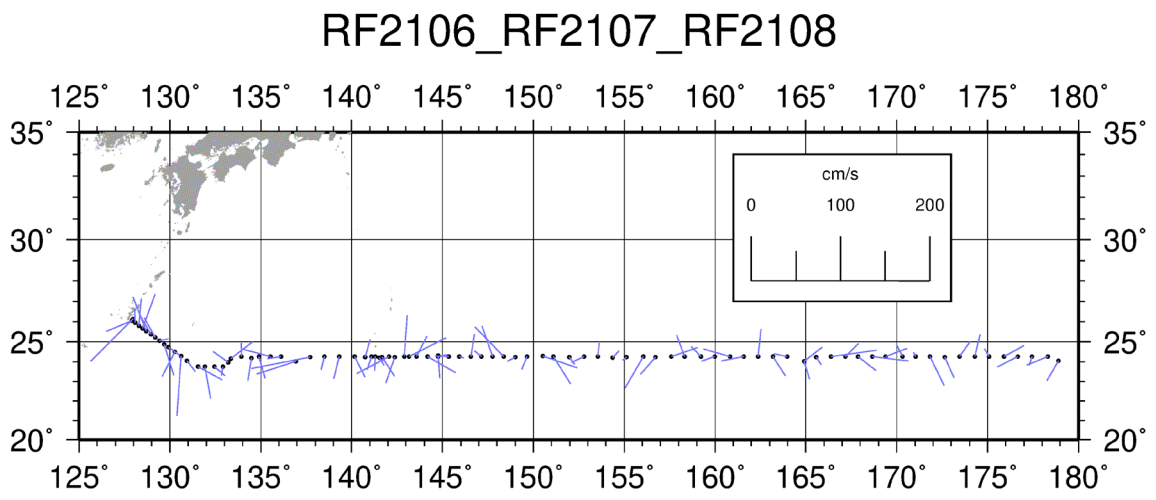

Figure B.7.1. Surface current at the depth of 36 m.

Reference

Joyce, T. M. (1988), On in-situ "calibration" of shipboard ADCPs. *J. Atmos. Oceanic Technol.*, 6, 169172.

C. Hydrographic Measurement Techniques and Calibration

1. $CTDO_2$ Measurements

25 November 2021

(1) Personnel

WADA Kouichi （JMA）

ETO Tetsuhiro （JMA）

IDA Togo （JMA）

TSUZUKI Takato （JMA、RF2106）

OE Mitsuho （JMA、RF2106）

CHIBA Yasuomi （JMA、RF2107, RF2108）

HATANAKA Kenichiro （JMA、RF2107, RF2108）

(2) $CTDO_2$ measurement system

（*Software*: SEASAVEwin32 ver7.23.2）

Deck unit	*Serial number*	*Station*
SBE 11plus (SBE)	11P35251 – 0683	RF6860 – 6974
Under-water unit	***Serial number***	***Station***
SBE 9plus (SBE)	09P35251 – 0761 (Pressure : 91530)	RF6860 – 6974
Temperature	***Serial number***	***Station***
SBE 3plus (SBE)	03P4436 (primary)	RF6860 – 6974

	03P5632 (secondary)	RF6860 – 6974
SBE 35 (SBE)	0093	RF6860 – 6974
Conductivity	*Serial number*	*Station*
SBE 4C (SBE)	042987 (primary)	RF6860 – 6974
	043682 (secondary)	RF6860 – 6974
Pump	*Serial number*	*Station*
SBE 5T (SBE)	056552 (primary)	RF6860 – 6974
	057934 (secondary)	RF6860 – 6974
Oxygen	*Serial number*	*Station*
RINKO III (JFE)	392 (foil number:193028A)	RF6860 – 6974
	356 (foil number:193028A)	RF6860 – 6974
Water sampler (36 position)	*Serial number*	*Station*
SBE 32 (SBE)	32 – 1270	RF6860 – 6974
Altimeter	*Serial number*	*Station*
VA500 (VA)	69758	RF6860 – 6974
Water sampling bottle		*Station*
Niskin Bottle (GO)		RF6860 – 6974

SBE: Sea- Bird Electronics, Inc., USA

JFE: JFE Advantech Co., Ltd., Japan

VA: VALEPORT, Inc., UK

GO: General Oceanics, Inc., USA

(3) Pre-cruise calibration

(3.1) Pressure

S/N 0761, *15 Jan. 2021*

c_1	=	-4.651547×10^{4}	t_1	=	3.020363×10
c_2	=	9.130672×10^{-2}	t_2	=	-2.641135×10^{-4}
c_3	=	1.439800×10^{-2}	t_3	=	4.172110×10^{-6}
d_1	=	3.778300×10^{-2}	t_4	=	3.125100×10^{-9}
d_2	=	0.000000	t_5	=	0.000000

Formula:

$$c = c_1 + c_2 \times U + c_3 \times U^2$$
$$d = d_1 + d_2 \times U$$
$$t_0 = t_1 + t_2 \times U + t_3 \times U^2 + t_4 \times U^3 + t_5 \times U^4$$

U (*degrees Celsius*) = $M \times$ (*12-bit pressure temperature compensation word*) + B

U: temperature in degrees Celsius

S/N 0761 coefficients in SEASOFT (configuration sheet dated on 15 *Jan. 2021)*

$M = 1.28617 \times 10^{-2}$, $B = -8.41688$

Finally, pressure is computed as

$$P(psi) = c \times (1 - t_0^2 / t^2) \times \{1 - d \times (1 - t_0^2 / t^2)\}$$

t: pressure period (μ sec)

The drift-corrected pressure is computed as

$$Drift\ corrected\ pressure(dbar) = slope \times (computed\ pressure\ in\ dbar) + offset$$

$$Slope = 0.99990,\ Offset = -0.5234$$

(3.2) Temperature (ITS-90): SBE 3plus

S/N 03P4436 (primary), 01 Dec. 2020

$g = 4.33671540 \times 10^{-3}$ $\quad j = 1.84135076 \times 10^{-6}$

$h = 6.38168848 \times 10^{-4}$ $\quad f_0 = 1000.0$

$i = 2.12668822 \times 10^{-5}$

S/N 03P5632 (secondary), 04 Dec. 2020

$g = 4.34077936 \times 10^{-3}$ $\quad j = 1.39823691 \times 10^{-6}$

$h = 6.28182709 \times 10^{-4}$ $\quad f_0 = 1000.0$

$i = 1.94913513 \times 10^{-5}$

Formula:

$$Temperature(ITS-90) = \frac{1}{g + h \times \ln(f_0/f) + i \times \ln^2(f_0/f) + j \times \ln^3(f_0/f)} - 273.15$$

f: Instrument freq.[Hz]

(3.3) Deep Ocean Standards Thermometer Temperature (ITS-90): SBE 35

S/N 0093, 27 Oct. 2020

$a_0 = 4.12756963 \times 10^{-3}$ $a_3 = -9.36245277 \times 10^{-6}$

$a_1 = -1.08163464 \times 10^{-3}$ $a_4 = 2.00979198 \times 10^{-7}$

$a_2 = 1.67453817 \times 10^{-4}$

Formula:

$$Linearized\ temperature(ITS{-}90) = 1/\left\{a_0 + a_1 \times \ln(n) + a_2 \times \ln^2(n) + a_3 \times \ln^3(n) + a_4 \times \ln^4(n)\right\} - 273.15$$

n: instrument output

The slow time drift of the SBE 35

S/N 0093, 2 Nov. 2020 (2nd step: fixed point calibration)

Slope = 1.000004, Offset = -0.000188

Formula:

$$Temperature(ITS{-}90) = slope \times (Linearized\ temperature) + offset$$

(3.4) Conductivity: SBE 4C

S/N 042987 (primary), 28 Jan. 2021

g	=	–9.90116802	j	=	$-3.76254718 \times 10^{-5}$
h	=	1.35606673	CP_{cor}	=	-9.5700×10^{-8}
i	=	$1.99815553 \times 10^{-3}$	CT_{cor}	=	3.2500×10^{-6}

S/N 043682 (secondary), 24 Nov. 2020

g	=	-1.00118599×10	j	=	$3.15601132 \times 10^{-4}$
h	=	1.43233438	CP_{cor}	=	-9.5700×10^{-8}
i	=	$-2.92529308 \times 10^{-3}$	CT_{cor}	=	3.2500×10^{-6}

Conductivity of a fluid in the cell is expressed as:

$$C(S/m) = \left(g + h \times f^2 + i \times f^3 + j \times f^4\right) \Big/ \left\{10 \times \left(1 + CT_{cor} \times t + CP_{cor} \times p\right)\right\}$$

f: instrument frequency (kHz)

t: water temperature (degrees Celsius)

p: water pressure (dbar).

(3.5) Oxygen (RINKO III)

The RINKO III (JFE Advantech Co., Ltd., Japan) sensor is based on the ability of a selected substance to act as a dynamic fluorescence quencher. The RINKO III model is designed to be used with a CTD system that accepts an auxiliary analog sensor, and it is designed to operate down to 7000 m. The RINKO III output is expressed in voltage from 0 to 5 V.

(4) Quality control and data correction during the cruise

(4.1) Temporal change of deck pressure

The post-cruise drift corrected pressure was computed as follows:

$$Drift\ corrected\ pressure(dbar) = slope \times (computed\ pressure\ in\ dbar) + offset$$

S/N 09P35251 – 0761, 11 Mar. 2022

$$Slope = 0.99982, \quad Offset = -1.4530$$

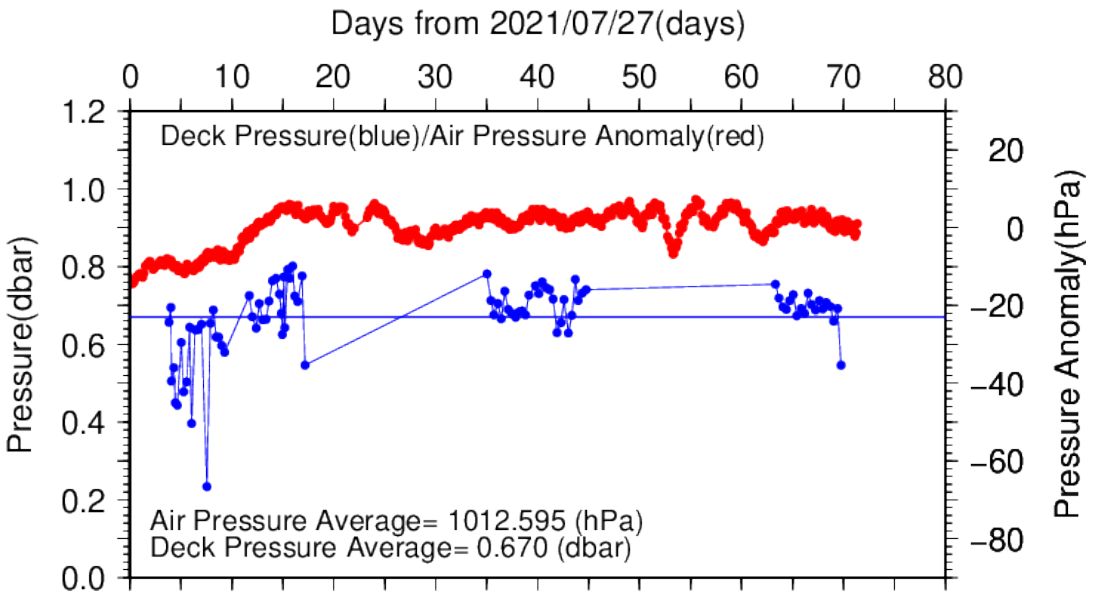

Figure C.1.1. Time series of the CTD deck pressure. Red line indicates atmospheric pressure anomaly. Blue line and dots indicate pre-cast deck pressure and average.

(4.2) Temperature sensor (SBE 3plus)

The practical corrections for the CTD temperature data can be made by using a SBE 35 and correcting the SBE 3plus so that it agrees with the SBE 35 (*McTaggart et al., 2010*; *Uchida et al., 2007*).

CTD temperature is corrected as follows:

$$Corrected\ temperature = T - (c_0 + c_1 \times P + c_2 \times P^2)$$

T: CTD temperature (degrees Celsius), *P:* pressure (dbar), and c_0, c_1, c_2: coefficients

Table C.1.1. Temperature correction summary (pressure ≥ 2000dbar). (Bold: accepted sensor)

S/N	*Num*	$c_0(K)$	$c_1(K/dbar)$	$C_2(K/dbar^2)$	*Stations*
03P4436	**372**	**5.437328×10^{-4}**	**1.098702×10^{-7}**	**0.000000**	**RF6860 – 6901**
03P4436	**446**	**6.992947×10^{-4}**	**-1.149782×10^{-7}**	**3.185994×10^{-11}**	**RF6902 – 6931** RF6932 (※) **RF6933 - 6937**
03P4436	**384**	**7.489255×10^{-4}**	**-1.149898×10^{-7}**	**2.979558×10^{-11}**	RF6938 – 6974
03P5632	372	3.653535×10^{-4}	-2.615938×10^{-7}	5.289684×10^{-11}	RF6860 – 6901
03P5632	446	7.466208×10^{-4}	-5.704204×10^{-7}	8.808326×10^{-11}	RF6902 – 6931 **RF6932 (※)** RF6933 - 6937
03P5632	384	8.837996×10^{-4}	-6.324936×10^{-7}	9.389582×10^{-11}	RF6938 – 6974

※ For station RF6932, the S/N 03P5632 was accepted instead of the S/N 03P4436 due to data shift. This shift was not determined except for RF6932.

Table C.1.2. Temperature correction summary for S/N 03P4436.

Stations	Pressure < 2000dbar			Pressure ≥ 2000 dbar		
	Num	Average (K)	Std (K)	Num	Average (K)	Std (K)

RF6860 – 6901	737	– 0.0002	0.0080	372	0.0000	0.0002
RF6902 – 6937	620	– 0.0008	0.0080	446	0.0000	0.0001
RF6938 – 6974	537	– 0.0002	0.0056	384	0.0000	0.0002

Table C.1.3. Temperature correction summary for S/N 03P5632.

Stations	Pressure < 2000dbar			Pressure ≥ 2000 dbar		
	Num	Average (K)	Std (K)	Num	Average (K)	Std (K)
RF6860 – 6901	737	– 0.0002	0.0092	372	0.0000	0.0002
RF6902 – 6937	620	– 0.0007	0.0074	446	0.0000	0.0001
RF6938 – 6974	537	– 0.0007	0.0059	384	0.0000	0.0001

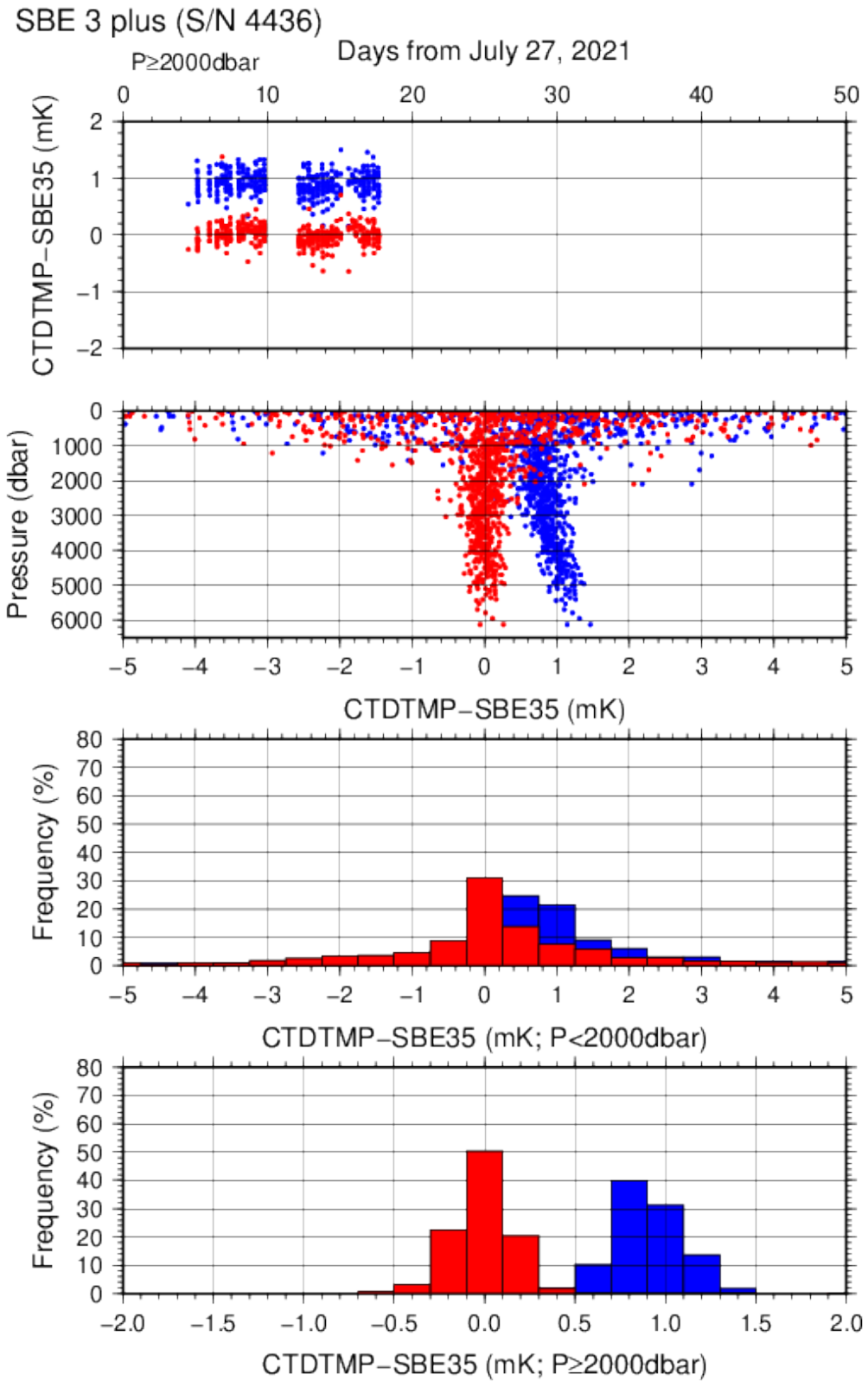

Figure C.1.2. Difference between the CTD temperature (*S/N 03P4436*) and the Deep Ocean Standards thermometer (SBE 35) on RF21-06 Leg 2. Blue and red dots indicate before and after the correction using SBE 35 data, respectively. Lower two panels show histograms of the differences after correction.

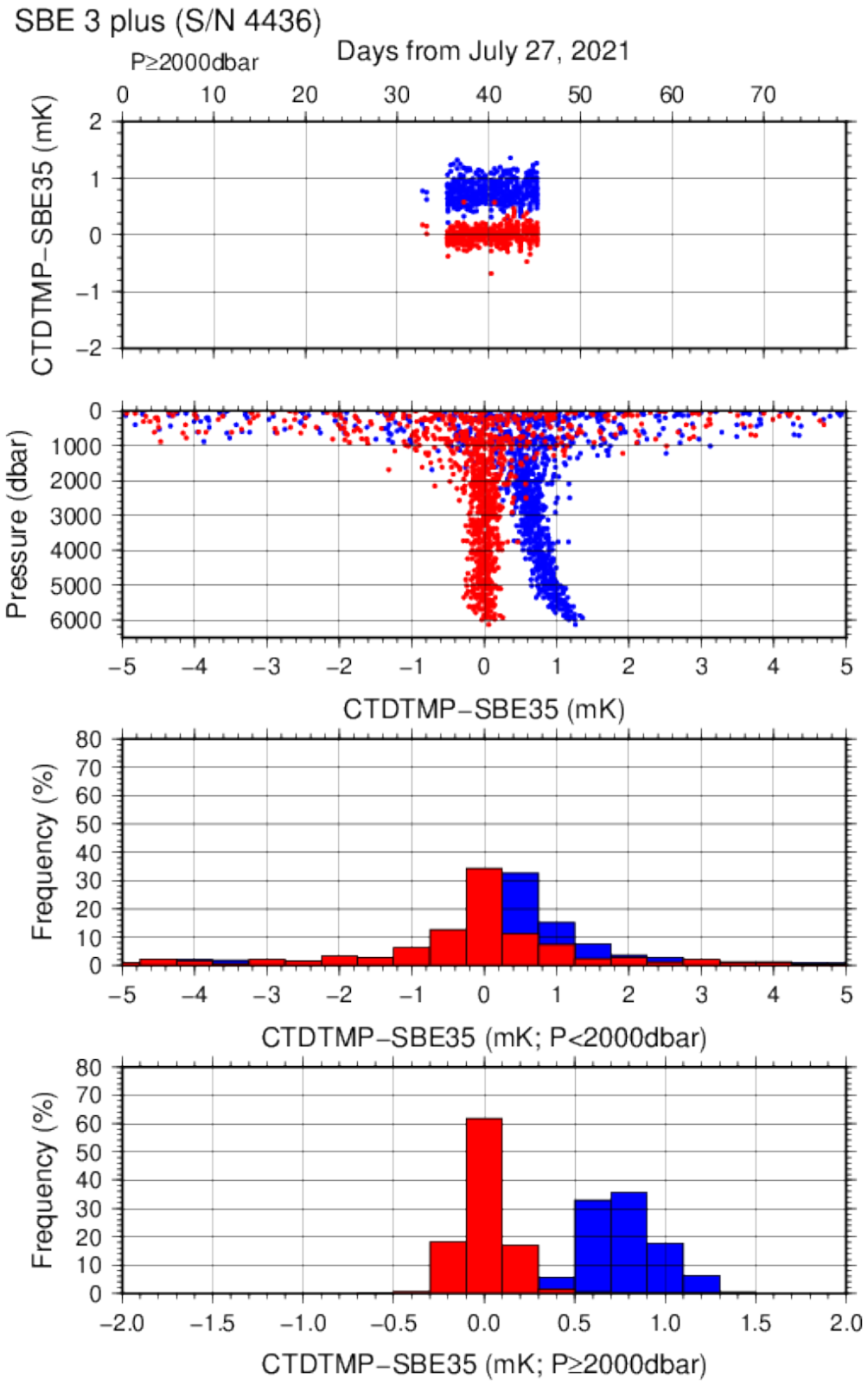

Figure C.1.3. Difference between the CTD temperature (*S/N 03P4436*) and the Deep Ocean Standards thermometer (SBE 35) on RF21-07. Blue and red dots indicate before and after the

correction using SBE 35 data, respectively. Lower two panels show histograms of the differences after correction.

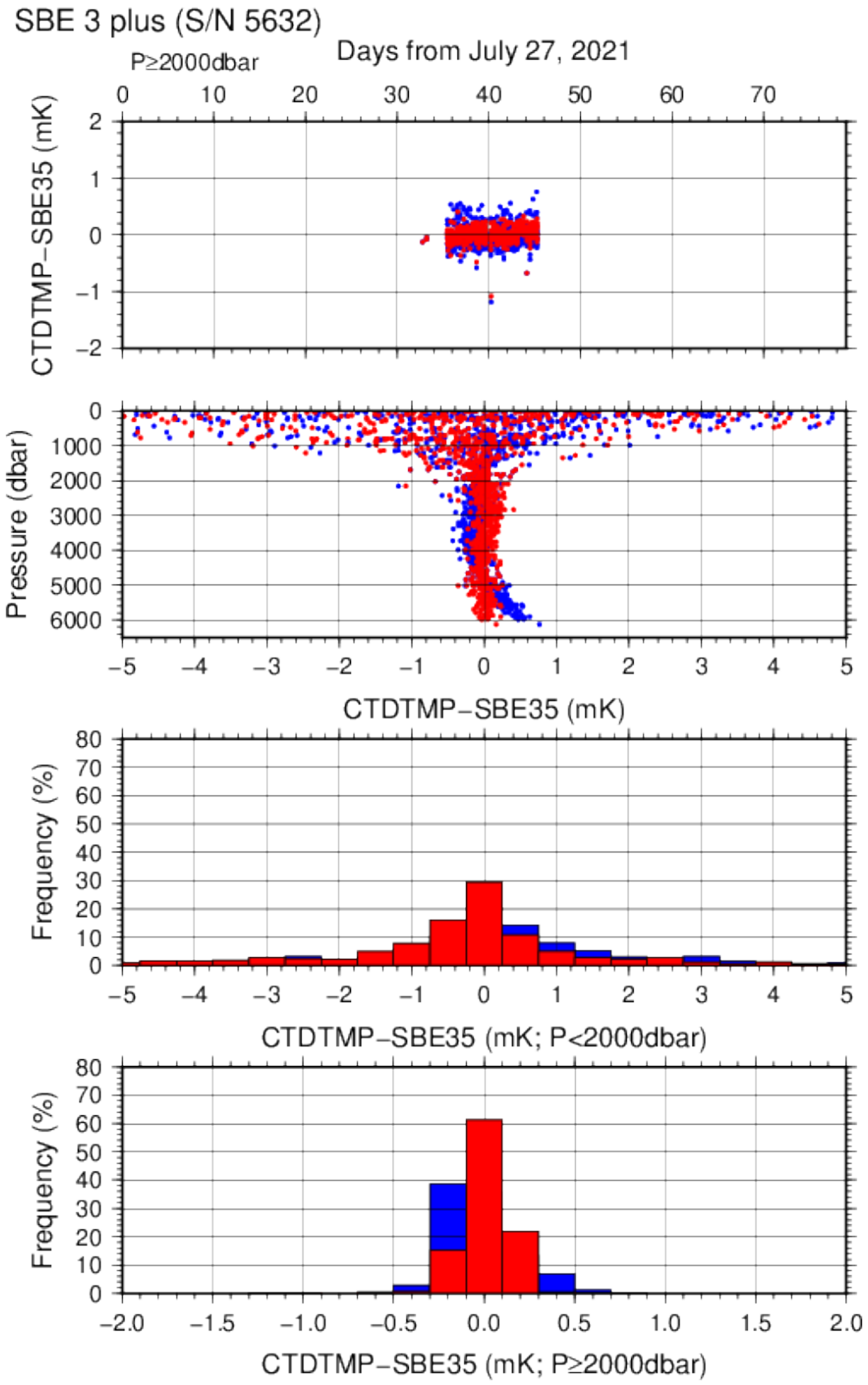

Figure C.1.4. Difference between the CTD temperature (*S/N 03P5632*) and the Deep Ocean Standards thermometer (SBE 35) on RF21-07. Blue and red dots indicate before and after the

correction using SBE 35 data, respectively. Lower two panels show histograms of the differences after correction.

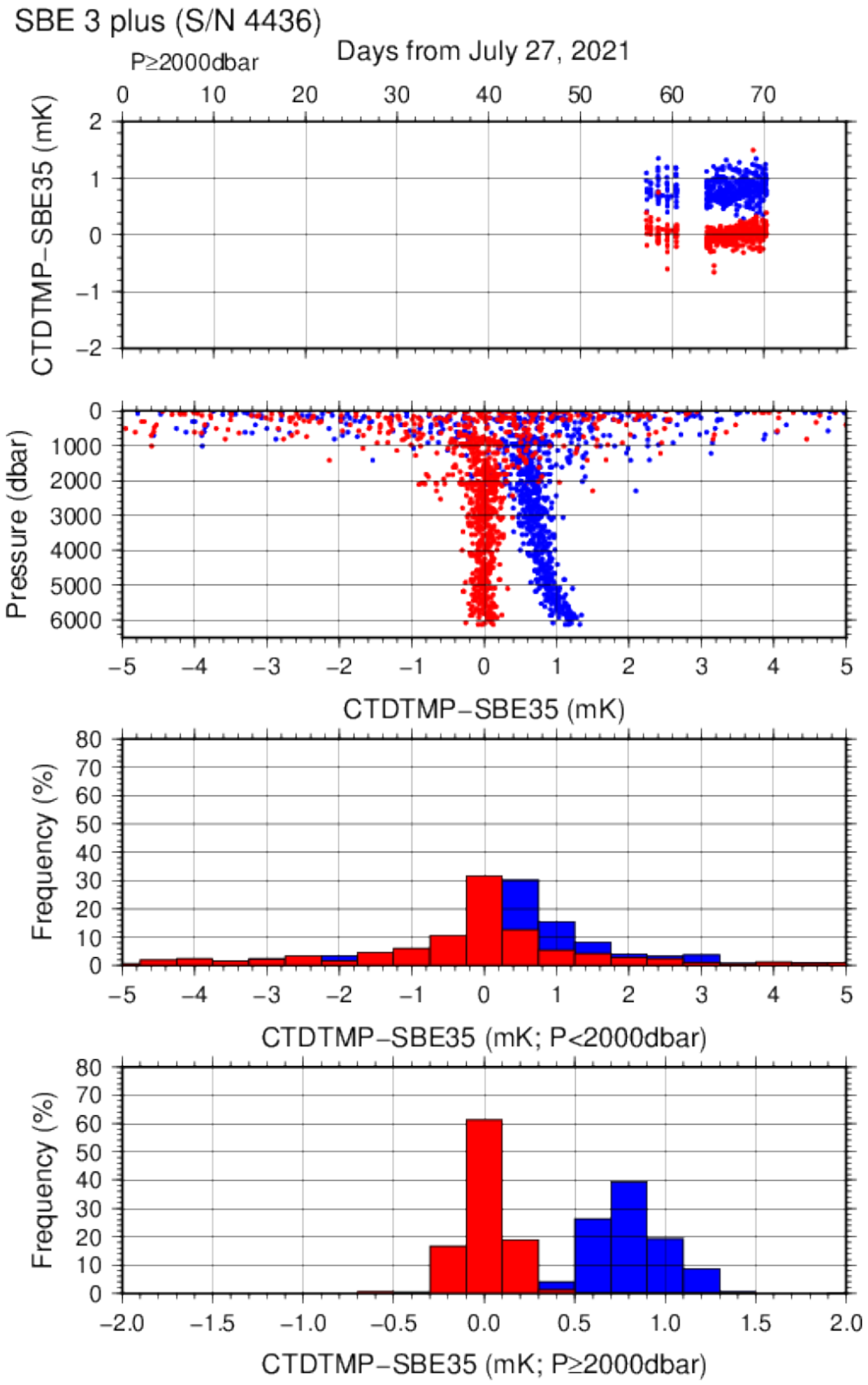

Figure C.1.5. Difference between the CTD temperature (*S/N 03P4436*) and the Deep Ocean Standards thermometer (SBE 35) on RF21-08. Blue and red dots indicate before and after the

correction using SBE 35 data, respectively. Lower two panels show histograms of the differences after correction.

(4.3) Conductivity sensor (SBE 4C)

The practical corrections for CTD conductivity data can be made by using bottle salinity data to correct the SBE 4C to agree with measured conductivity (*McTaggart et al., 2010*).

CTD conductivity was corrected as follows:

$$Corrected\ Conductivity = C - \left(\sum_{i=0}^{I} c_i \times C^i + \sum_{j=1}^{J} p_j \times P^j \right)$$

C: CTD conductivity, c_i and p_j: calibration coefficients

i, j: determined by use of the AIC (*Akaike*, 1974). In accord with *McTaggart et al.* (2010), the maximum of I and J are 2.

Table C.1.4. Conductivity correction coefficient summary. (Bold: accepted sensor)

S/N	*Num*	c_0(S/m)	c_1	c_2(m/S)	*Stations*
			p_1(S/m/dbar)	p_2(S/m/dbar^2)	
042987	576	-7.8668 × 10^{-4}	–4.8018 × 10^{-6}	6.9212 × 10^{-5}	RF6860 – 6901
			3.5637 × 10^{-8}	0.0000	
042987	564	-8.7024 × 10^{-4}	8.2765 × 10^{-5}	6.0423 × 10^{-5}	RF6902 – 6931
			4.5645 × 10^{-8}	–3.0751 × 10^{-12}	RF6932 (※) RF6933 - 6937
042987	542	- 4.0535 × 10^{-4}	–1.5552 × 10^{-4}	9.1640 × 10^{-5}	RF6938 – 6974
			5.9684 × 10^{-8}	-4.8822 × 10^{-12}	

043682	576	1.4895×10^{-3}	-9.8482×10^{-4}	1.7983×10^{-4}	RF6860 – 6901
			1.4452×10^{-8}	0.0000	
043682	568	2.1282×10^{-3}	-1.2598×10^{-3}	2.1145×10^{-4}	RF6902 – 6931
			0.0000	0.0000	**RF6932 (※)**
					RF6933 - 6937
043682	542	2.5221×10^{-3}	-1.4789×10^{-3}	2.3924×10^{-4}	RF6938 – 6974
			2.2088×10^{-8}	-3.3332×10^{-12}	

※ For station RF6932, the S/N 043682 was accepted instead of the S/N 042987 due to data shift.

This shift was not determined except for RF6932.

Table C.1.5. Conductivity correction and salinity correction summary for S/N 042987.

Stations	Pressure < 1900dbar					
	Conductivity			Salinity		
	Num	Average (S/m)	Std (S/m)	Num	Average	Std
RF6860 – 6901	391	0.0000	0.0002	391	0.0000	0.0013
RF6902 – 6937	346	0.0000	0.0002	346	0.0000	0.0019
RF6938 – 6974	313	0.0000	0.0002	313	0.0000	0.0015
Stations	Pressure ≥ 1900 dbar					
	Conductivity			Salinity		
	Num	Average (S/m)	Std (S/m)	Num	Average	Std
RF6860 – 6901	185	0.0000	0.0000	185	0.0000	0.0005
RF6902 – 6937	218	0.0000	0.0000	218	0.0000	0.0003
RF6938 – 6974	229	0.0000	0.0000	229	0.0000	0.0004

Table C.1.6. Conductivity correction and salinity correction summary for S/N 043682.

Stations	Pressure < 1900dbar					
	Conductivity			Salinity		
	Num	Average (S/m)	Std (S/m)	Num	Average	Std

RF6860 – 6901	391	0.0000	0.0002	391	0.0000	0.0016
RF6902 – 6937	345	0.0000	0.0002	345	0.0000	0.0019
RF6938 – 6974	313	0.0000	0.0002	313	0.0000	0.0015

Stations	Pressure ≥ 1900 dbar					
	Conductivity			Salinity		
	Num	Average (S/m)	Std (S/m)	Num	Average	Std
RF6860 – 6901	185	0.0000	0.0000	185	0.0000	0.0005
RF6902 – 6937	223	0.0000	0.0000	223	0.0000	0.0003
RF6938 – 6974	229	0.0000	0.0000	229	0.0000	0.0003

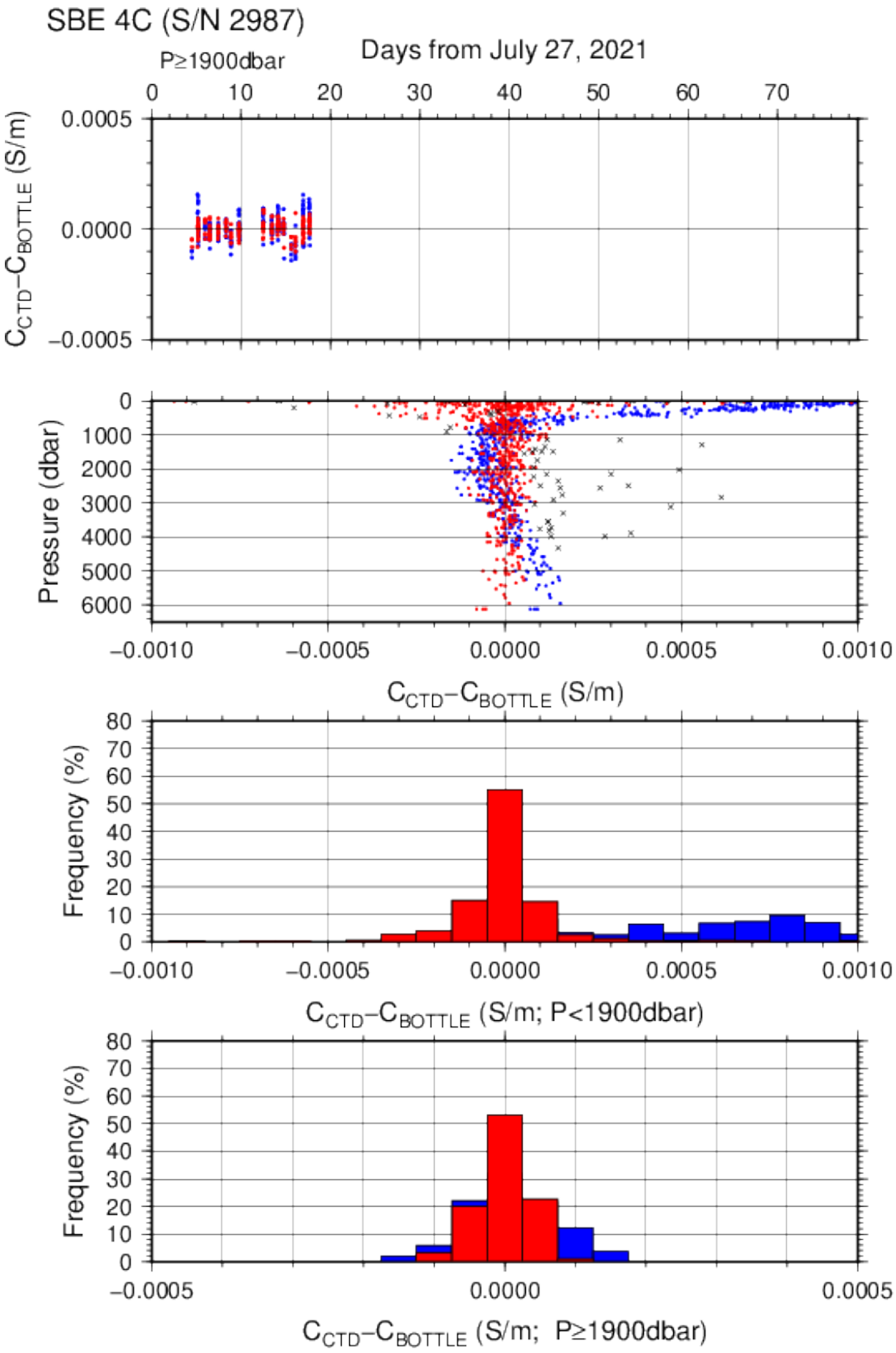

Figure C.1.6. Difference between the CTD conductivity (*S/N 042987*) and the bottle conductivity on RF21-06 Leg 2. Blue and red dots indicate before and after the calibration using bottle data, respectively. Lower two panels show histograms of the differences before and after calibration.

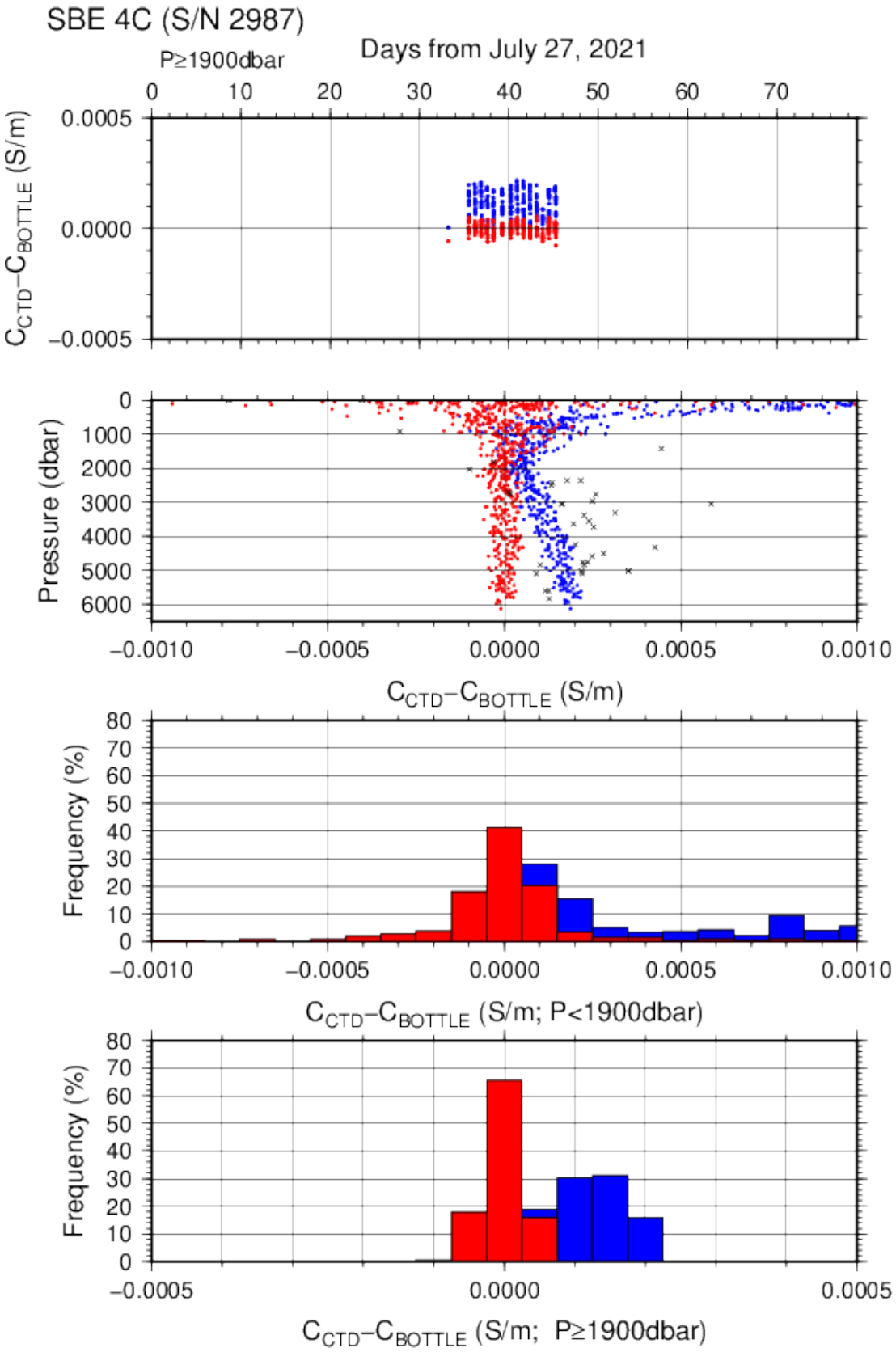

Figure C.1.7. Difference between the CTD conductivity (*S/N 042987*) and the bottle conductivity on RF21-07. Blue and red dots indicate before and after the calibration using bottle data, respectively. Lower two panels show histograms of the differences before and after calibration.

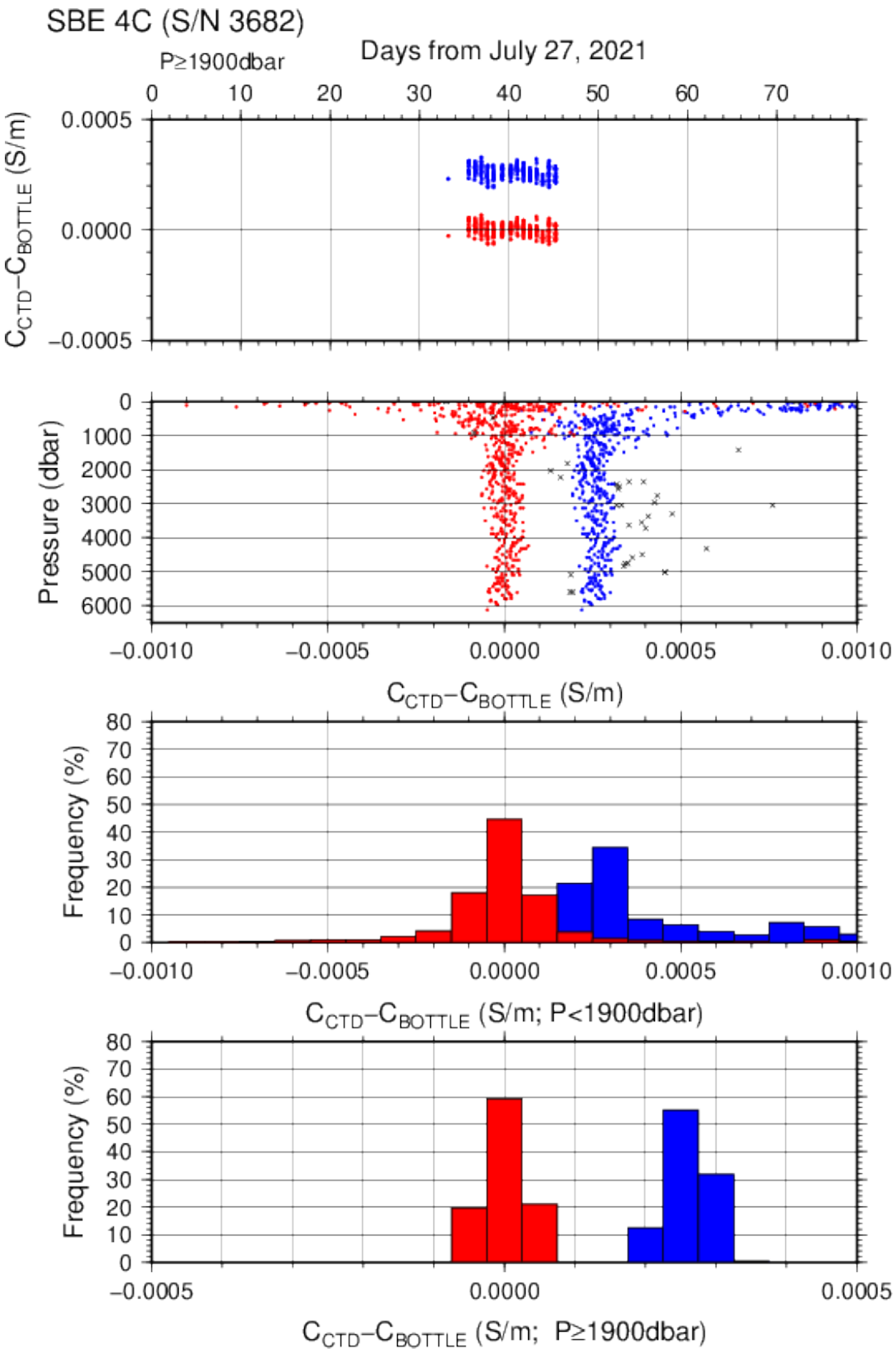

Figure C.1.8. Difference between the CTD conductivity (*S/N 043682*) and the bottle conductivity on RF21-07. Blue and red dots indicate before and after the calibration using bottle data, respectively.

Lower two panels show histograms of the differences before and after calibration.

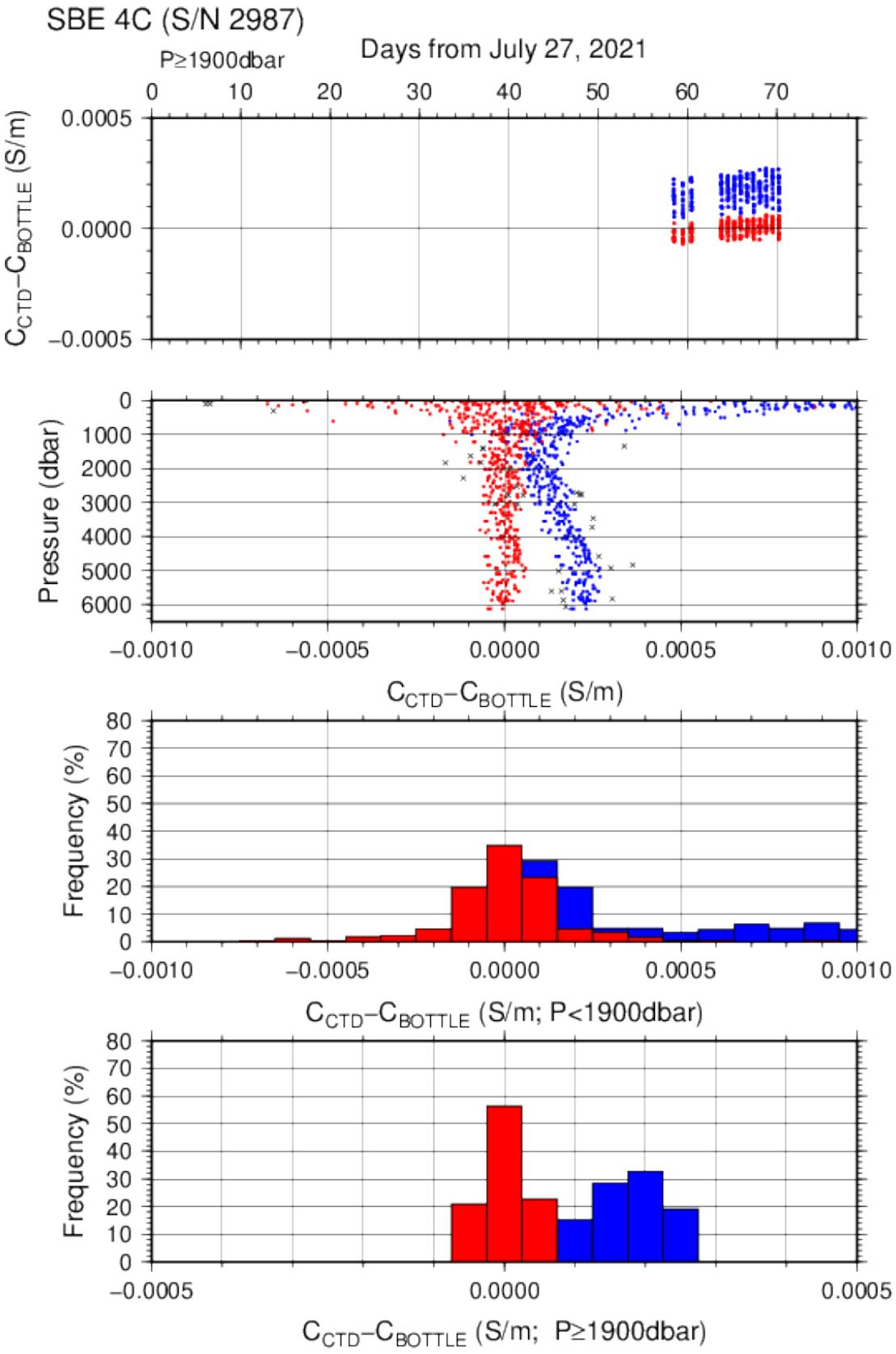

Figure C.1.9. Difference between the CTD conductivity (*S/N 042987*) and the bottle conductivity on RF21-08. Blue and red dots indicate before and after the calibration using bottle data, respectively. Lower two panels show histograms of the differences before and after calibration.

(4.4) Oxygen sensor (RINKO III)

The CTD oxygen concentration was calculated using the RINKO III output (voltage) with the Stern-Volmer equation in accord with the method of Uchida et al. (2008) and Uchida et al. (2010). The pressure hysteresis for the RINKO III output (voltage) was corrected in accord with Sea-bird Electronics (2009) and Uchida et al. (2010). The equations were as follows:

$$P_0 = 1.0 + c_4 \times t$$
$$P_c = c_5 + c_6 \times v + c_7 \times T + c_8 \times T \times v$$
$$K_{sv} = c_1 + c_2 \times t + c_3 \times t^2$$
$$coef = (1.0 + c_9 \times P/1000)^{1/3}$$
$$[O_2] = O_2^{sat} \times \{(P_0/P_c - 1.0)/K_{sv} \times coef\}$$

P: pressure (dbar), t: potential temperature, v: RINKO output voltage (volt)

T: elapsed time of the sensor from the beginning of first station in calculation group in day

O_2^{sat}: dissolved oxygen saturation by Garcìa and Gordon (1992) (μ mol/kg)

$[O_2]$: dissolved oxygen concentration (μ mol/kg)

c_1–c_9: determined by minimizing differences between CTD oxygen concentration and bottle dissolved oxygen concentration by quasi-newton method (*Shanno, 1970*).

Table C.1.7. Dissolved oxygen correction coefficient summary. (Bold: accepted sensor)

S/N	*Stations*	c_1	c_2	c_3	c_4	c_5
		c_6	c_7	c_8	c_9	
0392	**RF6860 – 6901**	**1.71748**	**2.32914×10^{-2}**	**2.77573×10^{-4}**	**-1.68331×10^{-4}**	**-1.43710×10^{-1}**
		3.08753×10^{-1}	**2.64411×10^{-4}**	**1.87630×10^{-4}**	**8.62170×10^{-2}**	
0392	RF6902 – 6937	1.69381	1.94596×10^{-2}	2.46605×10^{-4}	-7.33923×10^{-4}	-1.29783×10^{-1}
		3.06309×10^{-1}	1.34390×10^{-4}	1.53219×10^{-4}	8.97566×10^{-2}	
0392	**RF6938 – 6974**	**1.71884**	**2.41620×10^{-2}**	**2.58729×10^{-4}**	**-1.67454×10^{-4}**	**-1.43759×10^{-1}**
		3.10902×10^{-1}	**2.06382×10^{-5}**	**1.46204×10^{-4}**	**8.39368×10^{-2}**	
0356	RF6860 – 6901	1.72686	2.73896×10^{-2}	1.58460×10^{-4}	5.30533×10^{-4}	-1.34605×10^{-1}
		3.10240×10^{-1}	5.35585×10^{-4}	-3.80529×10^{-5}	8.51756×10^{-2}	
0356	**RF6902 – 6937**	**1.70374**	**2.30838×10^{-2}**	**1.33419×10^{-4}**	**-2.28257×10^{-4}**	**-1.20650×10^{-1}**
		3.06966×10^{-1}	**1.00118×10^{-4}**	**8.07451×10^{-5}**	**8.70983×10^{-2}**	
0356	RF6938 – 6974	1.71839	2.56171×10^{-2}	1.28693×10^{-4}	-1.81806×10^{-5}	-1.29483×10^{-1}
		3.09772×10^{-1}	3.28179×10^{-4}	$-3.03434 \times 10^{-}$	8.32957×10^{-2}	

				5		

Table C.1.8. Dissolved oxygen correction summary for S/N 0392.

Stations	Pressure < 950dbar			Pressure ≥ 950 dbar		
	Num	Average (μ mol/kg)	Std (μ mol/kg)	Num	Average (μ mol/kg)	Std (μ mol/kg)
RF6860 – 6901	555	0.04	0.72	542	-0.00	0.34
RF6902 – 6937	455	–0.03	0.56	603	0.01	0.26
RF6938 – 6974	390	–0.00	0.60	527	0.00	0.23

Table C.1.9. Dissolved oxygen correction summary for S/N 0356.

Stations	Pressure < 950dbar			Pressure ≥ 950 dbar		
	Num	Average (μ mol/kg)	Std (μ mol/kg)	Num	Average (μ mol/kg)	Std (μ mol/kg)
RF6860 – 6901	555	–0.01	0.62	542	-0.00	0.34
RF6902 – 6937	455	–0.03	0.49	603	0.00	0.25
RF6938 – 6974	390	-0.03	0.53	527	0.00	0.23

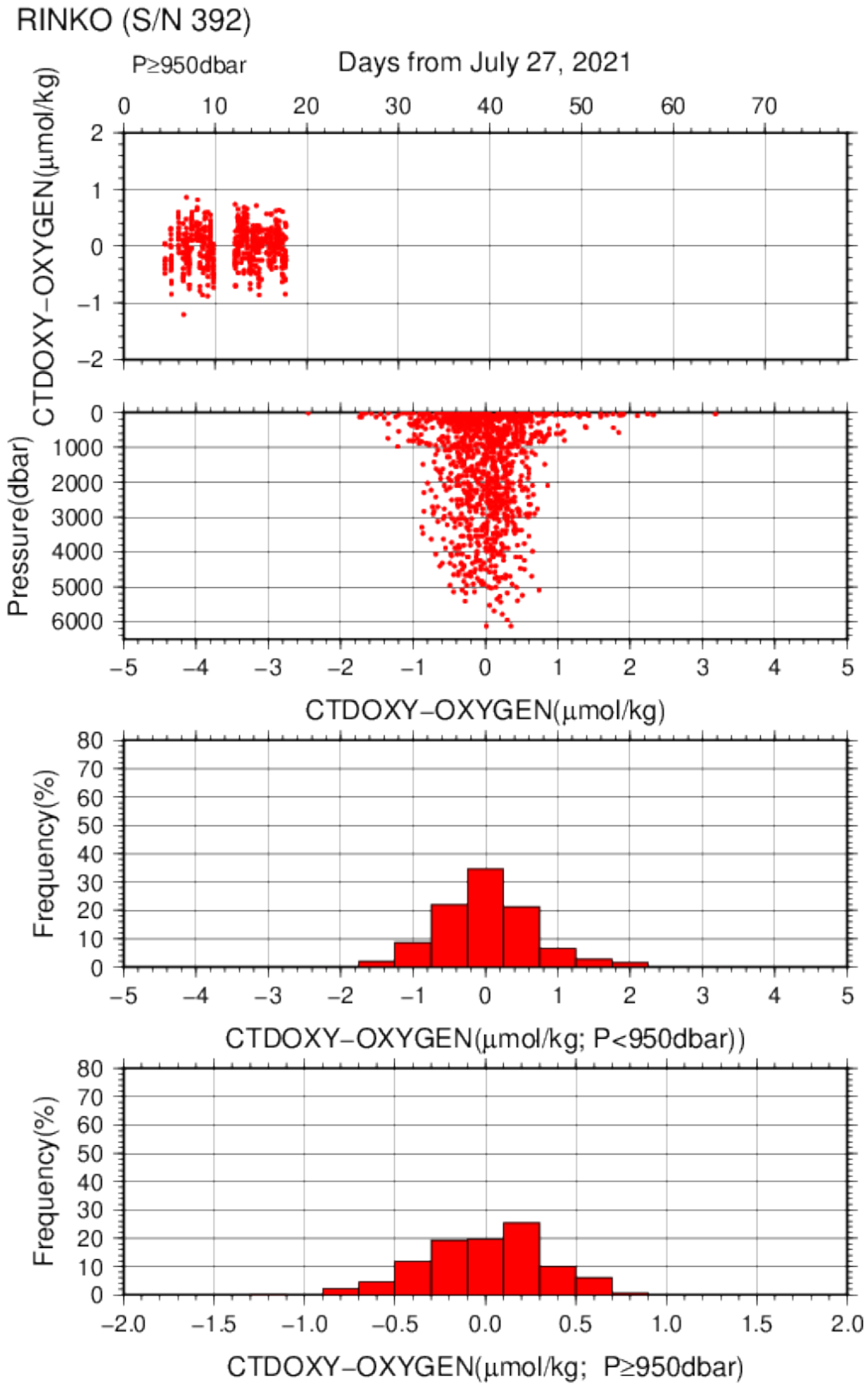

Figure C.1.10. Difference between the CTD oxygen (*S/N 0392*) and bottle dissolved oxygen on RF21-06 Leg 2. Red dots in upper two panels indicate the result of calibration. Lower two panels

show histograms of the differences between calibrated oxygen concentration and bottle oxygen concentration.

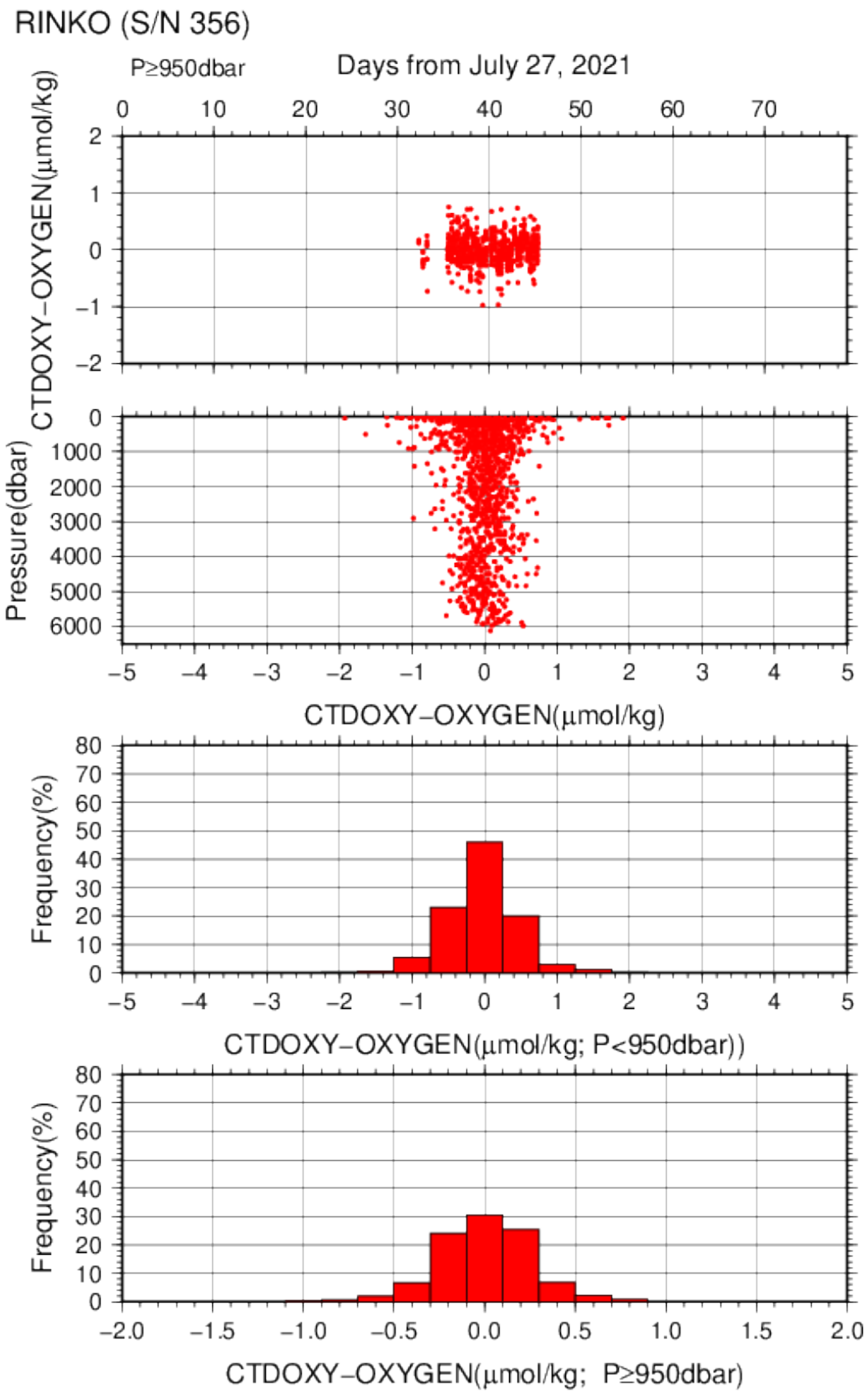
RINKO (S/N 356)
P≥950dbar
Days from July 27, 2021
CTDOXY−OXYGEN(µmol/kg)
Pressure(dbar)
CTDOXY−OXYGEN(µmol/kg)
Frequency(%)
CTDOXY−OXYGEN(µmol/kg; P<950dbar))
Frequency(%)
CTDOXY−OXYGEN(µmol/kg; P≥950dbar)

Figure C.1.11. Difference between the CTD oxygen (*S/N 0356*) and bottle dissolved oxygen on RF21-07. Red dots in upper two panels indicate the result of calibration. Lower two panels show histograms of the differences between calibrated oxygen concentration and bottle oxygen concentration.

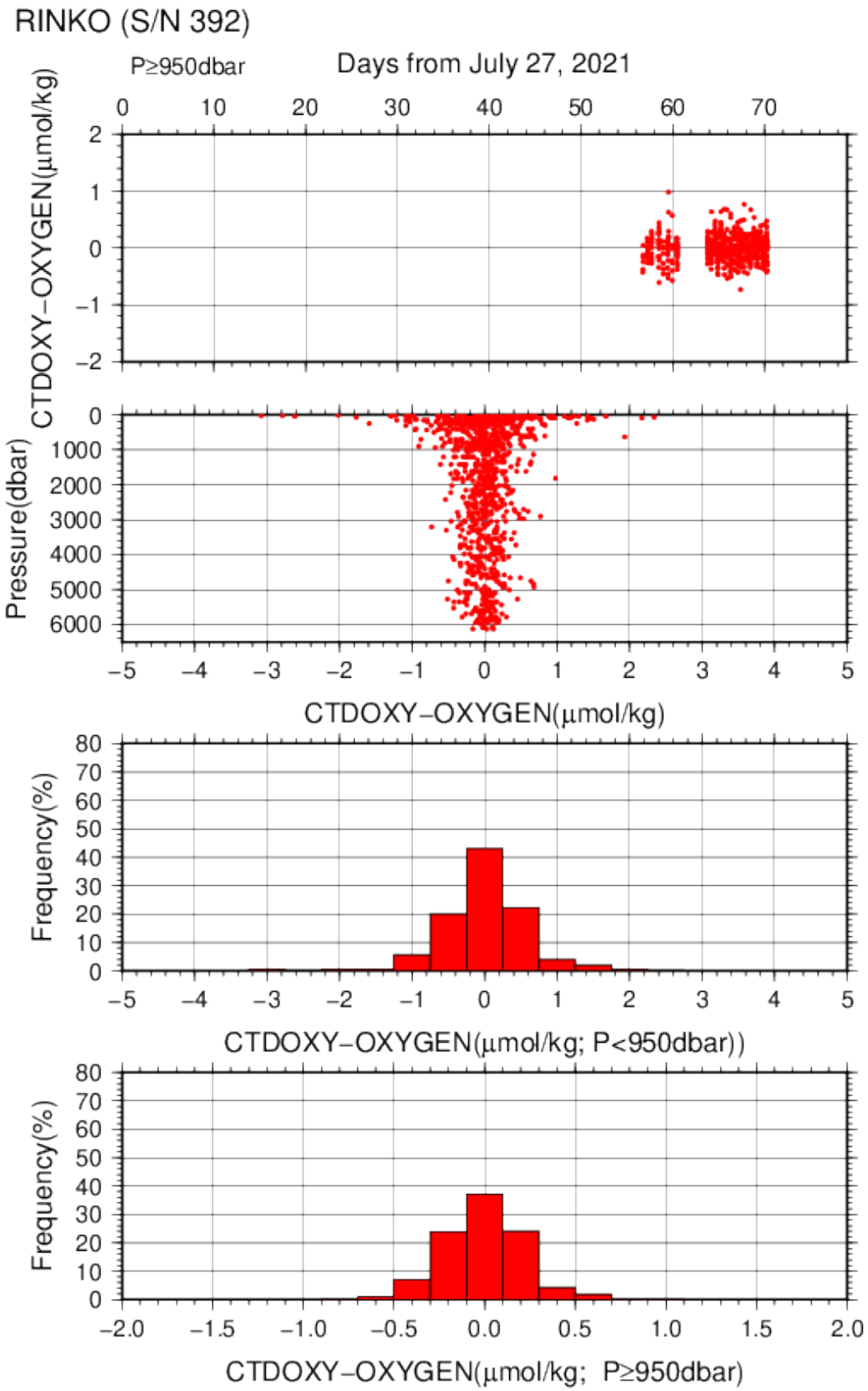
RINKO (S/N 392)
P≥950dbar
Days from July 27, 2021
CTDOXY−OXYGEN(µmol/kg)
Pressure(dbar)
CTDOXY−OXYGEN(µmol/kg)
Frequency(%)
CTDOXY−OXYGEN(µmol/kg; P<950dbar))
Frequency(%)
CTDOXY−OXYGEN(µmol/kg; P≥950dbar)

Figure C.1.12. Difference between the CTD oxygen (*S/N 0392*) and bottle dissolved oxygen on RF21-08. Red dots in upper two panels indicate the result of calibration. Lower two panels show histograms of the differences between calibrated oxygen concentration and bottle oxygen concentration.

(4.5) Results of detection of sea floor by the altimeter (VA500)

The altimeter detected the sea floor at 80 of 89 stations and that of final detection of sea floor was 14.6 m. The summary of detection of VA500 was shown in Figure C.1. 13.

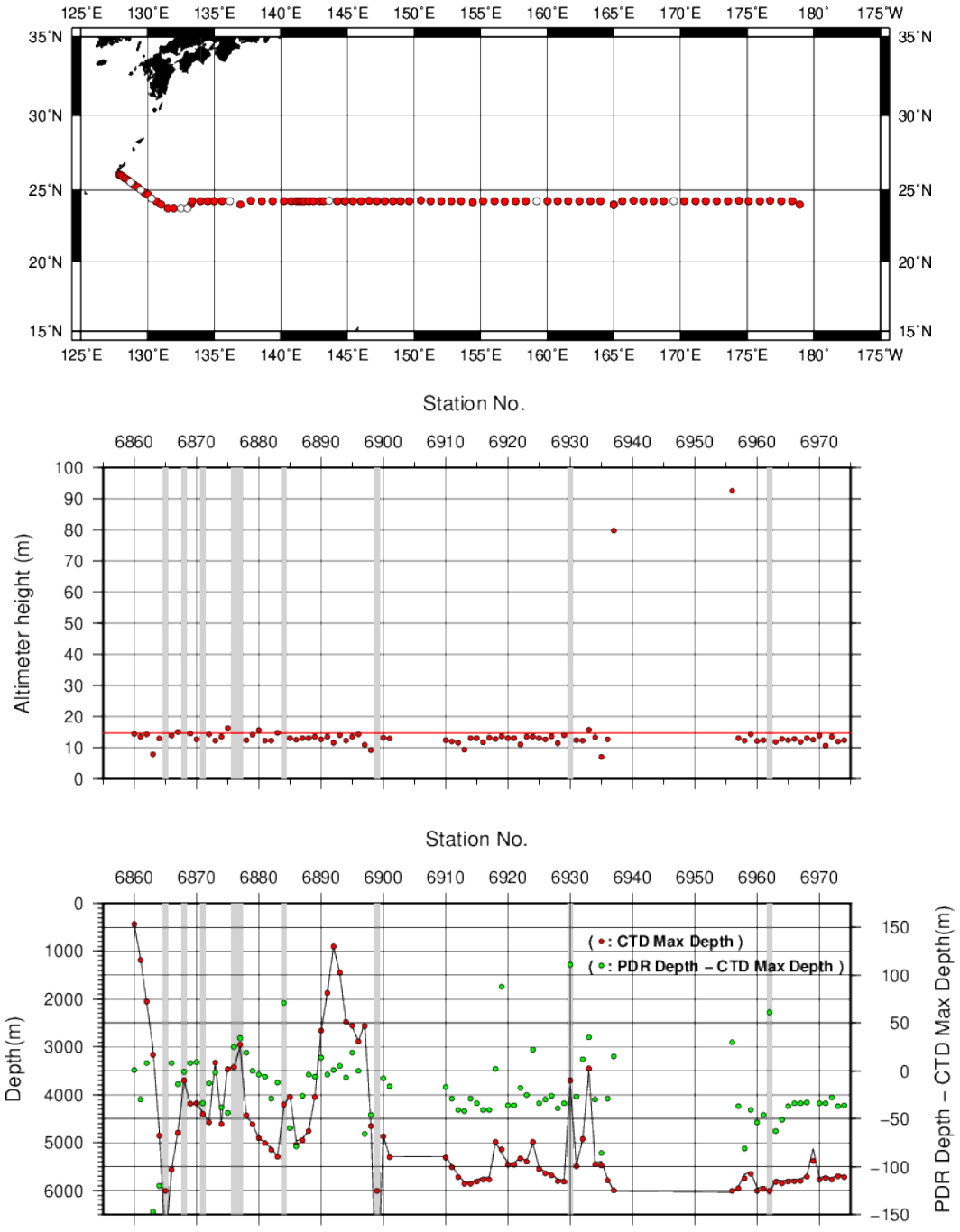

Figure C.1.13. The upper panel shows the stations of the detection along the P3 section. The middle panel shows altimeter height of VA500 in the stations. The lower panel shows maximum depth of CTD

observation (left Y-axis) and difference between bathymetry (PDR depth) and the CTD depth (right Y-axis) in the stations. Open circles (the upper panel) and gray shade (the other two panels) indicate stations where the sea floor cannot detected.

(5) Post-cruise calibration

After the cruise, post-cruise calibration of sensors was performed by the manufacturer, as shown below. We confirmed that the calibration of these sensors did not change significantly during the cruise.

(5.1) Temperature (ITS-90): SBE 3plus

S/N 03P4436 (primary), 21 Dec. 2021

$g = 4.33657874 \times 10^{-3}$ $\quad j = 1.78510112 \times 10^{-6}$

$h = 6.37856931 \times 10^{-4}$ $\quad f_0 = 1000.0$

$i = 2.10338369 \times 10^{-5}$

S/N 03P5632 (secondary), 21 Dec. 2021

$g = 4.34073662 \times 10^{-3}$ $\quad j = 1.38437092 \times 10^{-6}$

$h = 6.28102586 \times 10^{-4}$ $\quad f_0 = 1000.0$

i = $1.94331032 \times 10^{-5}$

(5.2) Deep Ocean Standards Thermometer Temperature (ITS-90): SBE 35

S/N 0093, 27 Oct. 2020

a_0 = $4.12756963 \times 10^{-3}$ a_3 = $-9.36245277 \times 10^{-6}$

a_1 = $-1.08163464 \times 10^{-3}$ a_4 = $2.00979198 \times 10^{-7}$

a_2 = $1.67453817 \times 10^{-4}$

Formula:

$$Linearized\ temperature(ITS-90) = 1/\left\{a_0 + a_1 \times \ln(n) + a_2 \times \ln^2(n) + a_3 \times \ln^3(n) + a_4 \times \ln^4(n)\right\} - 273.15$$

n: instrument output

The slow time drift of the SBE 35

S/N 0093, 18 Nov. 2021 (2nd step: fixed point calibration)

Slope = 1.000003, Offset = -0.000148

Formula:

$$Temperature(ITS-90) = slope \times (Linearized\ temperature) + offset$$

(5.3) Conductivity: SBE 4C

S/N 042987 (primary), 13 Jan. 2022

g	=	–9.91933438	j	=	$4.88610842 \times 10^{-5}$
h	=	1.36181919	CP_{cor}	=	-9.5700×10^{-8}
i	=	$5.85689368 \times 10^{-4}$	CT_{cor}	=	3.2500×10^{-6}

S/N 043682 (secondary), 07 Dec. 2021

g	=	–9.97135316	j	=	$3.91068913 \times 10^{-5}$
h	=	1.41854121	CP_{cor}	=	-9.5700×10^{-8}
i	=	$8.23390530 \times 10^{-4}$	CT_{cor}	=	3.2500×10^{-6}

References

Akaike, H. (1974): A new look at the statistical model identification. *IEEE Transactions on Automatic Control, **19**:716–722.*

Garcìa, H. E., and L. I. Gordon (1992): Oxygen solubility in seawater: Better fitting equations. *Limnol. Oceanogr., **37**, 1307–1312*.

McTaggart, K. E., G. C. Johnson, M. C. Johnson, F. M. Delahoyde, and J. H. Swift (2010): The GO-SHIP Repeat Hydrography Manual: A Collection of Expert Reports and guidelines. IOCCP Report No *14*, ICPO Publication Series No. 134, version 1, 2010.

Sea-Bird Electronics (2009): SBE 43 dissolved oxygen (DO) sensor – hysteresis corrections, *Application note no. 64-3, 7 pp.*

Shanno, David F. (1970): Conditioning of quasi-Newton methods for function minimization. *Math. Comput.* ***24****, 647–656. MR 42 #8905.*

Uchida, H., G. C. Johnson, McTaggart, K. E. (2010): CTD oxygen sensor calibration procedures. In: The GO-SHIP repeat hydrography manual: A Collection of Expert Reports and guidelines. IOCCP Report No ***14***, ICPO Publication Series No. 134, version 1, 2010.

Uchida, H., K. Ohyama, S. Ozawa, and M. Fukasawa (2007): In-situ calibration of the Sea-Bird 9plus CTD thermometer. *J. Atmos. Oceanic Technol.,* ***24****, 1961–1967.*

Uchida, H., T. Kawano, I. Kaneko, and M. Fukasawa (2008): In-situ calibration of optode-based oxygen sensors. *J. Atmos. Oceanic Technol.,* ***25****, 2271–2281.*

2. Bottle Salinity

25 November 2021

(1) Personnel

WADA Kouichi （JMA）

ETO Tetsuhiro （JMA）

IDA Togo （JMA）

TSUZUKI Takato （JMA、RF2106）

OE Mitsuho （JMA、RF2106）

CHIBA Yasuomi （JMA、RF2107, RF2108）

HATANAKA Kenichiro （JMA、RF2107, RF2108）

(2) Salinity measurement

Salinometer: AUTOSAL 8400B (Guildline Instruments Ltd., Canada ; S/N 72103, 73556)

Thermometer: 1502A Tweener thermometer readout (to monitor ambient temperature and bath temperature) (Fluke calibration, USA)

IAPSO Standard Seawater: P164 (K15=0.99985)

(3) Sampling and measurement

The measurement system was almost the same as the system described by Kawano (2010).

Algorithm for practical salinity scale, 1978 (PSS-78; UNESCO, 1981) was employed to

convert the conductivity ratios to salinities.

(4) Station occupied

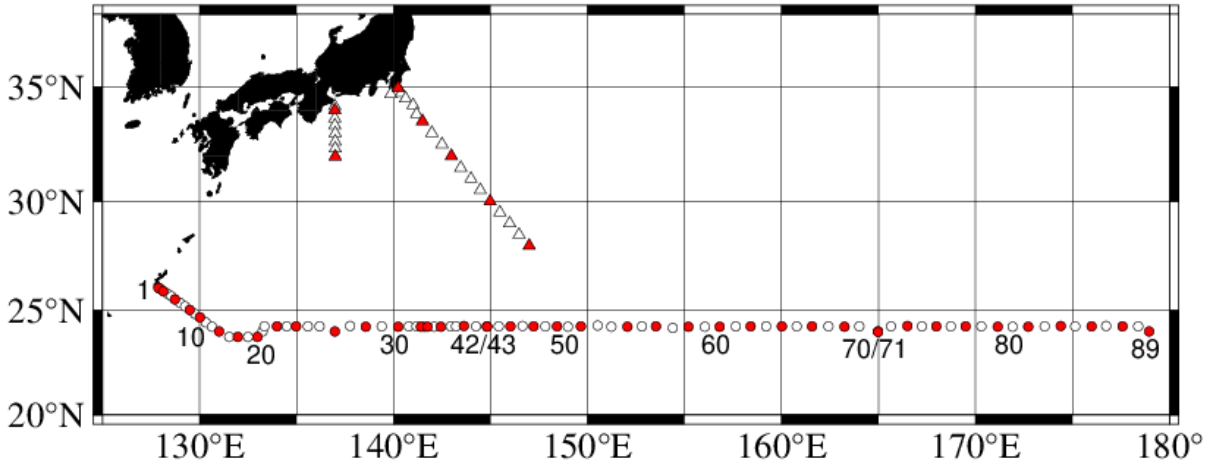

Figure C.2.1. Location of observation stations of bottle salinity. Closed and open circles indicate sampling and no-sampling station, respectively. Triangle shows a sampling station which is not reported in the bottle data file but is included in data processing. These data are available from the JMA web site (https://www.data.jma.go.jp/gmd/kaiyou/db/vessel_obs/datareport/html/ship/ship_e.php?year=2021&season=summer).

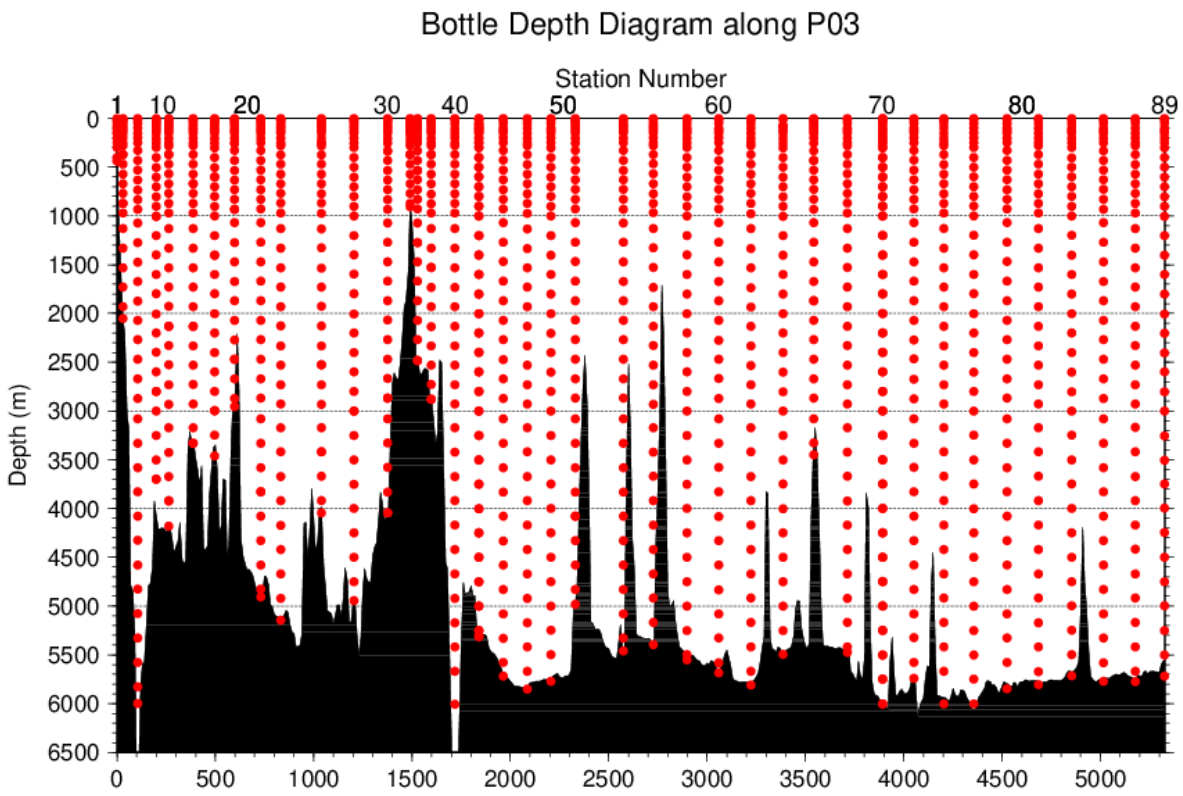

Figure C.2.2. Distance-depth distribution of sampling layers of bottle salinity.

(5) Result

(5.1) Ambient temperature, bath temperature and Standard Seawater measurements

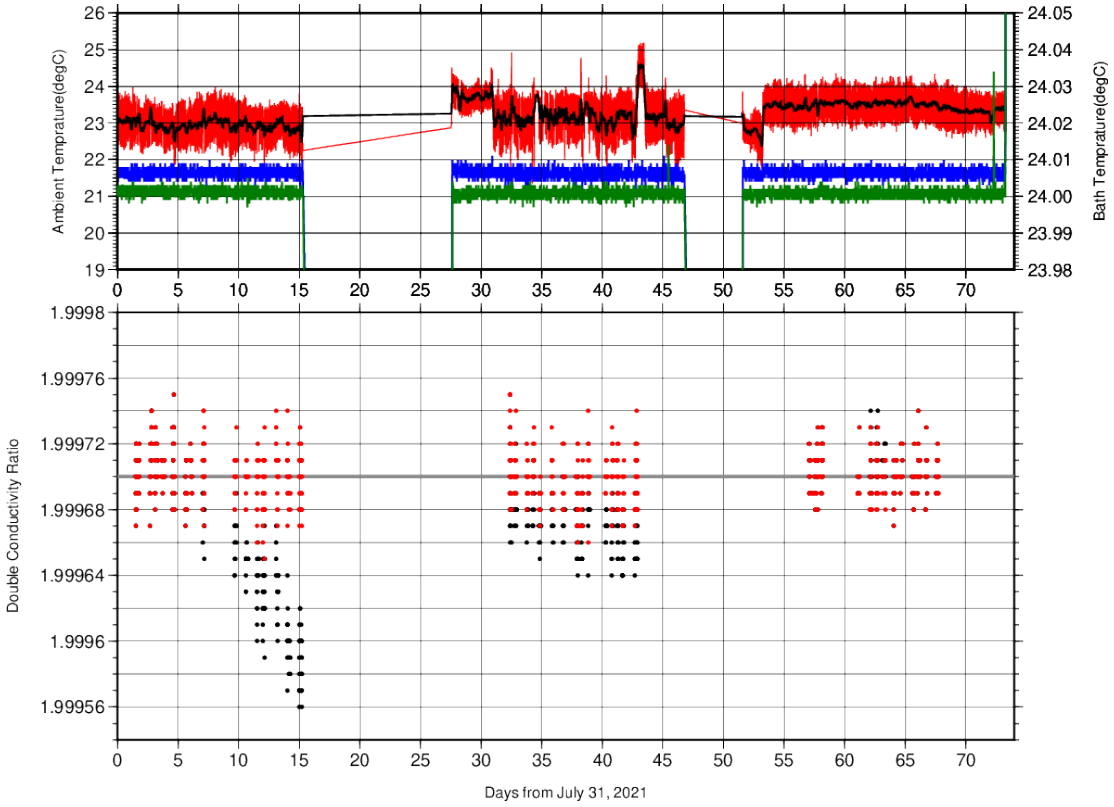

Figure C.2.3. The upper panel, red line, black line, green line, and blue line indicate time-series of ambient temperature, average ambient temperature, and bath temperature (green: Autosal S/N 72103, blue: S/N 73556) during cruise. The lower panel, black dots, and red dots indicate raw and corrected time-series of the double conductivity ratio of the standard seawater (P164).

(5.2) Replicate and duplicate samples

We took replicate (pair of water samples taken from a single Niskin bottle) and duplicate (pair of water samples taken from different Niskin bottles closed at the same depth) samples for bottle salinity throughout the cruise. Table C.2.1 summarizes the results of the analyses. Figure C.2.4 shows details of the results. The calculation of the standard deviation from the difference of sets was based on a procedure (SOP 23) in

DOE (1994).

Table C.2.1. Summary of replicate and duplicate salinity analyses.

Measurement	Average difference ± S.D.
Replicate sample	0.0002 ± 0.0002 (N = 170)
Duplicate sample	0.0005 ± 0.0006 (N = 32)

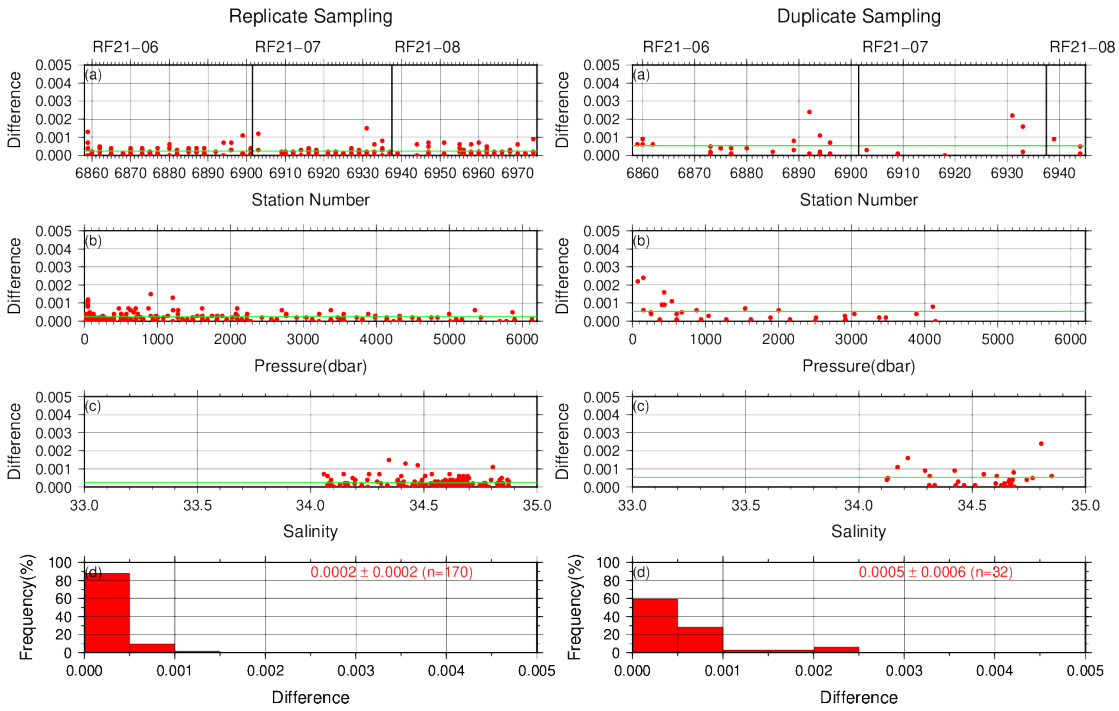

Figure C.2.4. Results of (left) replicate and (right) duplicate analyses during the cruise against (a)

station number, (b) pressure, (c) salinity, and (d) histogram of the measurements. Green line indicates the mean of the differences of salinity of replicate/duplicate analyses. These data are available from the JMA web site(https://www.data.jma.go.jp/gmd/kaiyou/db/vessel_obs/data-report/html/ship/ship_e.php?year=2021&season=summer).

(5.3) Summary of assigned quality control flags

Table C.2.2. Summary of assigned quality control flags

Flag	Definition	Number
2	Good	1215
3	Questionable	0
4	Bad (Faulty)	95
5	Not reported	1
6	Replicate measurements	152
Total number of samples		1463

References

DOE (1994), Handbook of methods for the analysis of the various parameters of the carbon dioxide system in sea water; version 2. *A. G. Dickson and C. Goyet (eds), ORNL/CDIAC-74.*

Kawano (2010), The GO-SHIP Repeat Hydrography Manual: A Collection of Expert Reports and Guidelines. *IOCCP Report No. 14, ICPO Publication Series No. 134, Version 1.*

UNESCO (1981), Tenth report of the Joint Panel on Oceanographic Tables and Standards. *UNESCO Tech. Papers in Mar. Sci., **36**, 25 pp.*

3. Bottle Oxygen

12 May 2022

(6) Personnel

SHINODA Yoshihiro

HASHIMOTO Susumu

SASAKI Takuya

OKAJIMA Shingo (RF21-06)

FUJII Takuya (RF21-06, RF21-08)

IMAI Yoichi (RF21-07)

KAKUYA Keita (RF21-07, RF21-08)

(7) Station occupied

A total of 81 stations (RF 21-06 Leg 2: 34, RF 21-07: 28, RF 21-08: 19) were occupied for dissolved oxygen measurements. Station location and sampling layers of bottle oxygen are shown in Figures C.3.1 and C.3.2, respectively.

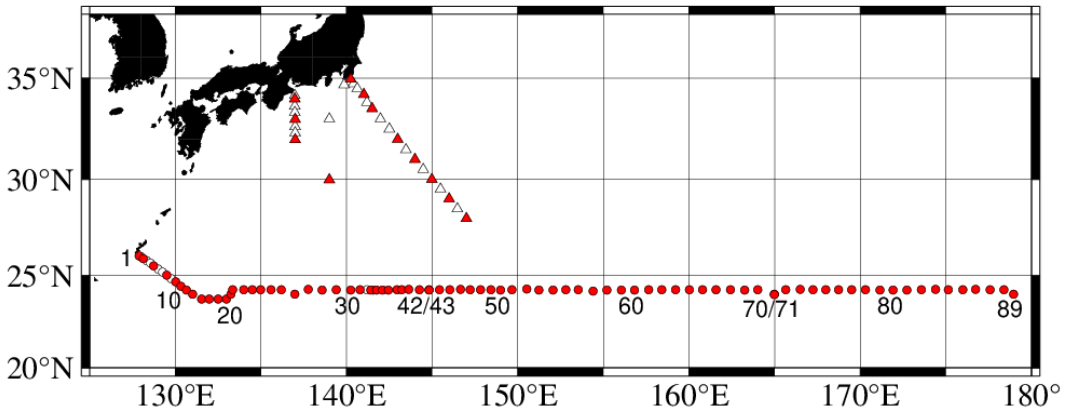

Figure C.3.1. Location of observation stations of bottle oxygen. Closed and open circles indicate sampling and no-sampling stations, respectively. Closed triangle

show sampling station which is not reported in the bottle data file but is used for quality control of dissolved oxygen. Open triangle shows no-sampling station which is not reported in the censor data. These data are available from the JMA (https://www.data.jma.go.jp/gmd/kaiyou/db/vessel_obs/data-report/html/ship/ship_e.php?year=2021&season=summer).

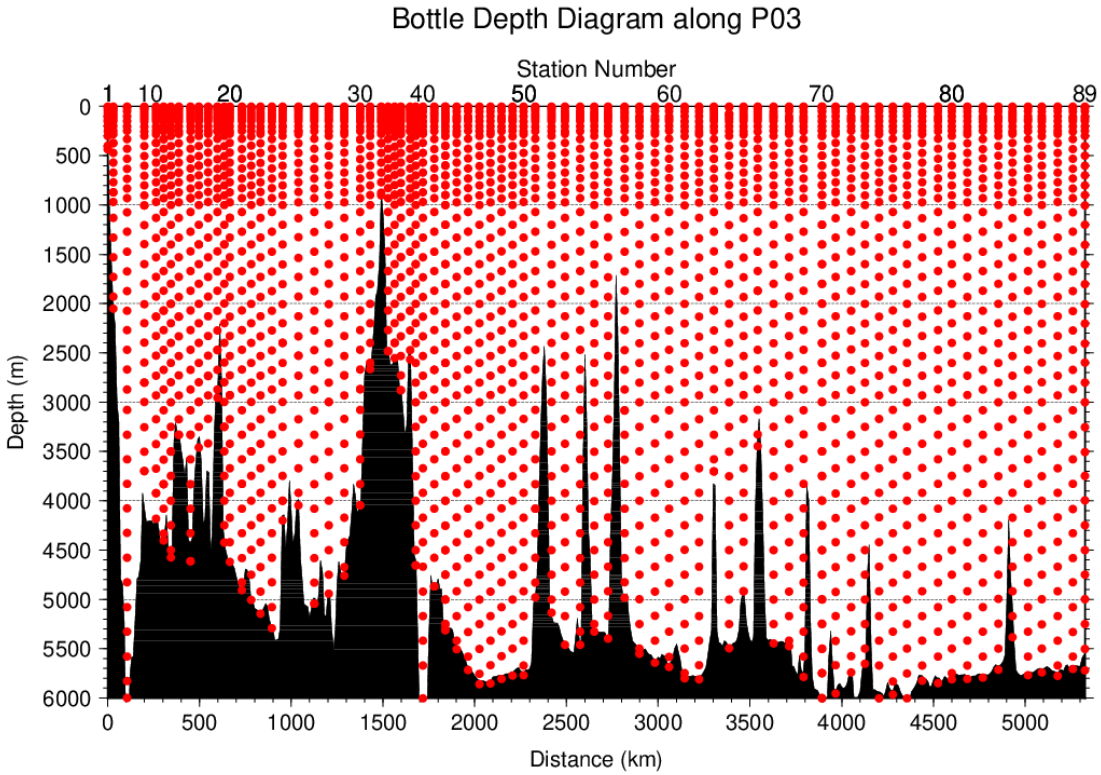

Figure C.3.2. Distance-depth distribution of sampling layers of bottle oxygen.

(8) Instrument

Detector: DOT-15X (KIMOTO ELECTRIC CO., LTD., Japan)

Burette: APB-610 (KYOTO ELECTRONICS MANUFACTURING CO., LTD., Japan)

(9) Sampling and measurement

Methods of seawater sampling, measurement, and calculation of dissolved oxygen concentration were based on an IOCCP Report (Langdon, 2010). Details of the methods are shown in Appendix A1.

The reagents for the measurement were prepared according to recipes described in Appendix A2. Standard KIO_3 solutions were prepared gravimetrically using the highest purity standard substance KIO_3 (Lot. No. KCN5512, FUJIFILM Wako Pure Chemical Corporation, Japan). Table C.3.1 shows the batch list of prepared standard KIO_3 solutions.

Table C.3.1. Batch list of the standard KIO_3 solutions.

KIO_3 batch	Cruise	Concentration and uncertainty (k=2) at 20 °C. Unit is mol L^{-1}.	Purpose of use
20201012-1	RF2106, RF2107, RF2108	0.0016670±0.0000007	Standardization (main use)
20201012-2	RF2106, RF2107	0.0016668±0.0000007	Mutual comparison
20210319-1	RF2108	0.0016664±0.0000007	Mutual comparison

(10) Standardization

The concentration of the $Na_2S_2O_3$ titrant was determined with the standard KIO_3 solution "20201012-1", based on the methods of an IOCCP Report (Langdon, 2010). Figure C.3.3 shows the results of standardization during the cruise. The standard deviation of the concentration at 20 ° C was determined through standardization and was used in the calculation of uncertainty.

(a)

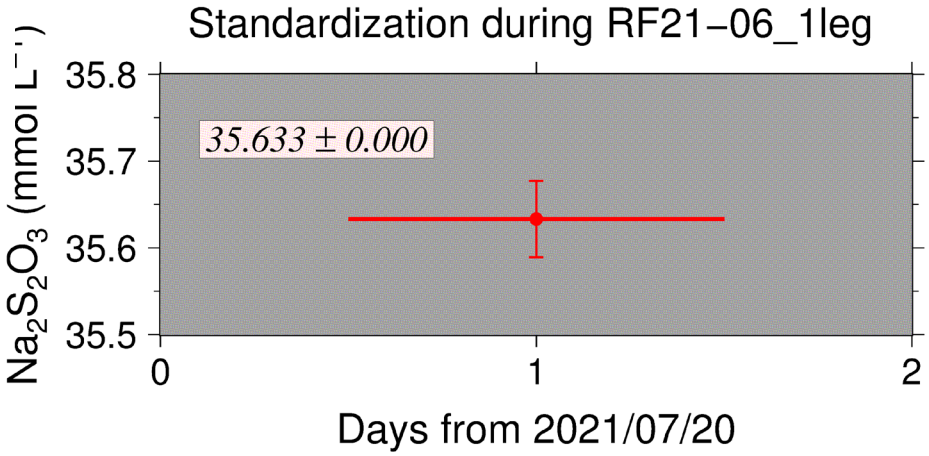

(b)

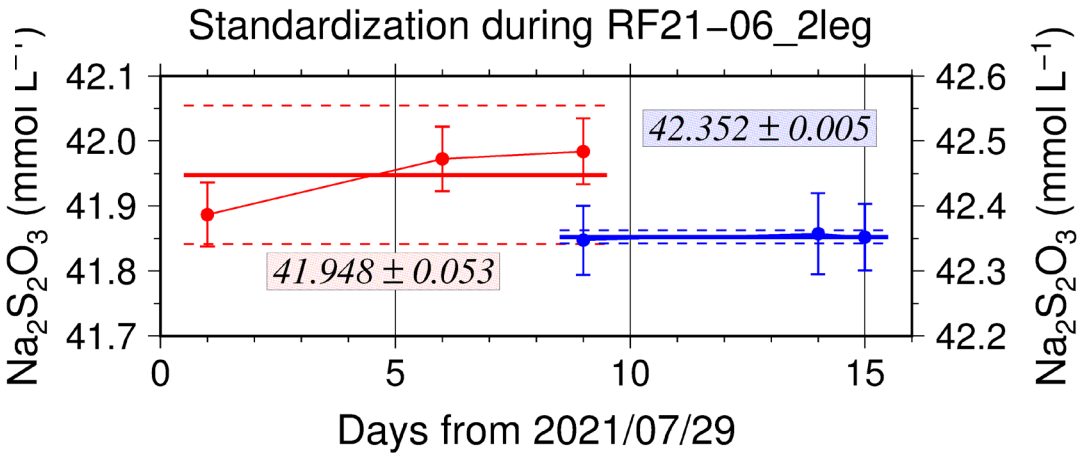

(c)

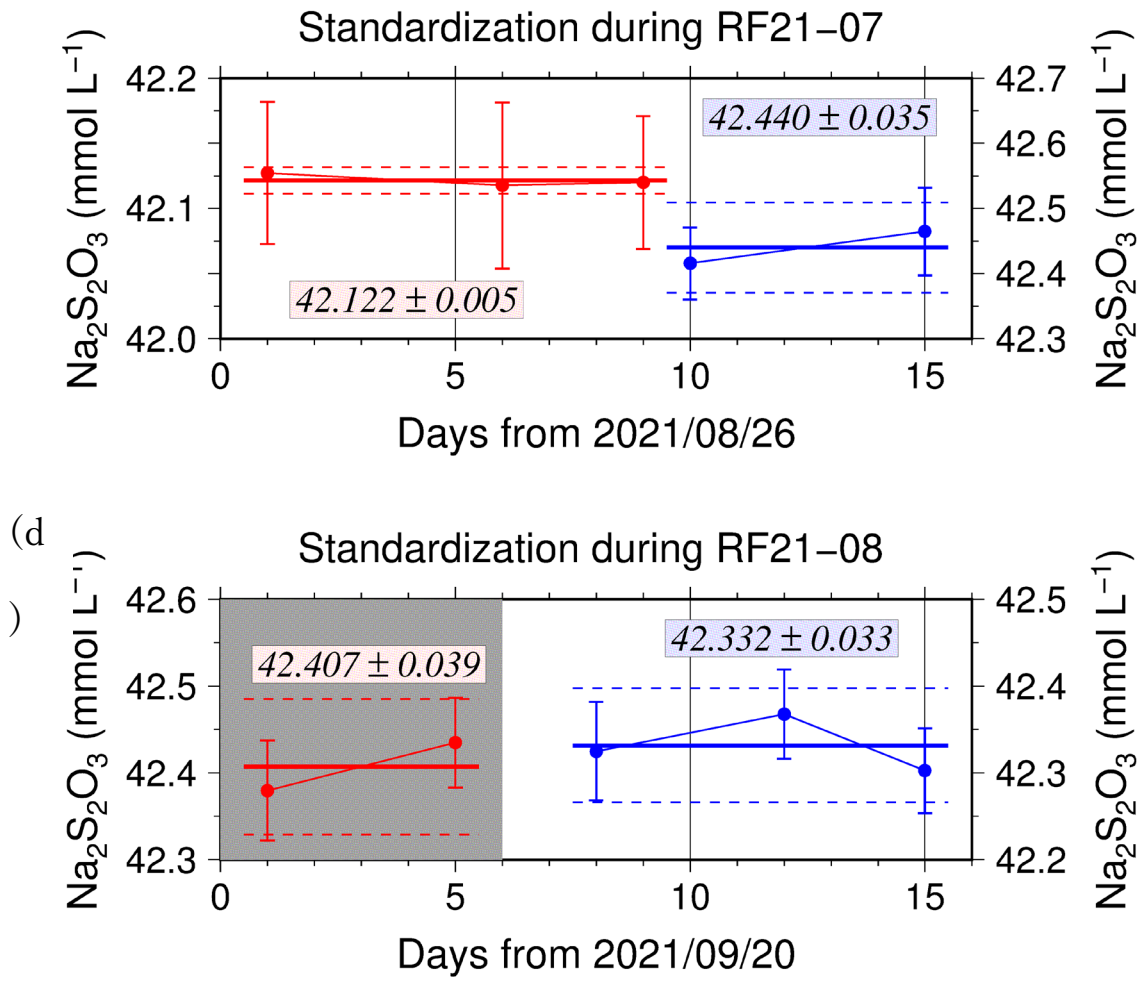

Figure C.3.3. Calculated concentration of $Na_2S_2O_3$ solution at 20 °C in standardization during (a) RF21-06 1leg and (b) RF21-06 2leg, (c) RF21-07, (d) RF21-08. Different colors of plots indicate different batches of $Na_2S_2O_3$ solution; red (blue) plots correspond to the left (right) y-axis. Error bars of plots show uncertainty of concentration of $Na_2S_2O_3$. Thick and dashed lines denote the mean and the mean ± twice the standard deviations for the batch measurements, respectively. The shaded regions indicate that the data in the regions are not used for calculations of measured data in P03 line.

(11) Blank

(6.1) Reagent blank

The blank in an oxygen measurement (reagent blank in distilled water; $V_{reg\text{-}blk}$) was determined by the methods described in the IOCCP Report (Langdon, 2010) using pure water. The blank reflects not only the interfering substances (oxidants or reductants) in the reagents but also the differences between the measured end-point and the equivalence point due to unknown causes in the titrator. Figure C.3.4 shows details of the results.

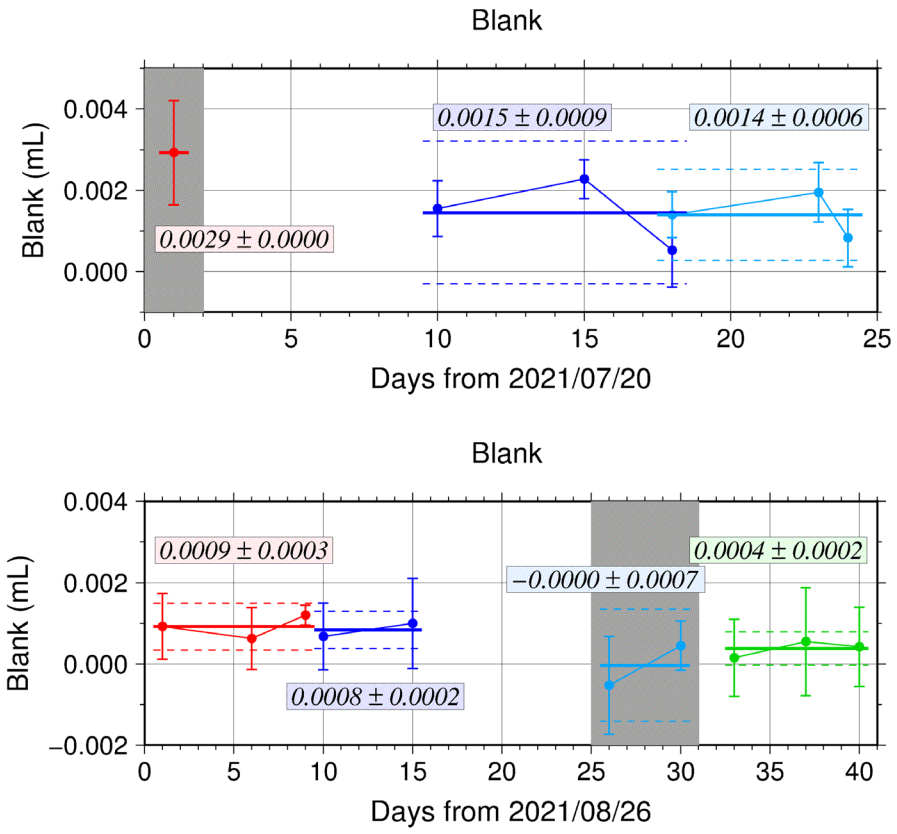

Figure C.3.4. Reagent blank ($V_{reg\text{-}blk}$) determination during RF21-06 (top), RF21-07 and RF21-08 (bottom). Error bars of plots show standard deviations of the measurements. Thick and dashed lines denote the mean and the mean ± twice the standard deviation for the batch measurement, respectively. The shaded regions

indicate that the data in the regions are not used for calculations of measured data in P03 line.

(6.2) Seawater blank

We also determined seawater blank ($V_{sw\text{-}blk}$) which reflects interfering substances in seawater. Although this blank is not included in determination of oxygen concentration, measurement of the blank would be necessary to improve traceability and comparability in dissolved oxygen concentration. Details are described in Appendix A3.

(12) Quality Control

(7.1) Replicate and duplicate analyses

We took replicate (pair of water samples taken from a single Niskin bottle) and duplicate (pair of water samples taken from different Niskin bottles closed at the same depth) samples of dissolved oxygen throughout the cruise. Table C.3.2 summarizes the results of the analyses. Figure C.3.5 shows details of the results. The calculation of the standard deviation from the difference of sets was based on a procedure (SOP 23) in DOE (1994).

Table C.3.2. Summary of replicate and duplicate measurements.

Measurement	Ave. ± S.D. (μmol kg^{-1})
Replicate	0.20±0.18 (N=338)
Duplicate	0.23±0.22 (N=96)

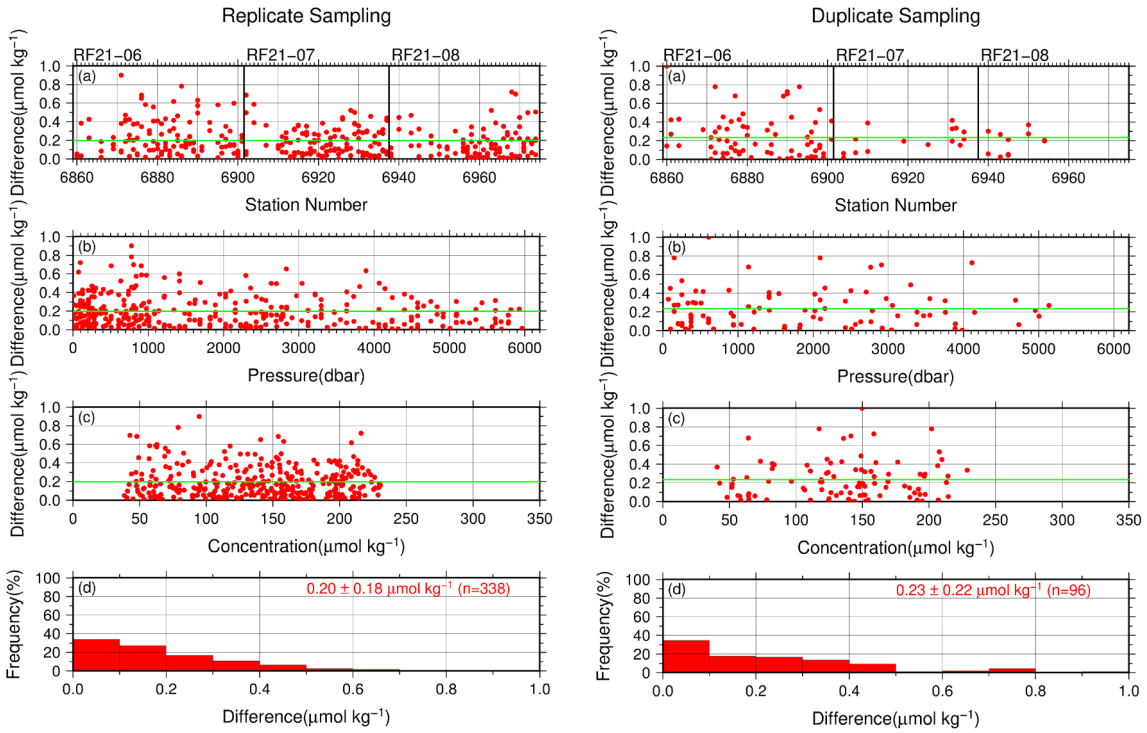

Figure C.3.5. Results of (left) replicate and (right) duplicate measurements during the cruise against (a) station number, (b) pressure, and (c) concentration of dissolved oxygen. Green lines denote the average of the measurements. Bottom panels (d) show histograms of the measurements.

(7.2) Comparisons between standard KIO_3 solutions

During the cruise, comparisons were made between different lots of standard KIO_3 solutions to confirm the accuracy of our oxygen measurements and the bias of a standard KIO_3 solution. A concentration of the standard KIO_3 solutions "20201012-2" and "20210319-1" was determined using $Na_2S_2O_3$ solution standardized with the KIO_3 solution "20201012-1", and the difference between the measured value and the theoretical one. Good agreement between two standards confirmed that there was no systematic shift in oxygen measurements during the cruise (Figure C.3.6).

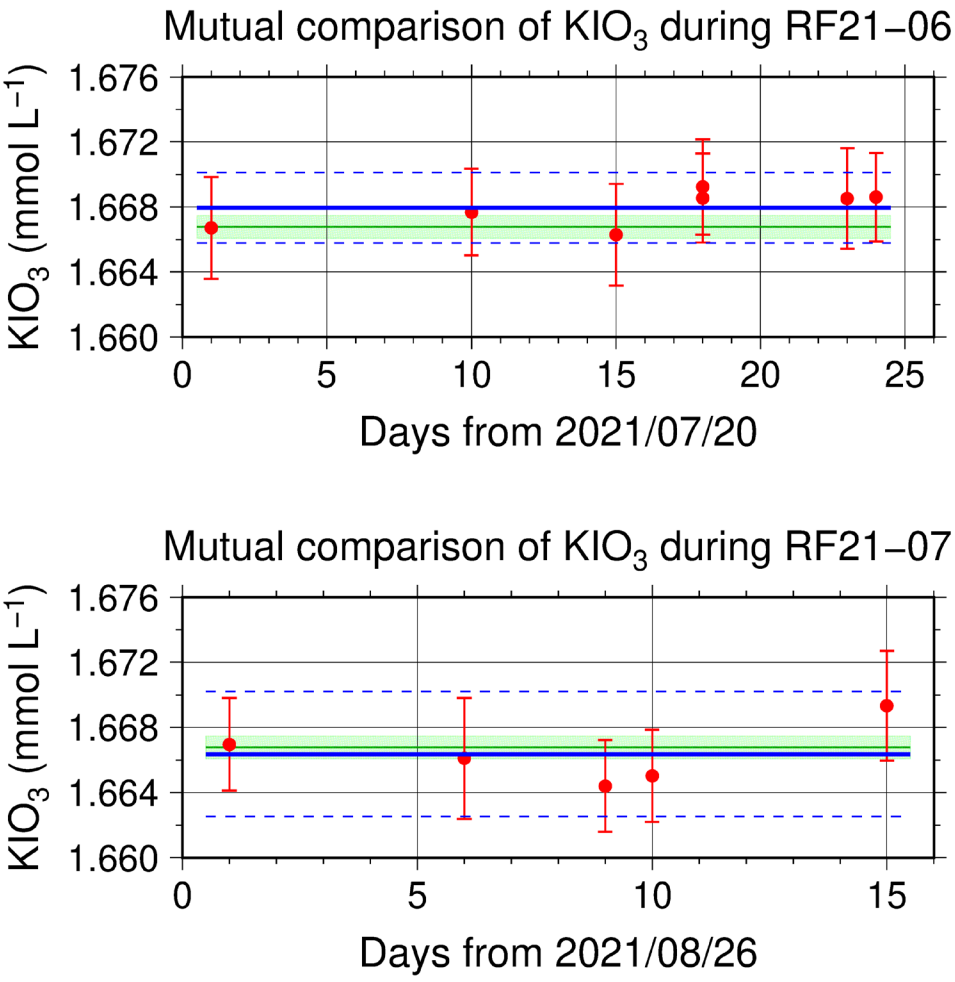

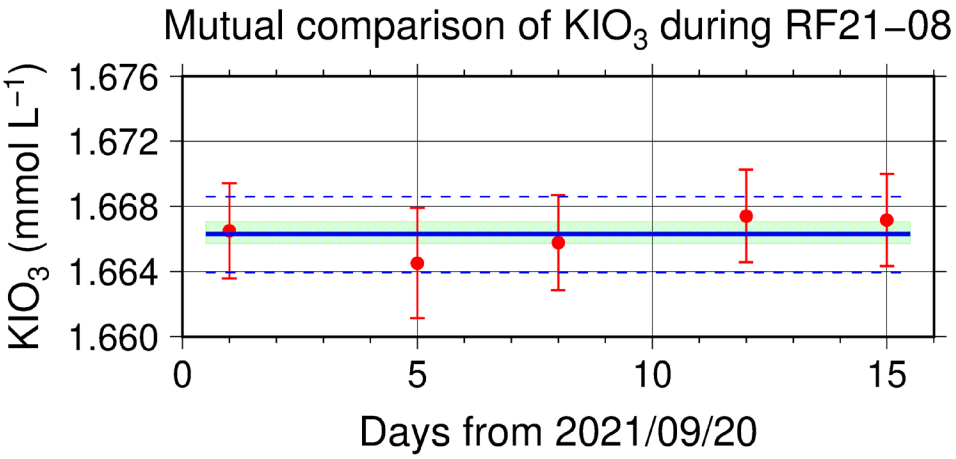

Figure C.3.6. Result of comparison of standard KIO_3 solutions during RF21-06 (top), RF21-07 (middle) and RF21-08 (bottom). Circles and error bars show mean of the measured value and its uncertainty (k=2), respectively. Thick and dashed lines in blue denote the mean and the mean ± twice the standard deviations, respectively, for the measurements throughout the cruise. Green thin line and light green thick line denote the nominal concentration and its uncertainty (k=2) of standard KIO_3 solutions "20201012-2" and "20210319-1", for RF21-06, RF21-07 and RF21-08, respectively.

(7.3) Quality control flag assignment

A quality flag value was assigned to oxygen measurements, as shown in Table C.3.3, using the code defined in IOCCP Report No.14 (Swift, 2010).

Table C.3.3. Summary of assigned quality control flags.

Flag	Definition	Number of samples
2	Good	2545
3	Questionable	9
4	Bad (Faulty)	12
5	Not reported	3
6	Replicate measurements	306
Total number of samples		2875

(13) Uncertainty

Oxygen measurement involves various uncertainties; determination of glass bottles volume, repeatability and systematic error of burette discharge, repeatability of pickling reagent discharges, determination of reagent blank, standardization of $Na_2S_2O_3$ solution, and uncertainty of KIO_3 concentration. After taking into consideration the above uncertainties that could be evaluated, the expanded uncertainty of bottle oxygen concentrations (T=20, S=34.5) was estimated, as shown in Table C.3.4. However, it is difficult to determine a strict uncertainty for oxygen concentration because there is no reference material for oxygen measurement.

Table C.3.4. Expanded uncertainty (k=2) of bottle oxygen during the cruise.

O_2 conc. (μmol kg^{-1})	Uncertainty (μmol kg^{-1})
20	0.28
30	0.30
50	0.32
70	0.35
100	0.41
150	0.53
200	0.66
250	0.79
300	0.94
400	1.22

Appendix

A1. Methods

(A1.1) Seawater sampling

Following procedure is based on a determination method in IOCCP Report (Langdon, 2010). Seawater samples were collected from 10-liters Niskin bottles attached the CTD-system and a stainless steel bucket for the surface. Seawater for bottle oxygen measurement was transferred from the Niskin bottle and a stainless steel bucket to a volumetrically calibrated dry glass bottles. At least three times the glass volume water was overflowed. Then, pickling reagent-I 1 mL and reagent-II 1mL were added immediately, and sample temperature was measured using a thermometer. After a stopper was inserted carefully into the glass, it was shaken vigorously to mix the content

and to disperse the precipitate finely. After the precipitate has settled at least halfway down the glass, the glass was shaken again. The sample glasses containing pickled samples were stored in a laboratory until they were titrated. To prevent air from entering the glass, deionized water (DW) was added to its neck after sampling.

(A1.2) Sample measurement

At least 15 minutes after the re-shaking, the samples were measured on board. Added 1 mL H_2SO_4 solution and a magnetic stirrer bar into the sample glass, samples were titrated with $Na_2S_2O_3$ solution whose molarity was determined with KIO_3 solution. During the titration, the absorbance of iodine in the solution was monitored using a detector. Also, temperature of $Na_2S_2O_3$ solution during the titration was recorded using a thermometer. Dissolved oxygen concentration (μmol kg^{-1}) was calculated from sample temperature at the fixation, CTD salinity, glass volume, and titrated volume of the $Na_2S_2O_3$ solution, and oxygen in the pickling reagents-I (1 mL) and II (1 mL) (7.6×10^{-8} mol; Murray *et al.*, 1968).

A2. Reagents recipes

Pickling reagent-I; Manganous chloride solution (3 mol L^{-1})

Dissolve 600 g of $MnCl_2 \cdot 4H_2O$ in DW, then dilute the solution with DW to a final volume of 1 L.

Pickling reagent-II; Sodium hydroxide (8 mol L^{-1}) / sodium iodide solution (4 mol L^{-1})

Dissolve 320 g of NaOH in about 500 mL of DW, allow to cool, then add 600 g NaI and dilute with DW to a final volume of 1 L.

H_2SO_4 solution; Sulfuric acid solution (5 mol L^{-1})

Slowly add 280 mL concentrated H_2SO_4 to roughly 500 mL of DW. After cooling the final volume should be 1 L.

$Na_2S_2O_3$ solution; Sodium thiosulfate solution (0.04 mol L^{-1})

Dissolve 50 g of $Na_2S_2O_3 \cdot 5H_2O$ and 0.4 g of Na_2CO_3 in DW, then dilute the solution with DW to a final volume of 5 L.

KIO_3 solution; Potassium iodate solution (0.001667 mol L^{-1})

Dry high purity KIO_3 for two hours in an oven at 130 ° C. After weight out accurately KIO_3, dissolve it in DW in a 5 L flask. Concentration of potassium iodate is determined by a gravimetric method.

A3. Seawater blank

Blank due to redox species other than oxygen in seawater ($V_{sw\text{-}blk}$) can be a potential source of measurement error. Total blank ($V_{tot\text{-}blk}$) in seawater measurement can be represented as follows;

$$V_{tot\text{-}blk,} = V_{reg\text{-}blk} + V_{sw\text{-}blk}. \qquad \text{(C3.A1)}$$

Because the reagent blank ($V_{reg\text{-}blk}$) determined for pure water is expected to be equal to that in seawater, the difference between blanks for seawater ($V_{tot\text{-}blk}$) and for pure water gives the $V_{sw\text{-}blk}$.

Here, $V_{sw\text{-}blk}$ was determined by following procedure. Seawater was collected in the calibrated volumetric glass without the pickling solution. Then 1 mL of the standard KIO_3 solution, H_2SO_4 solution, and reagent solution-II and I each were added in sequence into the glass. After that, the sample was titrated to the end-point by $Na_2S_2O_3$ solution. Similarly, a glass contained 100 mL of DW added with 1 mL of the standard KIO_3 solution, H_2SO_4 solution, pickling reagent solution-II and I were titrated with $Na_2S_2O_3$ solution. The difference of the titrant volume of the seawater and DW glasses gave $V_{sw\text{-}blk}$.

The seawater blank has been reported from 0.4 to 0.8 μmol kg^{-1} in the previous study (Culberson *et al.*, 1991). Additionally, these errors are expected to be the same to all investigators and not to affect the comparison of results from different investigators (Culberson, 1994). However, the magnitude and variability of the seawater blank have not yet been documented. Understanding of the magnitude and variability is important to improve traceability and comparability in oxygen concentration. The determined seawater blanks are shown in Table C.3.A1.

Table C.3.A1. Results of seawater blank determinations.

Station: RF6890 24°-15′ N/140°-48′ E		Station: RF6937 24°-01′ N/164°-59′ E		Station: RF6974 24°-00′ N/178°-57′ E	
Depth (m)	Blank (μmol kg^{-1})	Depth (m)	Blank (μmol kg^{-1})	Depth (m)	Blank (μmol kg^{-1})
50	0.88	48	0.48	48	0.59
252	0.86	201	0.65	126	0.49
400	0.77	201	0.70	249	0.71
502	0.83	400	0.70	249	0.74
701	0.79	799	0.69	402	0.73
1000	0.82	1401	0.70	900	0.72
1401	0.79	2200	0.75	1202	0.70
2399	0.86	2998	0.73	2405	0.77
2664	0.80	3997	0.68	3002	0.74
2664	0.84	4998	0.81	3995	0.77
		6001	0.70	3995	0.70
		6001	0.60	5502	0.75

Reference

Culberson, A.H. (1994), Dissolved oxygen, in WHPO Pub. 91-1 Rev. 1, November

1994, Woods Hole, Mass., USA.

Culberson, A.H., G. Knapp, M.C. Stalcup, R.T. Williams, and F. Zemlyak (1991), A comparison of methods for the determination of dissolved oxygen in seawater, WHPO Pub. 91-2, August 1991, Woods Hole, Mass., USA.

Langdon, C. (2010), Determination of dissolved oxygen in seawater by Winkler titration using the amperometric technique, *IOCCP Report No.14, ICPO Pub. 134, 2010 ver.1*

Murray, C. N., J. P. Riley and T. R. S. Wilson (1968), The solubility of oxygen in Winkler reagents used for the determination of dissolved oxygen. *Deep-Sea Res.* 15, 237–238.

Swift, J. H. (2010), Reference-quality water sample data: Notes on acquisition, record keeping, and evaluation. *IOCCP Report No.14, ICPO Pub. 134, 2010 ver.1.*

4. Nutrients

31 March 2022

(1) Personnel

SHINODA Yoshihiro

HASHIMOTO Susumu

SASAKI Takuya

OKAJIMA Shingo (RF21-06)

FUJII Takuya (RF21-06, RF21-08)

IMAI Yoichi (RF21-07)

KAKUYA Keita (RF21-07, RF21-08)

(14) Station occupied

A total of 81 stations (RF 21-06 Leg 2: 34, RF 21-07: 28, RF 21-08: 19) were occupied for nutrients measurements. Station location and sampling layers of nutrients are shown in Figures C.4.1 and C.4.2.

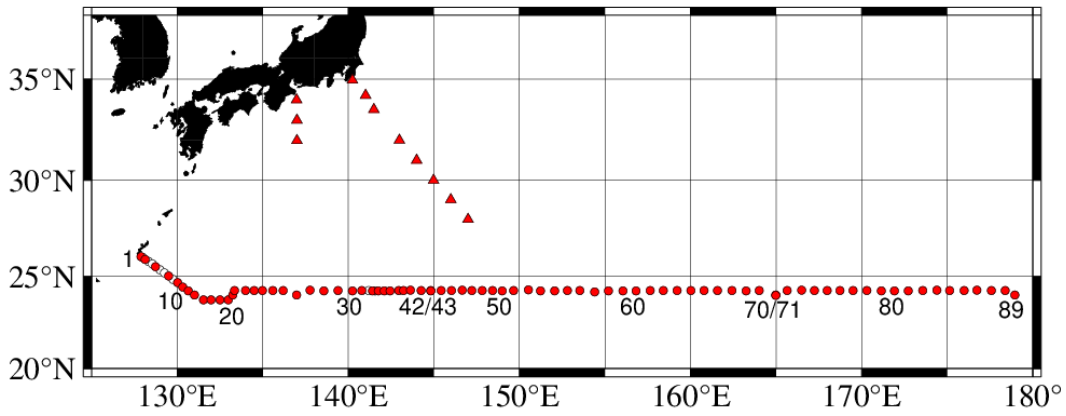

Figure C.4.1. Location of observation stations of nutrients. Closed and open circles indicate sampling and no-sampling stations, respectively. Triangle shows a sampling station which is not reported in the bottle data file but is included in data processing. These data are available from the JMA (https://www.data.jma.go.jp/gmd/kaiyou/db/vessel_obs/data-report/html/ship/ship_e.php?year=2021&season=summer).

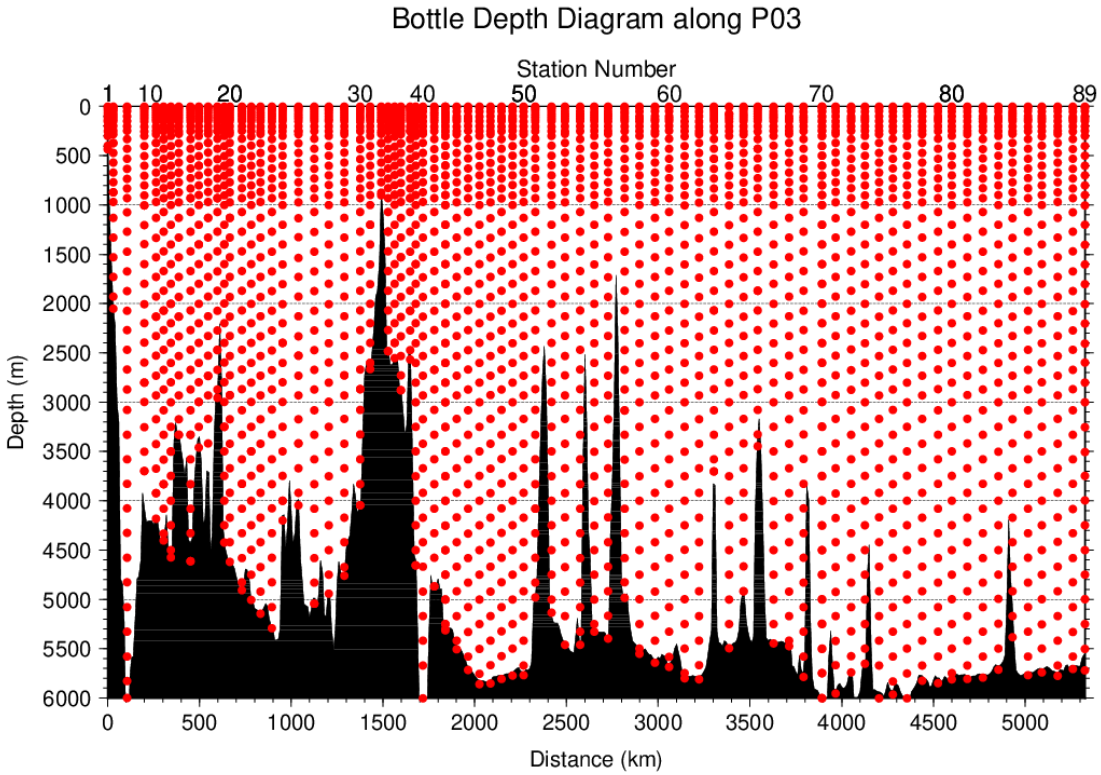

Figure C.4.2. Distance-depth distributions of sampling layers of nutrients.

(15) Instrument

The nutrients analyses were carried out on a four-channel Auto Analyzer III (BL TEC K.K., Japan) for four nutrients nitrate+nitrite, nitrite, phosphate, and silicate.

(16) Sampling and measurement

Methods of seawater sampling, measurement, and data processing of nutrient concentration were described in Appendixes A1, A2, and A3, respectively. The reagents for the measurement were prepared according to recipes shown in Appendix A4.

(17) Nutrients standards

(5.1) Volumetric laboratory ware of in-house standards

All volumetric wares were gravimetrically calibrated. The weights obtained in the calibration weighing were corrected for the density of water and for air buoyancy. Polymethylpenten volumetric flasks were gravimetrically calibrated at the temperature of use within 4–6 °C. All pipettes have nominal calibration tolerances of 0.1 % or better. These were gravimetrically calibrated in order to verify and improve upon this nominal tolerance.

(5.2) Reagents of standard

The batches of the reagents used for standards are listed in Table C.4.1.

Table C.4.1. List of reagents for the standards used in the cruise.

	Name	CAS No	Lot. No	Industries
Nitrate	Potassium nitrate 99.995 suprapur®	7757-79-1	B1706365	Merck KGaA
Nitrite	Sodium nitrite GR for analysis ACS, Reag. Ph Eur	7632-00-0	A1611049	Merck KGaA
Phosphate	Potassium dihydrogen	7778-77-	B1781408	Merck

	phosphate anhydrous 99.995 suprapur®	0		KGaA
Silicate	Silicon standard solution 1000 mg/l Si*	-	HC01345036	Merck KGaA

* Traceable to NIST-SRM3150

(5.3) Low nutrient seawater (LNSW)

Surface water with sufficiently low nutrient concentration was taken and filtered using 10 μm pore size membrane filter in our previous cruise. This water was stored in 15 liter flexible container with paper box.

(5.4) In-house standard solutions

Nutrient concentrations for A, B and C standards were set as shown in Table C.4.2. A and B standards were prepared with deionized water (DW). C standard (full scale of working standard) was mixture of B-1 and B-2 standards, and was prepared with LNSW. C-1 standard, whose concentrations of nutrient were nearly zero, was prepared as LNSW slightly added with DW to be equal with mixing ratio of LNSW and DW in C standard. The C-2 to -5 standards were prepared with mixture of C-1 and C standards in stages as 1/4, 2/4, 3/4, and 4/4 (i.e., pure "C standard") concentration for full scale, respectively. The actual concentration of nutrients in each standard was calculated based on the solution temperature and factors of volumetric laboratory wares calibrated prior to use. Nominal zero concentration of nutrient was determined in measurement of DW after refraction error correction. The calibration curves for each run were

obtained using 5 levels of C-1 to -5 standards. These standard solutions were periodically renewed as shown in Table C.4.3.

Table C.4.2. Nominal concentrations of nutrients for A, B, and C standards at 20 ° C.

Unit is μ mol L^{-1}.

	A	B	C
Nitrate	27484	550	44.0
Nitrite	12503	250	2.0
Phosphate	2122	42.4	3.39
Silicate	35606	2136	171

Table C.4.3. Schedule of renewal of in-house standards.

Standard	Renewal
A-1 std. (NO_3)	No renewal
A-2 std. (NO_2)	No renewal
A-3 std. (PO_4)	No renewal
A-4 std. (Si)	Commercial prepared solution
B-1 std. (mixture of A-1, A-3, and A-4 stds.)	Maximum 8 days
B-2 std. (diluted A-2 std.)	Maximum 15 days
C-std. (mixture of B-1 and B-2 stds.)	Every measurement
C-1 to -5 stds.	Every measurement

(18) Certified reference material

Certified reference material for nutrients in seawater (hereafter CRM), which was prepared by the General Environmental Technos company (KANSO Technos, Japan), was used for every analysis at each hydrographic station. Use of CRMs for the analysis of seawater ensures stable comparability and uncertainty of data. CRMs used in the cruise are shown in Table C.4.4.

Table C.4.4. Certified concentration and uncertainty (k=2) of CRMs. Unit is μmol kg^{-1}.

	Nitrate	Nitrite	Phosphate	Silicate
CRM-CK	0.02±0.03*	0.011±0.008*	0.048±0.012	0.73±0.08*
CRM-CJ	16.2±0.2	0.031±0.007	1.19±0.02	38.5±0.4
CRM-CM	33.2±0.3	0.018±0.006*	2.38±0.03	100.5±0.5
CRM-CN	43.6±0.4	0.010±0.004*	2.94±0.03	152.7±0.8

* Reference value because concentration is under limit of quantitation

The CRMs were analyzed every run but were newly opened every two runs. Although this usage of CRM might be less common, we have confirmed a stability of the opened CRM bottles to be tolerance in our observation. The CRM bottles were stored at a laboratory in the ship, where the temperature was maintained at around 25 ° C.

It is noted that nutrient data in our report are calibrated not on CRM but on in-house standard solutions. Therefore, to calculate data based on CRM, it is necessary that

values of nutrient concentration in our report are correlated with CRM values measured in the same analysis run. The result of CRM measurements is attached as 49UP20210719_P03W_nut_CRM_measurement.csv.

(19) Quality Control

(7.1) Replicate and duplicate analyses

We took replicate (pair of water samples taken from a single Niskin bottle) and duplicate (pair of water samples taken from different Niskin bottles closed at the same depth) samples of nutrients throughout the cruise. Table C.4.5 summarizes the results of the analyses. Figures C.4.3–C.4.5 show details of the results. The calculation of the standard deviation from the difference of sets of samples was based on a procedure (SOP 23) in DOE (1994).

Table C.4.5. Average and standard deviation of difference of replicate and duplicate measurements throughout the cruise. Unit is μ mol kg^{-1}.

Samples	Nitrate+nitrite	Phosphate	Silicate
Replicate	0.026±0.024	0.002±0.002	0.130±0.125
	(N=337)	(N=337)	(N=337)
Duplicate	0.037±0.034	0.003±0.002	0.160±0.177
	(N=96)	(N=96)	(N=96)

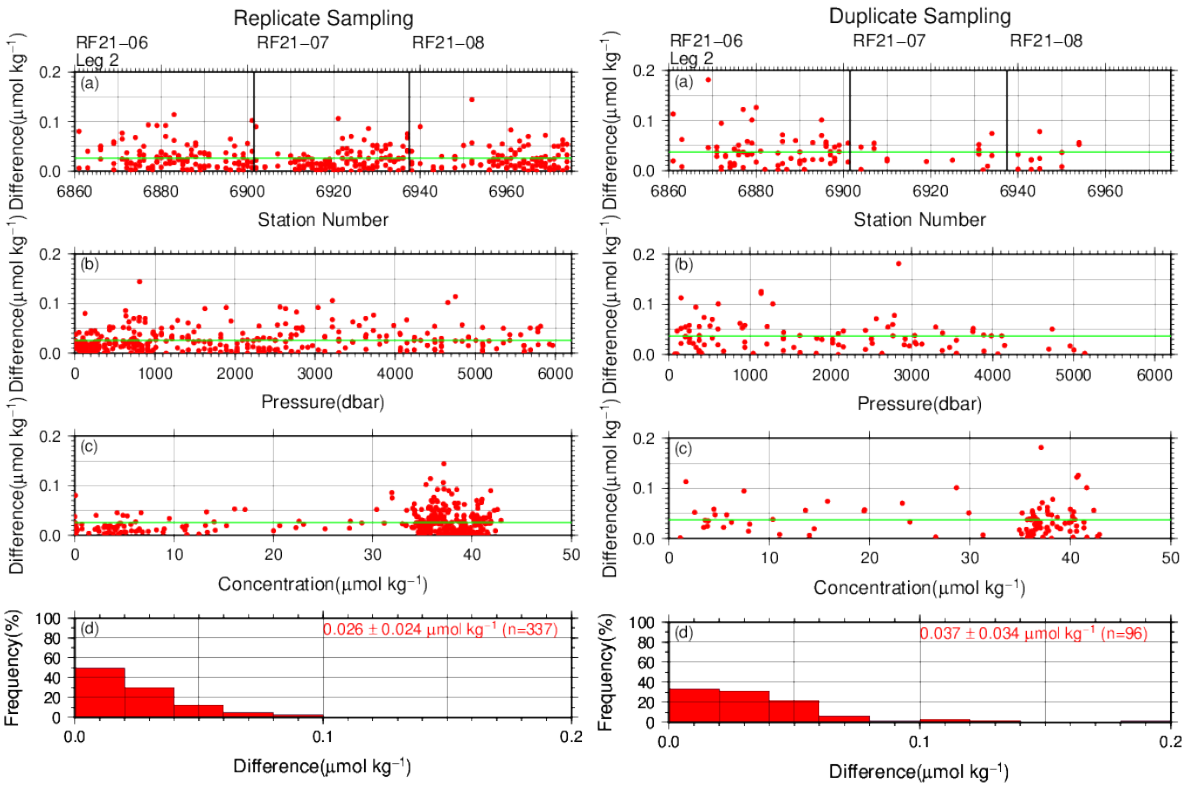

Figure C.4.3. Results of (left) replicate and (right) duplicate measurements of nitrate+nitrite throughout the cruise versus (a) station number, (b) sampling pressure, (c) concentration, and (d) histogram of the measurements. Green lines indicates the mean of the differences of concentrations based on replicate/duplicate analyses.

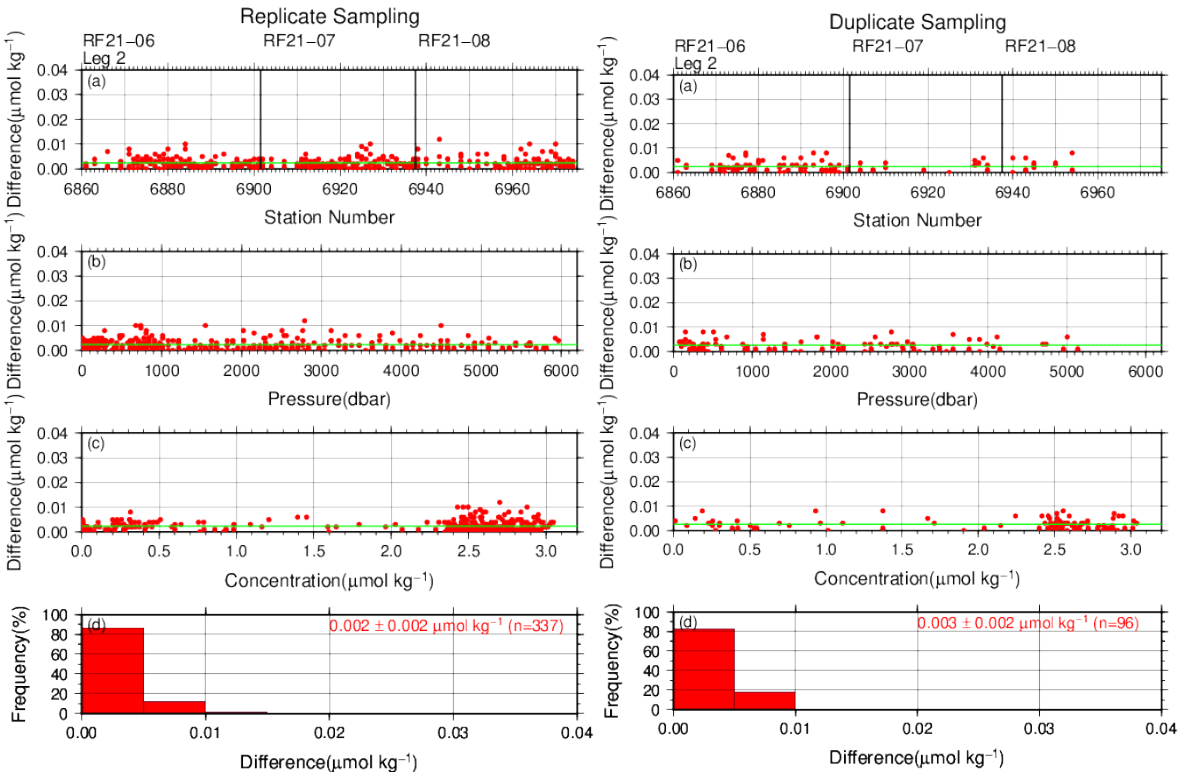

Figure C.4.4. Same as Figure C.4.3, but for phosphate.

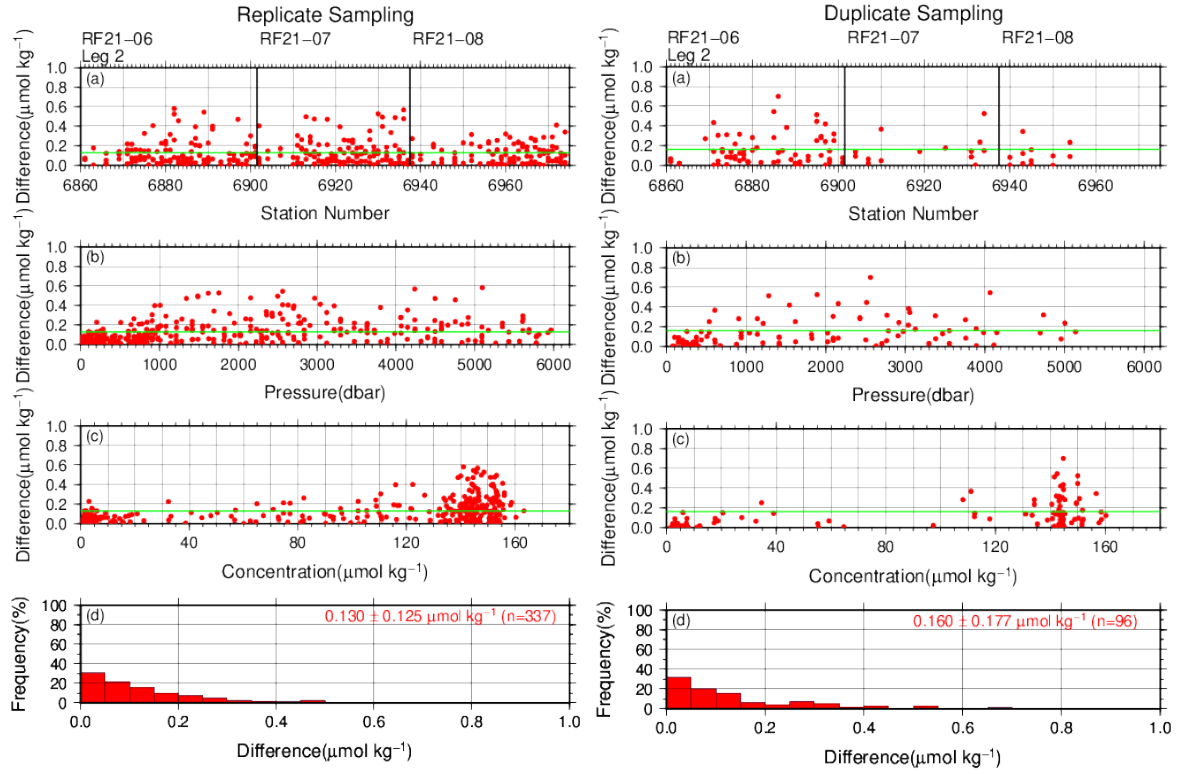

Figure C.4.5. Same as Figure C.4.3, but for silicate.

(7.2) Measurement of CRMs

Table C.4.6 summarizes the CRM measurements during the cruise. The CRM concentrations were assigned with in-house standard solutions. Figures C.4.6–C.4.9 show the measured concentrations of CRM-CN throughout the cruise.

Table C.4.6. Summary of (upper) mean concentration and its standard deviation (unit: μ mol kg^{-1}), (middle) coefficient of variation (%), and (lower) total number of CRMs measurements throughout the cruise.

	Nitrate+nitrite	Nitrite	Phosphate	Silicate
CRM-CK	0.070±0.049	0.039±0.002	0.061±0.005	0.81±0.14
	70.35 %	4.65 %	7.48 %	16.86 %
	(N=136)	(N=136)	(N=134)	(N=136)
CRM-CJ	16.26±0.06	0.047±0.002	1.20±0.01	38.88±0.17
	0.39 %	3.35 %	0.48 %	0.43 %
	(N=136)	(N=133)	(N=134)	(N=136)
CRM-CM	33.25±0.08	0.022±0.002	2.39±0.01	101.64±0.31
	0.25 %	7.61 %	0.28 %	0.30 %
	(N=136)	(N=135)	(N=136)	(N=136)
CRM-CN	43.67±0.10	0.013±0.002	2.94±0.01	154.52±0.39
	0.22 %	14.87 %	0.26 %	0.26 %
	(N=137)	(N=137)	(N=135)	(N=137)

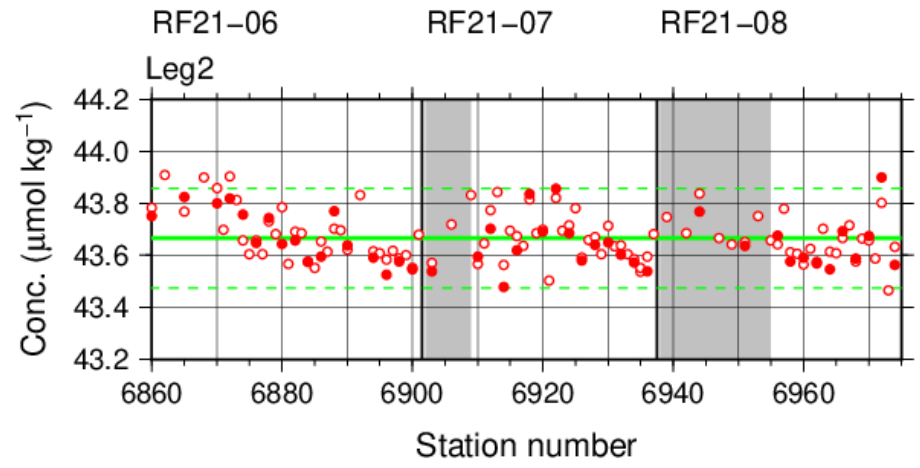

Figure C.4.6. Time-series of measured concentration of nitrate+nitrite of CRM-CN throughout the cruise. Closed and open circles indicate the newly and previously opened bottle, respectively. Thick and dashed lines denote the mean and the mean ± twice the standard deviations of the measurements throughout the cruise, respectively. Gray shade indicates an observation period of a sampling station which is not reported in the bottle data file.

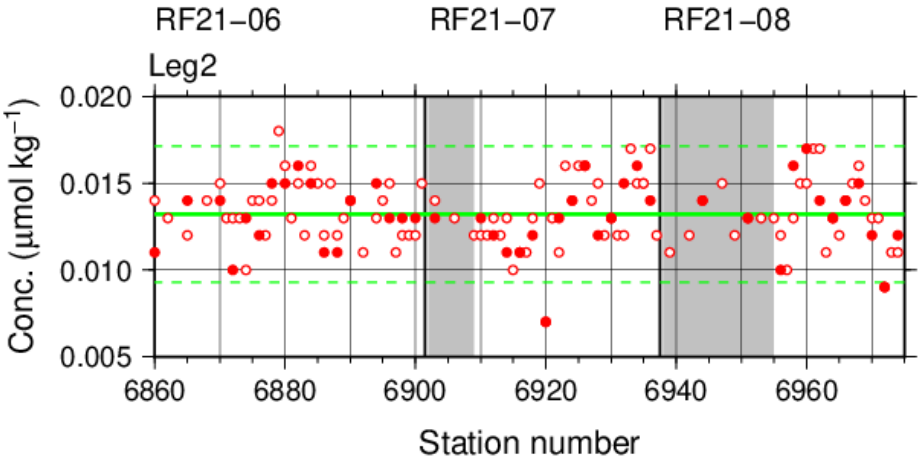

Figure C.4.7. Same as Figure C.4.6, but for nitrite.

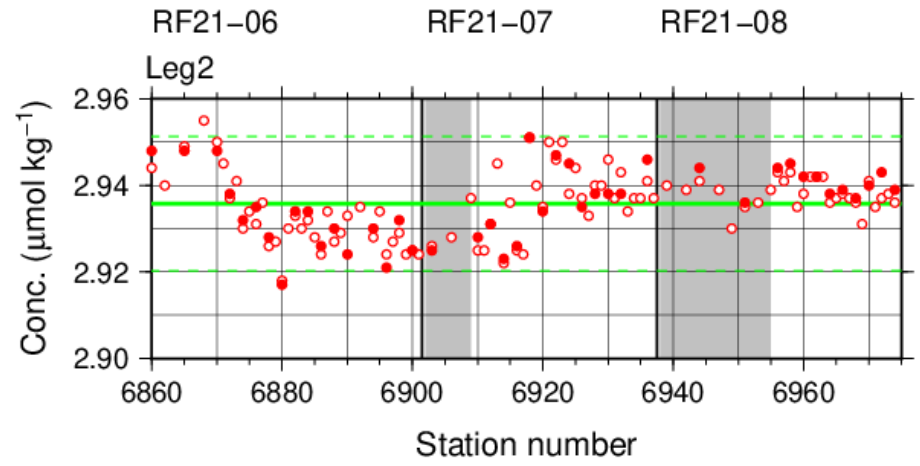

Figure C.4.8. Same as Figure C.4.6, but for phosphate.

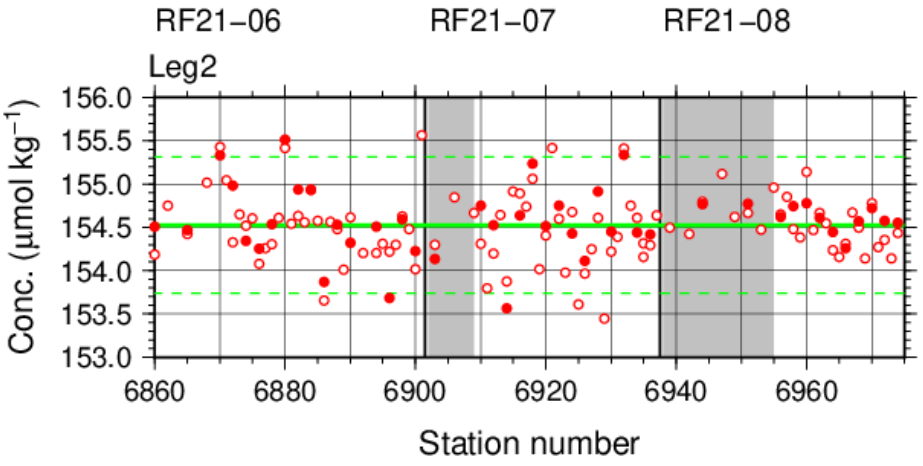

Figure C.4.9. Same as Figure C.4.6, but for silicate.

(7.3) Precision of analysis in a run

To monitor the precision of the analyses, the same samples were repeatedly measured in a sample array during a run. For this purpose, a C-5 standard solution was randomly inserted in every 2–10 samples as a "check standard" (the number of standards was about 8–9) in the run. The precision was estimated in terms of the coefficient of variation of the measurements. Table C.4.7 summarizes the results. The time series are shown in Figures C.4.10–C.4.13.

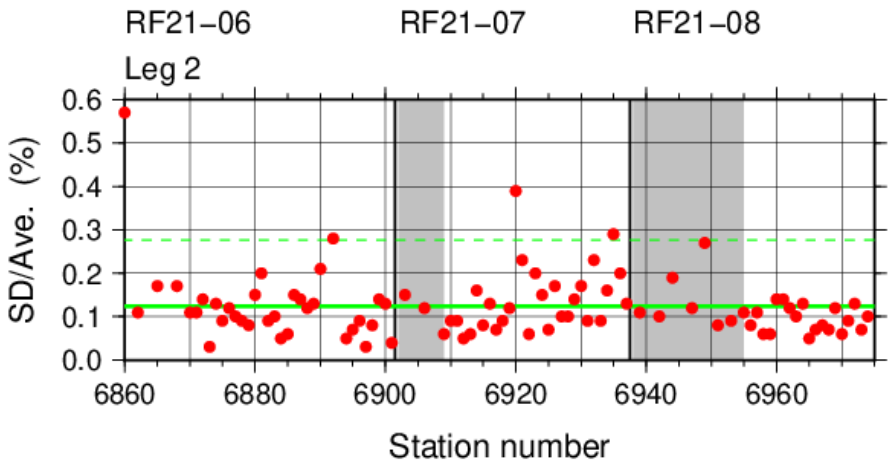

Figure C.4.10. Time-series of the coefficients of variation of "check standard" measurements of nitrate+nitrite throughout the cruise. Thick and dashed lines denote the mean and the mean ± twice the standard deviations of the measurements throughout the cruise, respectively. Gray shade indicates an observation period of a sampling station which is not reported in the bottle data file.

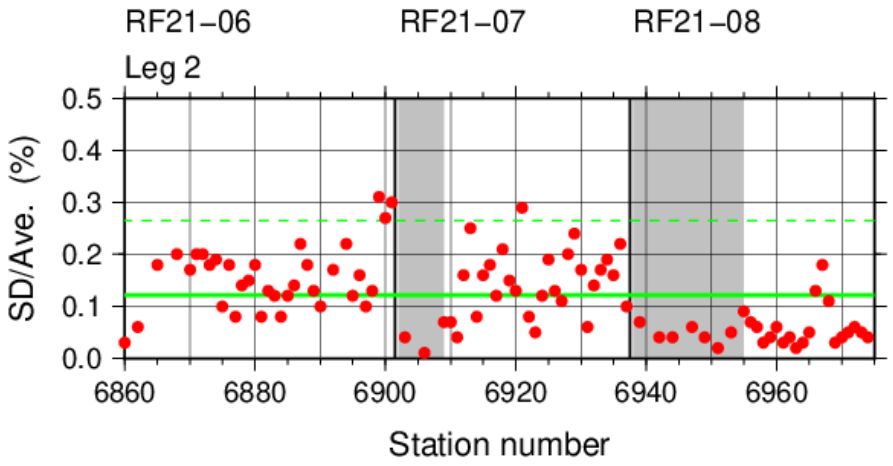

Figure C.4.11. Same as Figure C.4.10, but for nitrite.

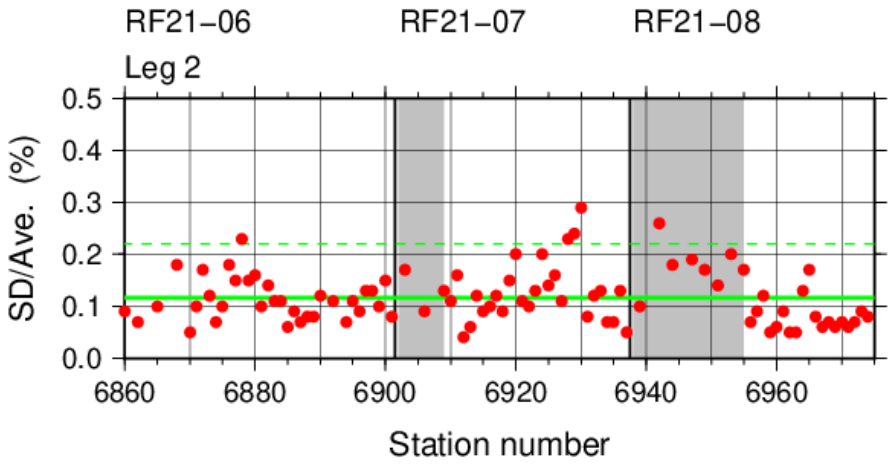

Figure C.4.12. Same as Figure C.4.10, but for phosphate.

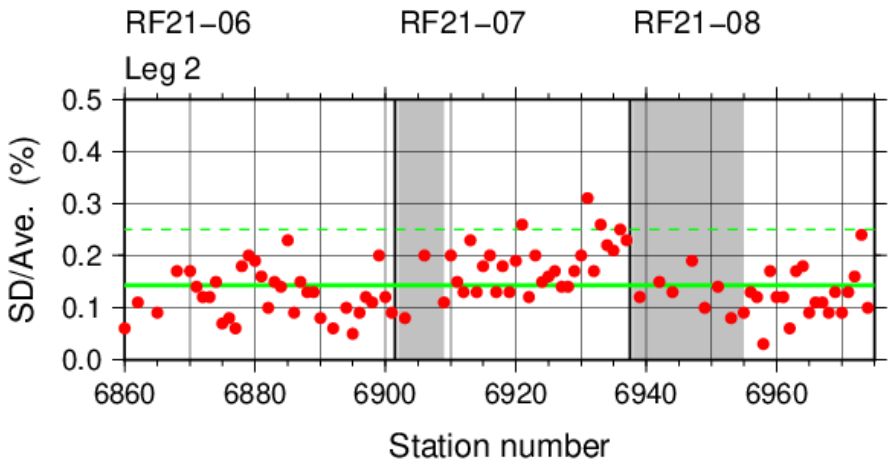

Figure C.4.13. Same as Figure C.4.10, but for silicate.

Table C.4.7. Summary of precisions of nutrient assays during the cruise.

	Nitrate+nitrite	Nitrite	Phosphate	Silicate
Median	0.11 %	0.12 %	0.11 %	0.13 %
Mean	0.12 %	0.12 %	0.12 %	0.14 %
Minimum	0.03 %	0.01 %	0.04 %	0.03 %
Maximum	0.57 %	0.31 %	0.29 %	0.31 %
Number	92	92	92	92

(7.4) Carryover

Carryover coefficients were determined during each analytical run. The C-5 standard (high standard) was followed by two C-1 standards (low standards). Figures C.4.14–17 show the time series of the carryover coefficients.

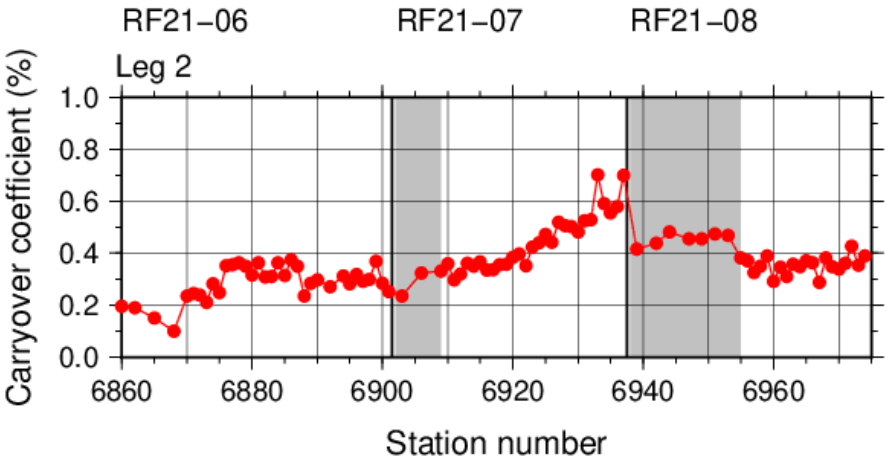

Figure C.4.14. Time-series of carryover coefficients in measurement of nitrate+nitrite throughout the cruise. Gray shade indicates an observation period of a sampling station which is not reported in the bottle data file.

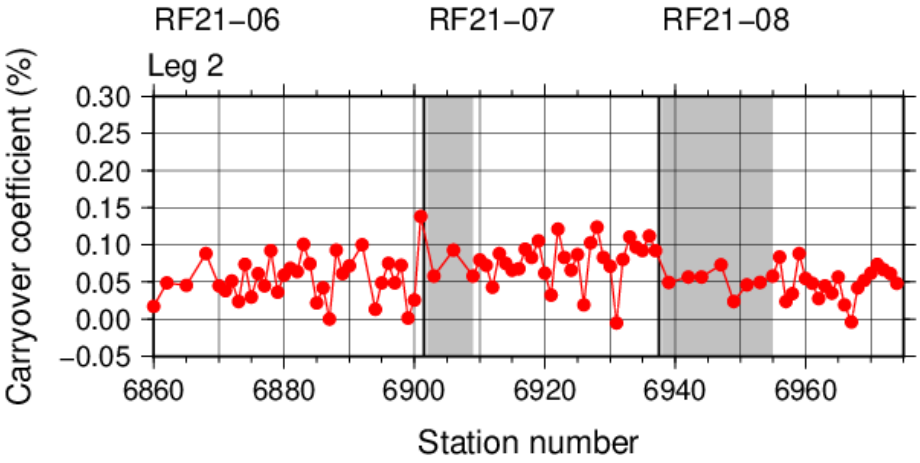

Figure C.4.15. Same as Figure C.4.14, but for nitrite.

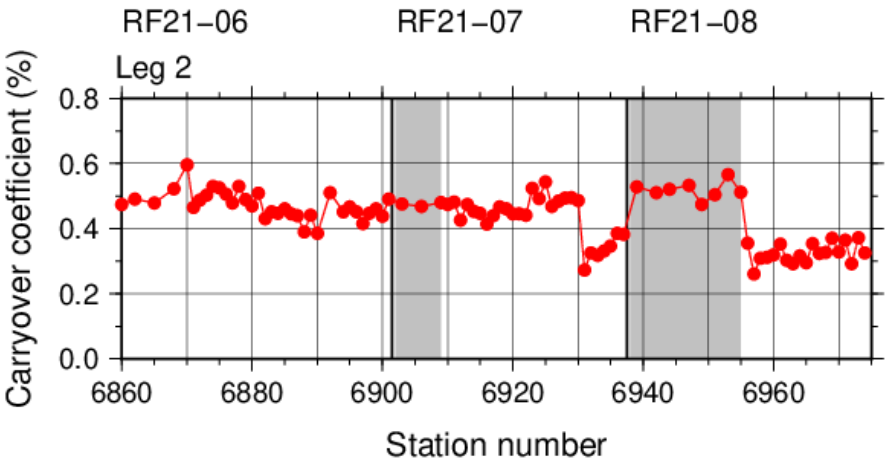

Figure C.4.16. Same as Figure C.4.14, but for phosphate.

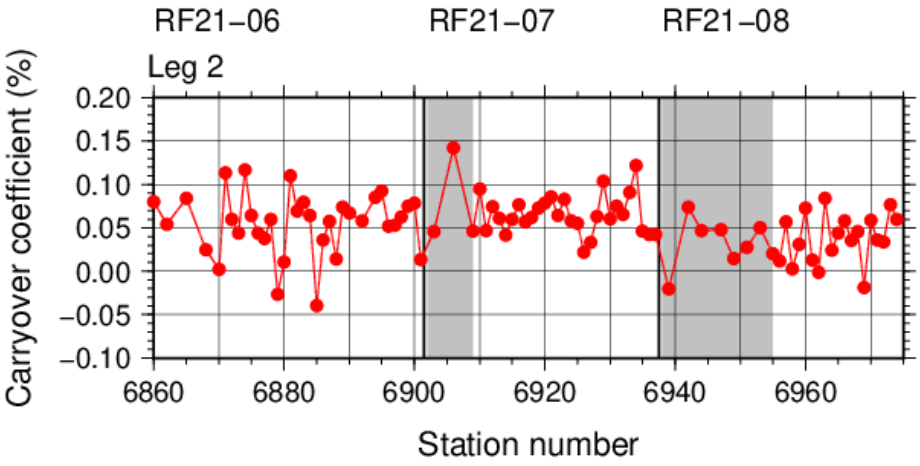

Figure C.4.17. Same as Figure C.4.14, but for silicate.

(7.5) Limit of detection/quantitation of measurement

Limit of detection (LOD) and quantitation (LOQ) of nutrient measurement were estimated from standard deviation (σ) of repeated measurements of nutrients concentration in C-1 standard as 3σ and 10σ, respectively. Summary of LOD and LOQ are shown in Table C.4.8.

Table C.4.8. Limit of detection (LOD) and quantitation (LOQ) of nutrient measurement in the cruise. Unit is μ mol kg^{-1}.

	LOD	LOQ
Nitrate+nitrite	0.049	0.165
Nitrite	0.001	0.005
Phosphate	0.009	0.031
Silicate	0.170	0.567

(7.6) Quality control flag assignment

A quality flag value was assigned to nutriment measurements as shown in Table C.4.9, using the code defined in IOCCP Report No.14 (Swift, 2010).

Table C.4.9. Summary of assigned quality control flags.

Flag	Definition	Nitrate+nitrite	Nitrite	Phosphate	Silicate
2	Good	2566	2567	2564	2566

3	Questionable	0	0	0	0
4	Bad (Faulty)	2	1	4	2
5	Not reported	0	0	0	0
6	Replicate measurements	307	307	307	307
Total number of samples		2875	2875	2875	2875

(20) Uncertainty

(8.1) Uncertainty associated with concentration level: U_c

Generally, an uncertainty of nutrient measurement is expressed as a function of its concentration level which reflects that some components of uncertainty are relatively large in low concentration. Empirically, the uncertainty associated with concentrations level (U_c) can be expressed as follows;

$$U_c\ (\%) = a + b \cdot (1/C_x) + c \cdot (1/C_x)^2, \quad \text{(C4.1)}$$

where C_x is the concentration of sample for parameter X.

Using the coefficients of variation of the CRM measurements throughout the cruise, uncertainty associated with concentrations of nitrate+nitrite, phosphate, and silicate were determined as follows:

$$U_{c\text{-}no3}\ (\%) = 0.013 + 2.342 \cdot (1/C_{no3}) + 0.002 \cdot (1/C_{no3})^2 \quad \text{(C4.2)}$$

$$U_{c\text{-}po4}\ (\%) = -0.066 + 0.396 \cdot (1/C_{po4}) \quad \text{(C4.3)}$$

$$U_{c\text{-}sil}\ (\%) = 0.08 + 5.49 \cdot (1/C_{sil}) + 1.10 \cdot (1/C_{sil})^2, \quad \text{(C4.4)}$$

where C_{no3}, C_{po4}, and C_{sil} represent concentrations of nitrate+nitrite, phosphate, and silicate, respectively, in μmol kg^{-1}. Figures C.4.18–C.4.20 show the calculated uncertainty graphically.

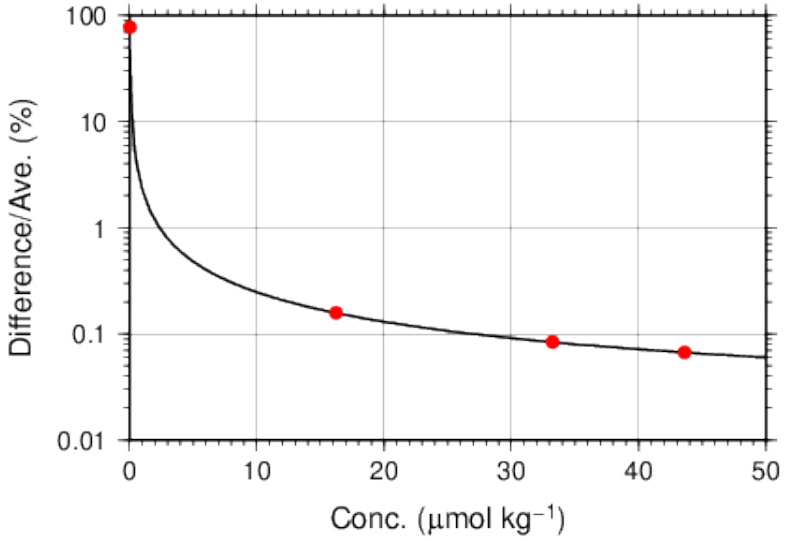

Figure C.4.18. Uncertainty of nitrate+nitrite associated with concentrations.

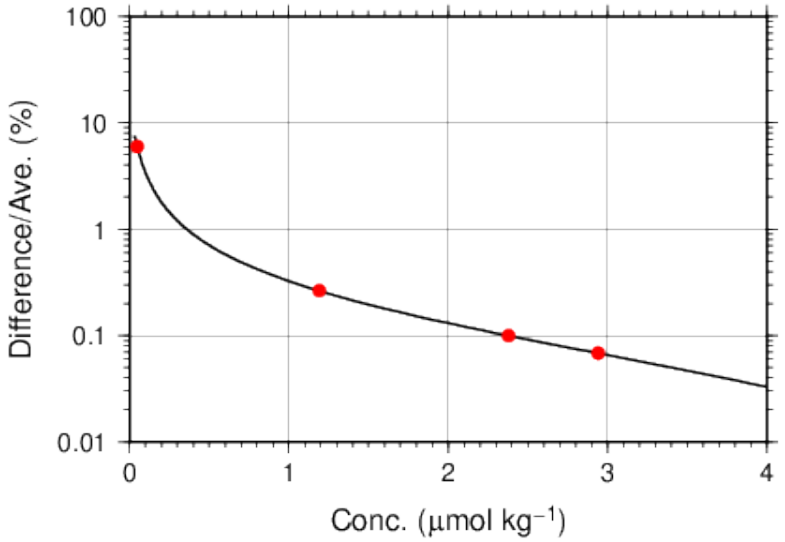

Figure C.4.19. Same as Figure C.4.18, but for phosphate.

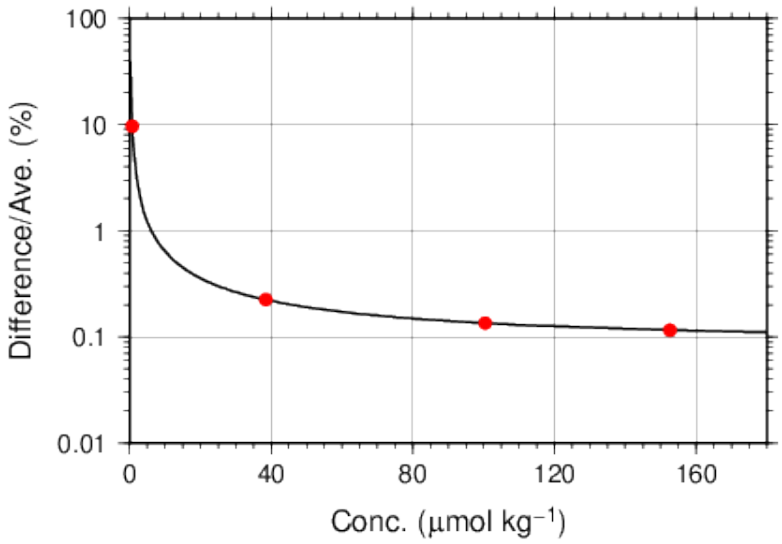

Figure C.4.20. Same as Figure C.4.18, but for silicate.

(8.2) Uncertainty of analysis between runs: U_s

Uncertainty of analysis among runs (U_s) was evaluated based on the coefficient of variation of measured concentrations of CRM-CN with the highest concentration among the CRM lots throughout the cruise, as shown in subsection (7.2). The reason for using the CRM lot to state U_s is to exclude the effect of uncertainty associated with lower concentration described previously. As is clear from the definition of U_c, U_s is equal to U_c at nutrients concentrations of the lot. It is important to note that U_s includes all of uncertainties during the measurements throughout stations, namely uncertainties of concentrations of in-house standard solutions prepared for each run, uncertainties of slopes and intercepts of the calibration curve in each run, precision of measurement in a run (U_a), and between-bottle homogeneity of the CRM.

(8.3) Uncertainty of analysis in a run: U_a

Uncertainty of analysis in a run (U_a) was evaluated based on the coefficient of variation of repeated measurements of the "check standard" solution, as shown in subsection (7.3). The U_a reflects the conditions associated with chemistry of colorimetric measurement of nutrients, and stability of electronic and optical parts of the instrument throughout a run. Under a well-controlled condition of the measurements, U_a might show Poisson distribution with a mean as shown in Figures C.4.10–C.4.13 and Table C.4.7 and treated as a precision of measurement. U_a is a part of U_c at the concentration as stated in a previous section for U_c.

However, U_a may show larger value which was not expected from Poisson distribution of U_a due to the malfunction of the instruments, larger ambient temperature change, human errors in handling samples and chemistries, and contaminations of samples in a run. In the cruise, we observed that U_a of our measurement was usually small and well-controlled in most runs as shown in Figures C.4.10–C.4.13 and Table C.4.7. However, in a few runs, U_a showed high values which were over the mean ± twice the standard deviations of U_a, suggesting that the measurement system might have some problems.

(8.4) Uncertainty of CRM concentration: U_r

In the certification of CRM, the uncertainty of CRM concentrations (U_r) was stated by the manufacturer (Table C.4.4) as expanded uncertainty at k=2. This expanded uncertainty reflects the uncertainty of the Japan Calibration Service System (JCSS) solutions, characterization in assignment, between-bottle homogeneity, and long term stability. We have ensured comparability between cruises by ensuring that at least two

lots of CRMs overlap between cruises. In comparison of nutrient concentrations between cruises using KANSO CRMs in an organization, it was not necessary to include U_r in the conclusive uncertainty of concentration of measured samples because comparability of measurements was ensured in an organization as stated previously.

(8.5) Conclusive uncertainty of nutrient measurements of samples: *U*

To determine the conclusive uncertainty of nutrient measurements of samples (U), we use two functions depending on U_a value acquired at each run as follows:

When U_a was small and measurement was well-controlled condition, the conclusive uncertainty of nutrient measurements of samples, U, might be as below:

$$U = U_c. \quad \text{(C4.5)}$$

When U_a was relative large and the measurement might have some problems, the conclusive uncertainty of nutrient measurements of samples, U, can be expanded as below:

$$U = \sqrt{U_c^2 + U_a^2}. \quad \text{(C4.6)}$$

When U_a was relative large and the measurement might have some problems, the equation of U is defined as to include U_a to evaluate U, although U_a partly overlaps with U_c. It means that the equation overestimates the conclusive uncertainty of samples. On the other hand, for low concentration there is a possibility that the equation not only overestimates but also underestimates the conclusive uncertainty because the functional shape of U_c in lower concentration might not be the same and cannot be verified. However, we believe that the applying the above function might be better way

to evaluate the conclusive uncertainty of nutrient measurements of samples because we can do realistic evaluation of uncertainties of nutrient concentrations of samples which were obtained under relatively unstable conditions, larger U_a as well as the evaluation of them under normal and good conditions of measurements of nutrients.

Appendix

A1. Seawater sampling

Seawater samples were collected from 10-liters Niskin bottle attached CTD-system and a stainless steel bucket for the surface. Samples were drawn into 10 mL polymethylpenten vials using sample drawing tubes. The vials were rinsed three times before water filling and were capped immediately after the drawing.

No transfer was made and the vials were set on an auto sampler tray directly. Samples were analyzed immediately after collection.

A2. Measurement

(A2.1) General

Auto Analyzer III is based on Continuous Flow Analysis method and consists of sampler, pump, manifolds, and colorimeters. As a baseline, we used artificial seawater (ASW).

(A2.2) Nitrate+nitrite and nitrite

Nitrate+nitrite and nitrite were analyzed according to the modification method of Armstrong (1967). The sample nitrate was reduced to nitrite in a glass tube which was filled with granular cadmium coated with copper. The sample stream with its equivalent nitrite was treated with an acidic, sulfanilamide reagent and the nitrite forms nitrous acid which reacts with the sulfanilamide to produce a diazonium ion. N-1-naphthylethylene-diamine was added to the sample stream then coupled with the diazonium ion to produce a red, azo dye. With reduction of the nitrate to nitrite, sum

of nitrate and nitrite were measured; without reduction, only nitrite was measured. Thus, for the nitrite analysis, no reduction was performed and the alkaline buffer was not necessary. The flow diagrams for each parameter are shown in Figures C.4.A1 and C.4.A2. If the reduction efficiency of the cadmium column became lower than 95 %, the column was replaced.

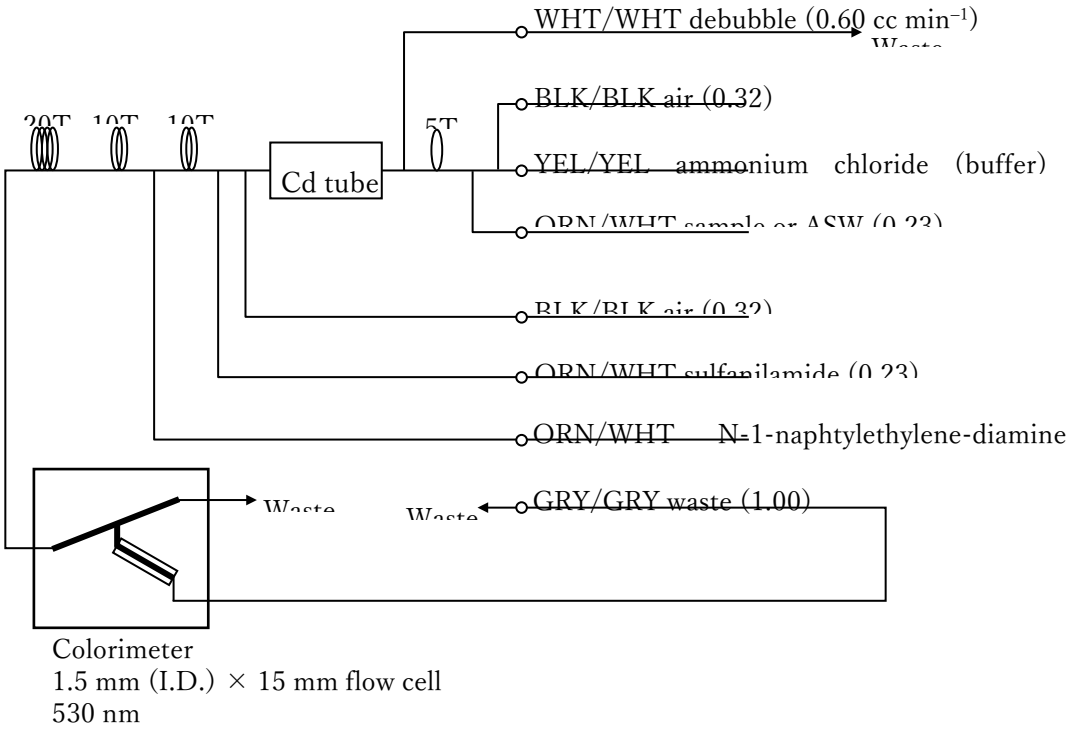

Figure C.4.A1. Nitrate+nitrite (ch. 1) flow diagram.

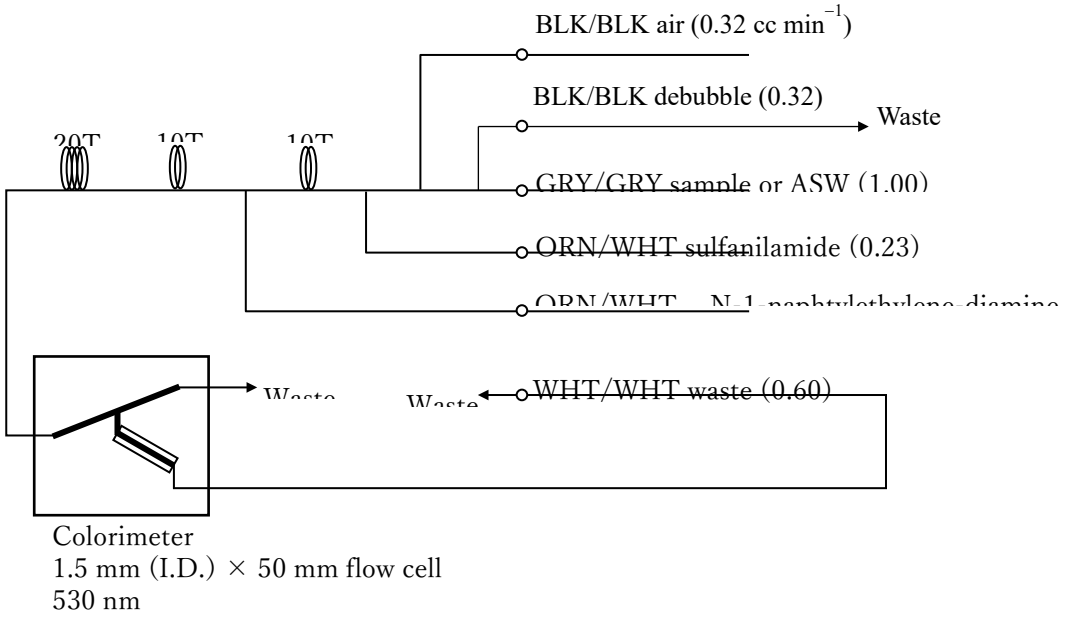

Figure C.4.A2. Nitrite (ch. 2) flow diagram.

(A2.3) Phosphate

The phosphate analysis was a modification of the procedure of Murphy and Riley (1962). Molybdic acid was added to the seawater sample to form phosphomolybdic acid which was in turn reduced to phosphomolybdous acid using L-ascorbic acid as the reductant. The flow diagram for phosphate is shown in Figure C.4.A3.

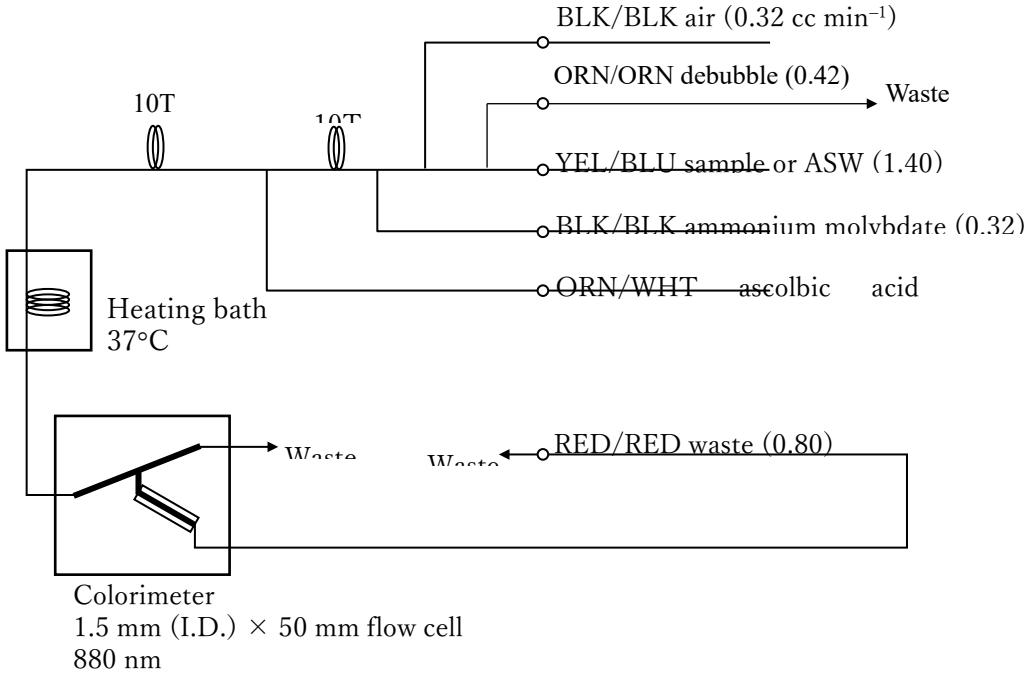

Figure C.4.A3. Phosphate (ch. 3) flow diagram.

(A2.4) Silicate

The silicate was analyzed according to the modification method of Grasshoff *et al.* (1983), wherein silicomolybdic acid was first formed from the silicate in the sample and added molybdic acid, then the silicomolybdic acid was reduced to silicomolybdous acid, or "molybdenum blue," using L-ascorbic acid as the reductant. The flow diagram for silicate is shown in Figure C.4.A4.

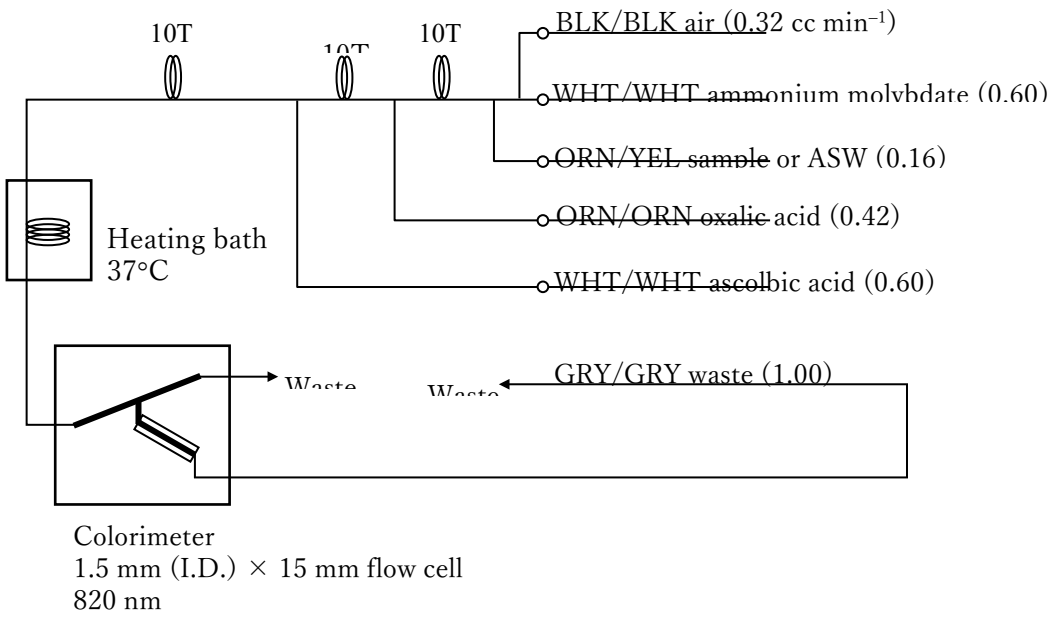

Figure C.4.A4. Silicate (ch. 4) flow diagram.

A3. Data processing

Raw data from Auto Analyzer III were recorded at 1-second interval and were treated as follows;

a. Check the shape of each peak and position of peak values taken, and then change the positions of peak values taken if necessary.

b. Baseline correction was done basically using linear regression.

c. Reagent blank correction was done basically using linear regression.

d. Carryover correction was applied to peak heights of each sample.

e. Sensitivity correction was applied to peak heights of each sample.

f. Refraction error correction was applied to peak heights of each seawater sample.

g. Calibration curves to get nutrients concentration were assumed quadratic

expression.

h. Concentrations were converted from μ mol L^{-1} to μ mol kg^{-1} using seawater density.

A4. Reagents recipes

(A4.1) Nitrate+nitrite

Ammonium chloride (buffer), 0.7 μ mol L^{-1} (0.04 % w/v);

Dissolve 190 g ammonium chloride, NH_4Cl, in ca. 5 L of DW, add about 5 mL ammonia(aq) to adjust pH of 8.2–8.5.

Sulfanilamide, 0.06 μ mol L^{-1} (1 % w/v);

Dissolve 5 g sulfanilamide, 4-$NH_2C_6H_4SO_3H$, in 430 mL DW, add 70 mL concentrated HCl. After mixing, add 1 mL Brij-35 (22 % w/w).

N-1-naphtylethylene-diamine dihydrochloride (NEDA), 0.004 μ mol L^{-1} (0.1 % w/v);

Dissolve 0.5 g NEDA, $C_{10}H_7NH_2CH_2CH_2NH_2 \cdot 2HCl$, in 500 mL DW.

(A4.2) Nitrite

Sulfanilamide, 0.06 μ mol L^{-1} (1 % w/v); Shared from nitrate reagent.

N-1-naphtylethylene-diamine dihydrochloride (NEDA), 0.004 μ mol L^{-1} (0.1 % w/v);

Shared from nitrate reagent.

(A4.3) Phosphate

Ammonium molybdate, 0.005 μ mol L^{-1} (0.6 % w/v);

Dissolve 3 g ammonium molybdate(VI) tetrahydrate, $(NH_4)_6Mo_7O_{24}{\cdot}4H_2O$, and 0.05 g potassium antimonyl tartrate, $C_8H_4K_2O_{12}Sb_2{\cdot}3H_2O$, in 400 mL DW and add 40 mL concentrated H_2SO_4. After mixing, dilute the solution with DW to final volume of 500 mL and add 2 mL sodium dodecyl sulfate (15 % solution in water).

L(+)-ascorbic acid, 0.08 μmol L^{-1} (1.5 % w/v);

Dissolve 4.5 g L(+)-ascorbic acid, $C_6H_8O_6$, in 300 mL DW. After mixing, add 10 mL acetone. This reagent was freshly prepared before every measurement.

(A4.4) Silicate

Ammonium molydate, 0.005 μmol L^{-1} (0.6 % w/v);

Dissolve 3 g ammonium molybdate(VI) tetrahydrate, $(NH_4)_6Mo_7O_{24}{\cdot}4H_2O$, in 500 mL DW and added concentrated 2 mL H_2SO_4. After mixing, add 2 mL sodium dodecyl sulfate (15 % solution in water).

Oxalic acid, 0.4 μmol L^{-1} (5 % w/v);

Dissolve 25 g oxalic acid dihydrate, $(COOH)_2{\cdot}2H_2O$, in 500 mL DW.

L(+)-ascorbic acid, 0.08 μmol L^{-1} (1.5 % w/v); Shared from phosphate reagent.

(A4.5) Baseline

Artificial seawater (salinity is ~34.7);

Dissolve 160.6 g sodium chloride, NaCl, 35.6 g magnesium sulfate heptahydrate, $MgSO_4{\cdot}7H_2O$, and 0.84 g sodium hydrogen carbonate, $NaHCO_3$, in 5 L DW.

References

Armstrong, F. A. J., C. R. Stearns and J. D. H. Strickland (1967), The measurement of upwelling and subsequent biological processes by means of the Technicon TM Autoanalyzer TM and associated equipment, *Deep-Sea Res.*, 14(3), 381–389.

Grasshoff, K., Ehrhardt, M., Kremling K. et al. (1983), Methods of seawater analysis. 2nd rev, *Weinheim: Verlag Chemie, Germany, West.*

Murphy, J. and Riley, J.P. (1962), Analytica chimica *Acta*, *27, 31-36.*

Swift, J. H. (2010), Reference-quality water sample data: Notes on acquisition, record keeping, and evaluation. *IOCCP Report No.14, ICPO Pub. 134, 2010 ver.1.*

5. Phytopigments (chlorophyll-a and phaeopigment)

31 March 2022

(1) Personnel

SHINODA Yoshihiro

HASHIMOTO Susumu

SASAKI Takuya

OKAJIMA Shingo (RF21-06)

FUJII Takuya (RF21-06, RF21-08)

IMAI Yoichi (RF21-07)

KAKUYA Keita (RF21-07, RF21-08)

(21) Station occupied

A total of 42 stations (RF 21-06 Leg 2: 18, RF 21-07: 14, RF21-08: 10) were occupied for phytopigment measurements. Station location and sampling layers of phytopigment are shown in Figures C.5.1 and C.5.2.

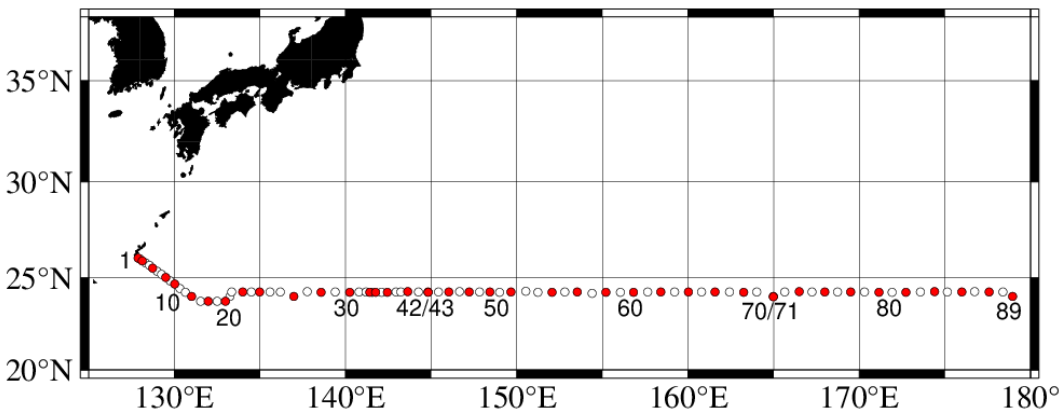

Figure C.5.1. Location of observation stations of chlorophyll-*a*. Closed and open circles indicate sampling and no-sampling stations, respectively.

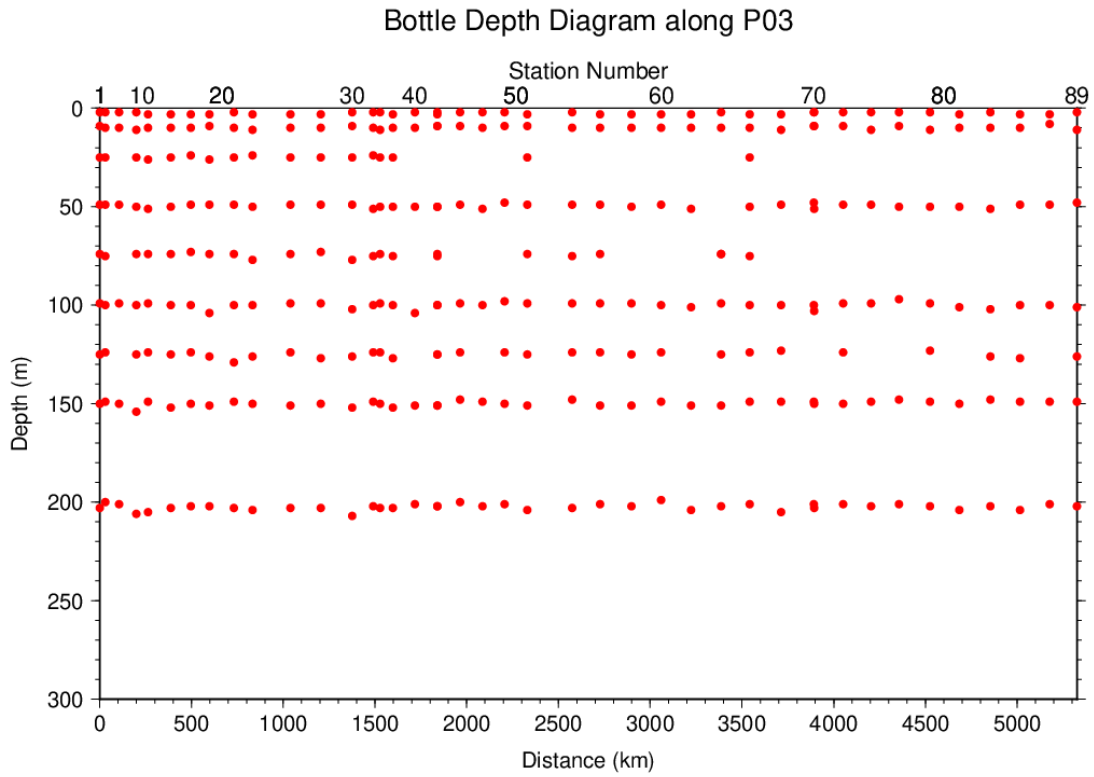

Figure C.5.2. Distance-depth distribution of sampling layers of chlorophyll-*a*.

(22) Reagents

N,N-dimethylformamide (DMF)

Hydrochloric acid (HCl), 0.5 mol L^{-1}

Chlorophyll-*a* standard from *Anacystis nidulans* algae (Sigma-Aldrich, United States)

Rhodamine WT (Turner Designs, United States)

(23) Instruments

Fluorometer: 10-AU (Turner Designs, United States)

Spectrophotometer: UV-1800 (Shimadzu, Japan)

(24) Standardization

(5.1) Determination of chlorophyll-*a* concentration of standard solution

To prepare the pure chlorophyll-*a* standard solution, reagent powder of chlorophyll-*a* standard was dissolved in DMF. A concentration of the chlorophyll-*a* solution was determined with the spectrophotometer as follows:

$$\text{chl. } a \text{ concentration } (\mu g\ mL^{-1}) = A_{chl} / a^*_{phy} \qquad (C5.1)$$

where A_{chl} is the difference between absorbance at 663.8 nm and 750 nm, and a^*_{phy} is specific absorption coefficient (UNESCO, 1994). The specific absorption coefficient is 88.74 L g^{-1} cm^{-1} (Porra *et al.*, 1989).

(5.2) Determination of R and f_{ph}

Before measurements, sensitivity of the fluorometer was calibrated with pure DMF and a rhodamine 1 ppm solution (diluted with deionized water).

The chlorophyll-*a* standard solution, whose concentration was precisely determined in subsection (5.1), was measured with the fluorometer, and after acidified with 1–2 drops 0.5 mol L^{-1} HCl the solution was also measured. The acidification coefficient (R) of the fluorometer was also calculated as the ratio of the unacidified and acidified readings of chlorophyll-*a* standard solution. The linear calibration factor (f_{ph}) of the fluorometer

was calculated as the slope of the acidified reading against chlorophyll-*a* concentration. The R and f_{ph} in the cruise are shown in Table C.9.1.

Table C.5.1. R and f_{ph} in the cruises.

Cruises number	RF21-06	RF21-07	RF21-08
Acidification coefficient (R)	2.0040	2.0015	1.9919
Linear calibration factor (f_{ph})	6.0970	6.1172	5.3501

(25) Seawater sampling and measurement

Water samples were collected from 10-liters Niskin bottle attached the CTD-system and a stainless steel bucket for the surface. A 200 mL seawater sample was immediately filtered through 25 mm GF/F filters by low vacuum pressure below 15 cmHg, the particulate matter collected on the filter. Phytopigments were extracted in vial with 9 mL of DMF. The extracts were stored for 24 hours in the refrigerator at –30 ° C until analysis.

After the extracts were put on the room temperature for at least one hour in the dark, the extracts were decanted from the vial to the cuvette. Fluorometer readings for each cuvette were taken before and after acidification with 1–2 drops 0.5 mol L^{-1} HCl. Chlorophyll-*a* and phaeopigment concentrations (μg mL^{-1}) in the sample are calculated as follows:

$$\text{chl } a \text{ conc.} = \frac{F_0 - F_a}{f_{ph} \cdot (R-1)} \cdot \frac{v}{V} \qquad \text{(C5.2)}$$

$$\text{phaeo. conc.} = \frac{R \cdot F_0 - F_a}{f_{ph} \cdot (R-1)} \cdot \frac{v}{V} \qquad \text{(C5.3)}$$

F_0: reading before acidification

F_a: reading after acidification

R: acidification coefficient (F_0/F_a) for pure chlorophyll-*a*

f_{ph}: linear calibration factor

v: extraction volume

V: sample volume.

(26) Quality control flag assignment

Quality flag value was assigned to oxygen measurements as shown in Table C.5.2, using the code defined in IOCCP Report No.14 (Swift, 2010).

Table C.5.2 Summary of assigned quality control flags.

Flag	Definition	Chl. *a*	Phaeo.
2	Good	329	329
3	Questionable	0	0
4	Bad (Faulty)	2	2
5	Not reported	0	0

Total number	331	331

References

Porra, R. J., W. A. Thompson and P. E. Kriedemann (1989), Determination of accurate coefficients and simultaneous equations for assaying chlorophylls *a* and *b* extracted with four different solvents: verification of the concentration of chlorophyll standards by atomic absotption spectroscopy. *Biochem. Biophy. Acta,* 975, 384-394.

Swift, J. H. (2010), Reference-quality water sample data: Notes on acquisition, record keeping, and evaluation. *IOCCP Report No.14, ICPO Pub. 134, 2010 ver.1.*

UNESCO (1994), Protocols for the joint global ocean flux study (JGOFS) core measurements: Measurement of chlorophyll *a* and phaeopigments by fluorometric analysis, *IOC manuals and guides 29, Chapter 14.*

6. Total Dissolved Inorganic Carbon (DIC)

30 September 2023

(27) Personnel

DEHARA Kohshiro

HAMANA Minoru

NAKAMURA Naoki

(28) Station occupied

A total of 45 stations (RF21-06: 18, RF21-07: 15, RF21-08: 12) were occupied for total dissolved inorganic carbon (DIC). Station location and sampling layers of them are shown in Figures C.6.1 and C.6.2, respectively.

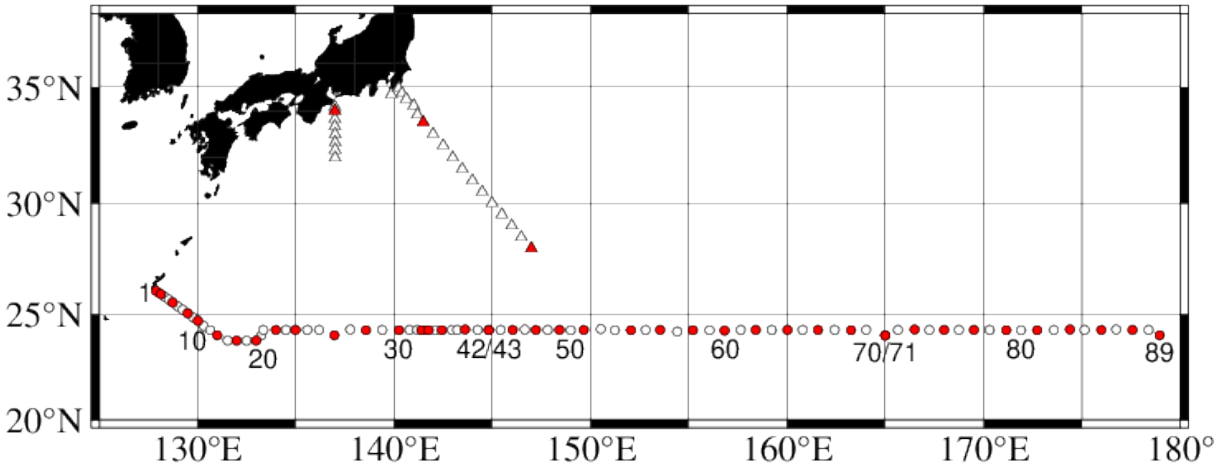

Figure C.6.1. Location of observation stations of DIC. Closed and open circles indicate sampling and no-sampling stations, respectively. Triangles show sampling station which are not reported in the bottle data file, but the data at closed triangles are used for quality control of DIC. These data are available from the JMA

(https://www.data.jma.go.jp/gmd/kaiyou/db/vessel_obs/data-report/html/ship/ship_e.php?year=2021&season=summer).

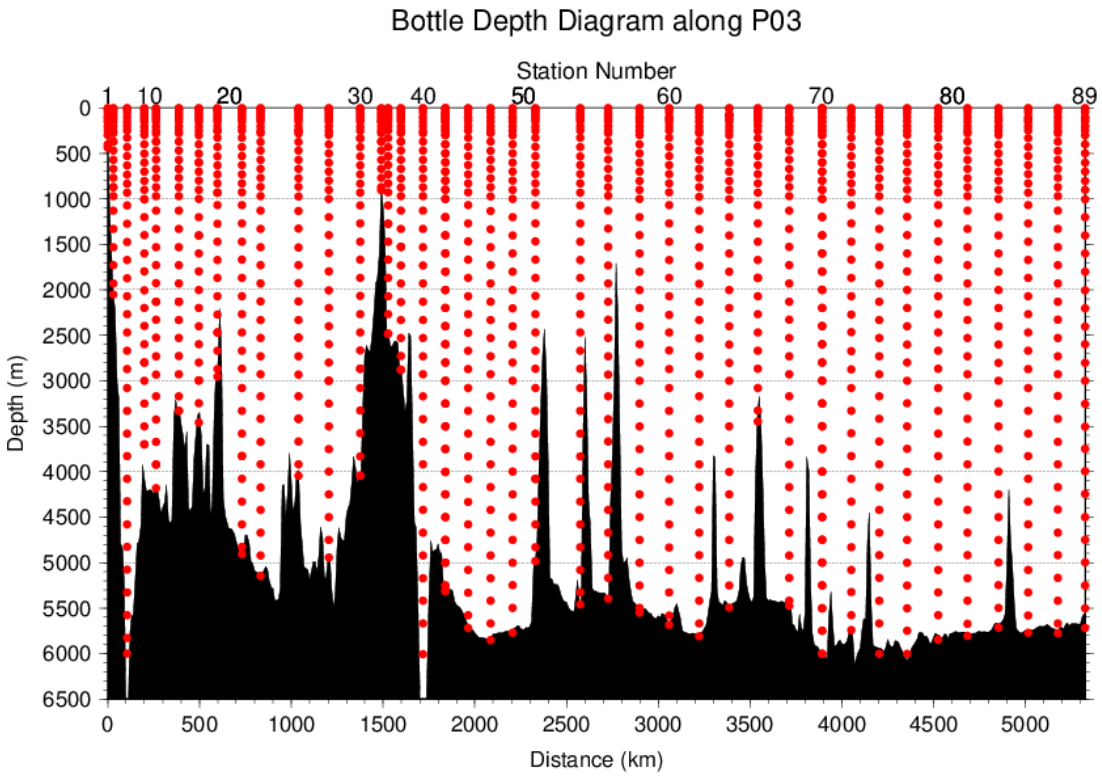

Figure C.6.2. Distance-depth distribution of sampling layers of DIC.

(29) Instrument

The measurement of DIC was carried out with DIC/TA analyzers (Nihon ANS Co. Ltd, Japan). We used two analyzers concurrently. These analyzers are designated as apparatus A and B.

(30) Sampling and measurement

Methods of seawater sampling, poisoning, measurement, and calculation of DIC

concentrations were based on the Standard Operating Procedure (SOP) described in PICES Special Publication 3, SOP-2 (Dickson et al., 2007). DIC was determined by coulometric analysis (Johnson et al., 1985, 1987) using an automated CO_2 extraction unit and a coulometer. Details of sampling and measurement are shown in Appendix A1.

(31) Calibration

The concentration of DIC (C_T) in moles per kilogram (mol kg^{-1}) of seawater was calculated from the following equation:

$$C_T = N_S / (cV \cdot \rho_S) \quad \text{(C6.1)}$$

where N_S is the counts of the coulometer (gC), cV is the calibration factor (gC (mol $L^{-1})^{-1}$), and ρ_S is density of seawater (kg L^{-1}), which is calculated from the salinity of the sample and the water temperature of the water-jacket for the sample pipette.

The determination of values of cV was based on measurements of in-house standard sea water (SSW) which was bottled in our laboratory at November 27th, 2019 (Appendix A2). The SSW show good homogeneity among bottles and good temporal stability of C_T at least 12 months. The C_T of SSW was determined in pre-cruise measurements at October 26th, 2020 using Certified Reference Materials (CRMs; provided by Dr. Andrew G. Dickson of the Scripps Institution of Oceanography). The list of SSW and CRM is shown in Table C.6.1.

Through the each cruise, the SSW measurement was carried out used as working reference material at every stations as shown in Subsection (6.2). After the cruise, a

value of cV was assigned to each apparatus (A, B) for each cruise. Table C.6.2 summarizes the cV values. Figure C.6.3 shows details.

Table C.6.1. Assigned C_T and standard deviation of SSW and certified C_T and standard deviation of CRM. Unit of C_T is μ mol kg^{-1}. More information about CRM is available at the NOAA web site (https://www.ncei.noaa.gov/access/ocean-carbon-acidification-data-system/oceans/Dickson_CRM/batches.html).

	SSW	CRM
Lot/batch	AH	187
C_T	2065.58 ± 0.59	2002.85 ± 0.40
Salinity	34.538	33.602

Table C.6.2. Assigned cV and standard deviation for each apparatus during the cruise. Unit is gC (mol L^{-1})$^{-1}$.

Apparatus	Cruise	cV
A	RF21-06	0.194080 ± 0.000087 (N=16)
	RF21-07	0.194066 ± 0.000135 (N=19)
	RF21-08	0.194194 ± 0.000128 (N=13)
B	RF21-06	0.189809 ± 0.000139 (N=21)
	RF21-07	0.189884 ± 0.000090 (N=16)
	RF21-08	0.189939 ± 0.000122 (N=16)

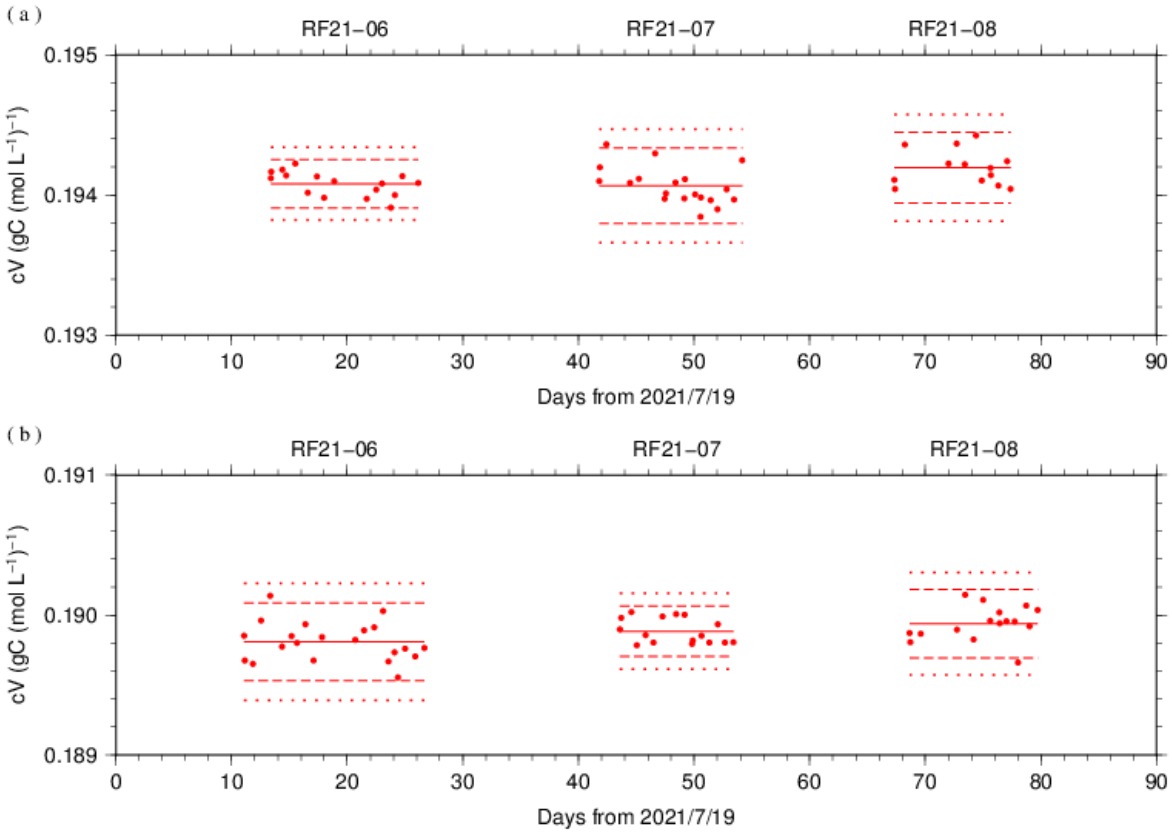

Figure C.6.3. Results of the cV at every stations for each cruise assigned for apparatus (a) A and (b) B. The solid, dashed, and dotted lines denote the mean, the mean ± 2S.D., and the mean ± 3S.D. for all measurements, respectively.

The precisions of the cV is equated to its coefficient of variation (= S.D. / mean). They were 0.045 % for apparatus A in RF21-06, 0.070 % for apparatus A in RF21-07, 0.066 % for apparatus A in RF21-08, 0.073 % for apparatus B in RF21-06, 0.047 % for apparatus B in RF21-07 and 0.064 % for apparatus B in RF21-08. They correspond to 0.93 μmol kg^{-1}, 1.44 μmol kg^{-1}, 1.36 μmol kg^{-1}, 1.51 μmol kg^{-1}, 0.98 μmol kg^{-1} and 1.33 μmol kg^{-1} in C_T of SSW batch AH, respectively.

Finally, the C_T was multiplied by 1.00067 (= 300.2 / 300.0) to correct dilution effect induced by addition of 0.2 mL of mercury (II) chloride ($HgCl_2$) solution in a sampling bottle with a volume of ~300 mL.

(32) Quality Control

(6.1) Replicate and duplicate analyses

We took replicate (pair of water samples taken from a single Niskin bottle) and duplicate (pair of water samples taken from different Niskin bottles closed at the same depth) samples of DIC during the cruise. Table C.6.3 summarizes the results of the measurements with each apparatus (A, B). Figures C.6.4–C.6.5 show details of the results. The calculation of the standard deviation from the difference of sets of measurements was based on a procedure (SOP 23) in DOE (1994).

Table C.6.3. Summary of replicate and duplicate measurements. Unit is μmol kg^{-1}.

	Apparatus A	Apparatus B
Measurement	Average magnitude of difference ± S.D.	
Replicate	2.1±2.0 (N=56)	0.9±0.9 (N=70)
Duplicate	1.9±1.9 (N=21)	0.9±0.8 (N=20)

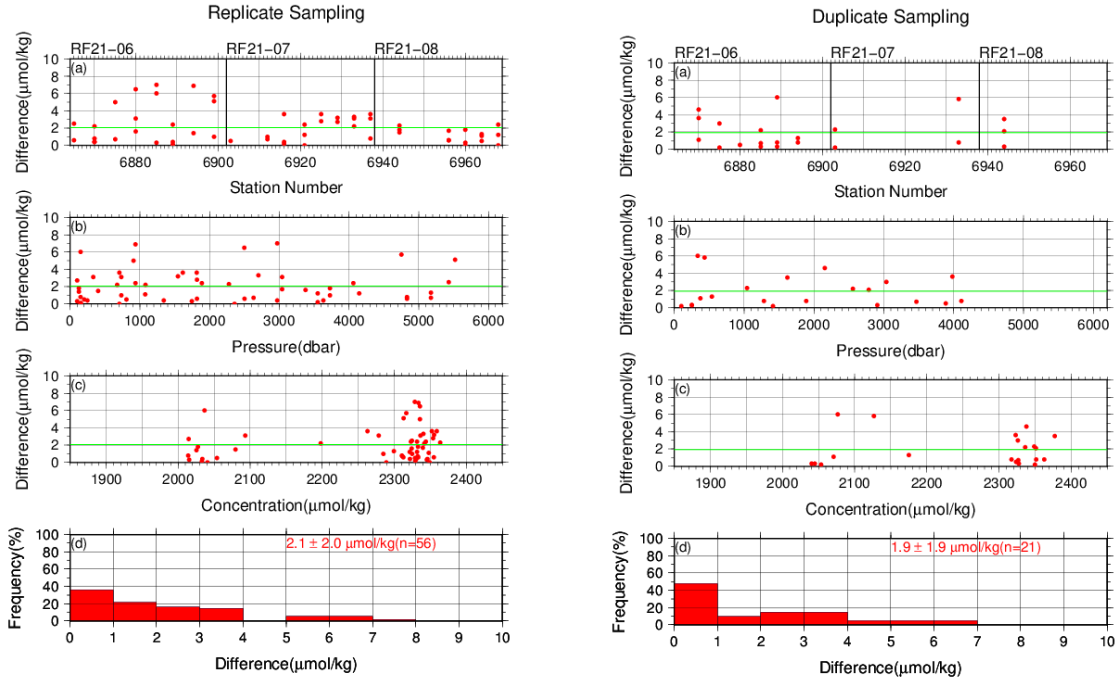

Figure C.6.4. Results of (left) replicate and (right) duplicate measurements during the cruise versus (a) station number, (b) pressure, and (c) C_T determined by apparatus A. The green lines denote the averages of the measurements. The bottom panels (d) show histograms of the measurements.

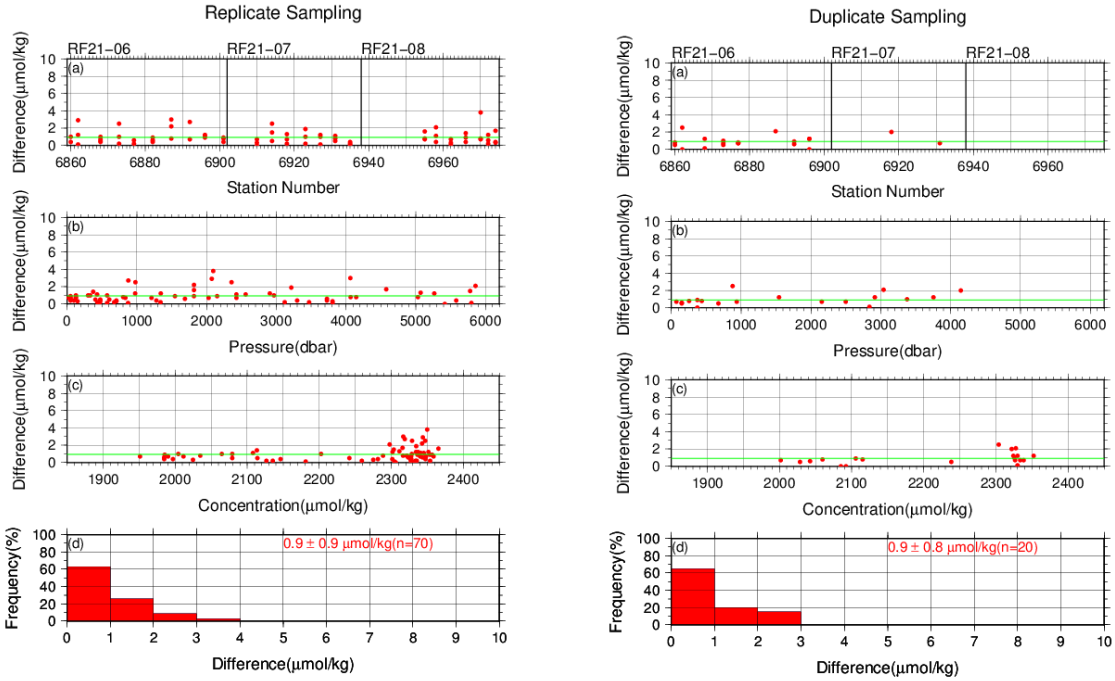

Figure C.6.5. Same as Figure C.6.4, but for apparatus B.

(6.2) Measurements of SSW and CRMs

The precision of the measurements was monitored by using SSW bottled in our laboratory (Appendix A2). At the beginning of the measurement of every station, we measured SSW as a working reference material. If the result were confirmed to be good, measurements of seawater samples were started. As a set of analysis, we measured all seawater samples acquired from a single station. At the end of the sequence of measurements, we measured another SSW bottle to confirm condition of the measurement again. Additionally, we measured a CRM bottle every few stations to confirm a temporal stability of measurement through the cruise. In the cruise, the CRM batch 187 was used (Table C.6.1). The CRM measurement was repeated twice consecutively from the same bottle. Table C.6.4 summarizes the mean C_T of SSW

measurements, the differences and the mean C_T of the repeated measurements of the CRM. Figures C.6.6–C.6.8 show detailed results.

Table C.6.4. Summary of the mean C_T of SSW, the differences and the mean C_T of the repeated measurements of the CRM. These data are based on good measurements. Unit is μ mol kg^{-1}.

Cruise	Apparatus	Mean Ave. ± S.D. (SSW)	Average magnitude of difference ± S.D. (CRM)	Mean Ave. ± S.D. (CRM)
RF21-06	A	2065.6±0.9 (N=16)	1.5±1.3 (N=3)	2004.4±0.1 (N=3)
	B	2065.6±1.5 (N=21)	0.7±0.5 (N=5)	2002.8±1.0 (N=5)
RF21-07	A	2065.6±1.4 (N=19)	2.5±2.0 (N=6)	2003.8±1.3 (N=6)
	B	2065.6±1.0 (N=16)	0.5±0.4 (N=6)	2002.8±1.1 (N=6)
RF21-08	A	2065.6±1.4 (N=13)	1.1±0.8 (N=4)	2003.4±1.1 (N=4)
	B	2065.6±1.3 (N=16)	1.2±1.1 (N=3)	2002.5±0.7 (N=3)

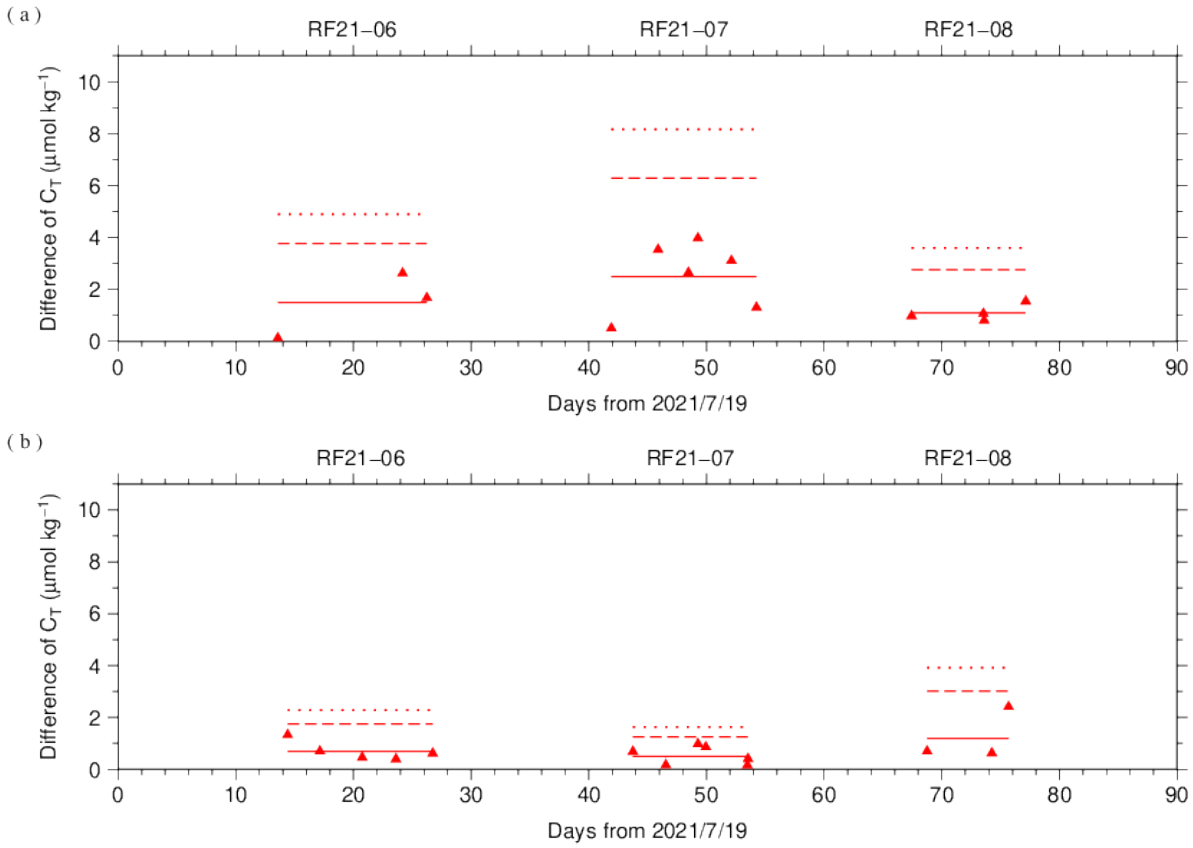

Figure C.6.6. The absolute difference (R) of C_T in repeated measurements of CRM determined by apparatus (a) A and (b) B. The solid line indicates the average of R ($\bar{R}$). The dashed and dotted lines denote the upper warning limit ($2.512\bar{R}$) and upper control limit ($3.267\bar{R}$), respectively (see Dickson et al., 2007).

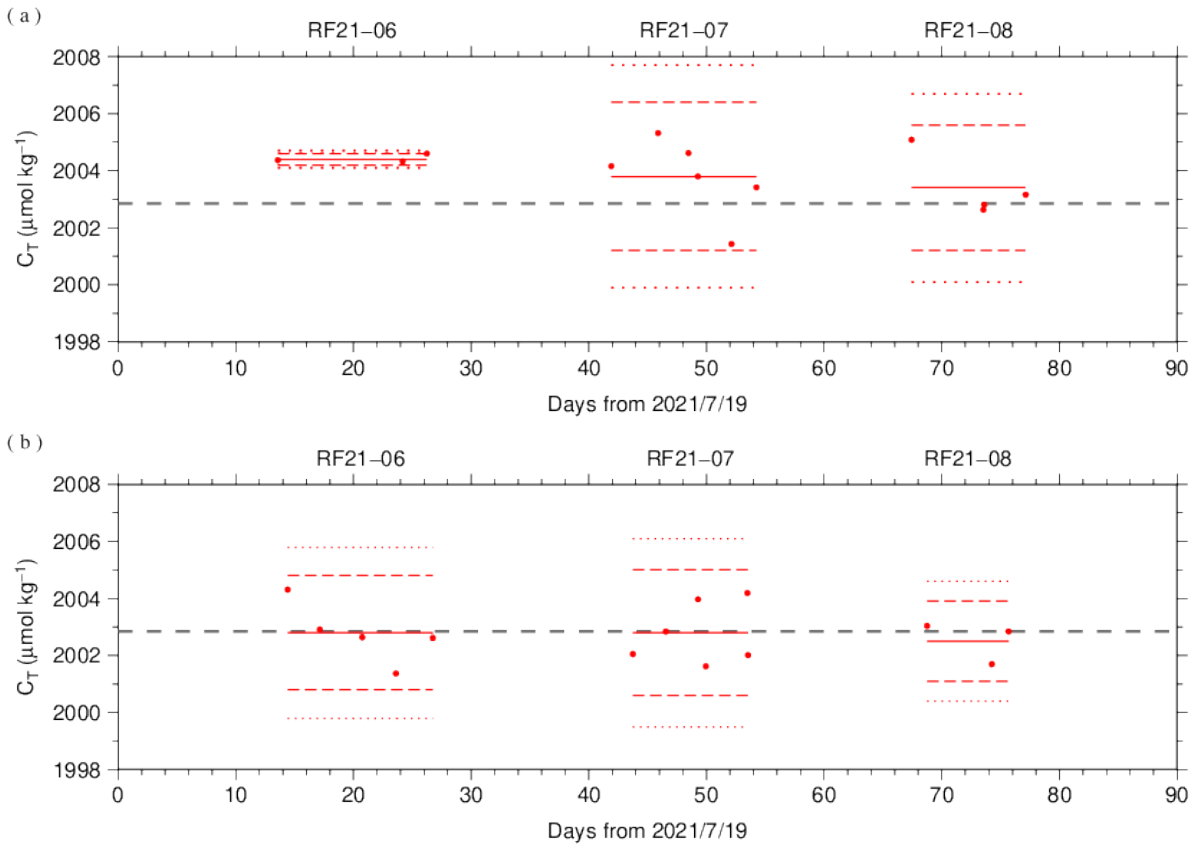

Figure C.6.7. The mean C_T of measurements of CRM. The panels show the results for apparatus (a) A and (b) B. The solid line indicates the mean of the measurements throughout the cruise. The dashed and dotted lines denote the upper/lower warning limit (mean ± 2S.D.) and the upper/lower control limit (mean ± 3S.D.), respectively. The gray dashed line denotes certified C_T of CRM.

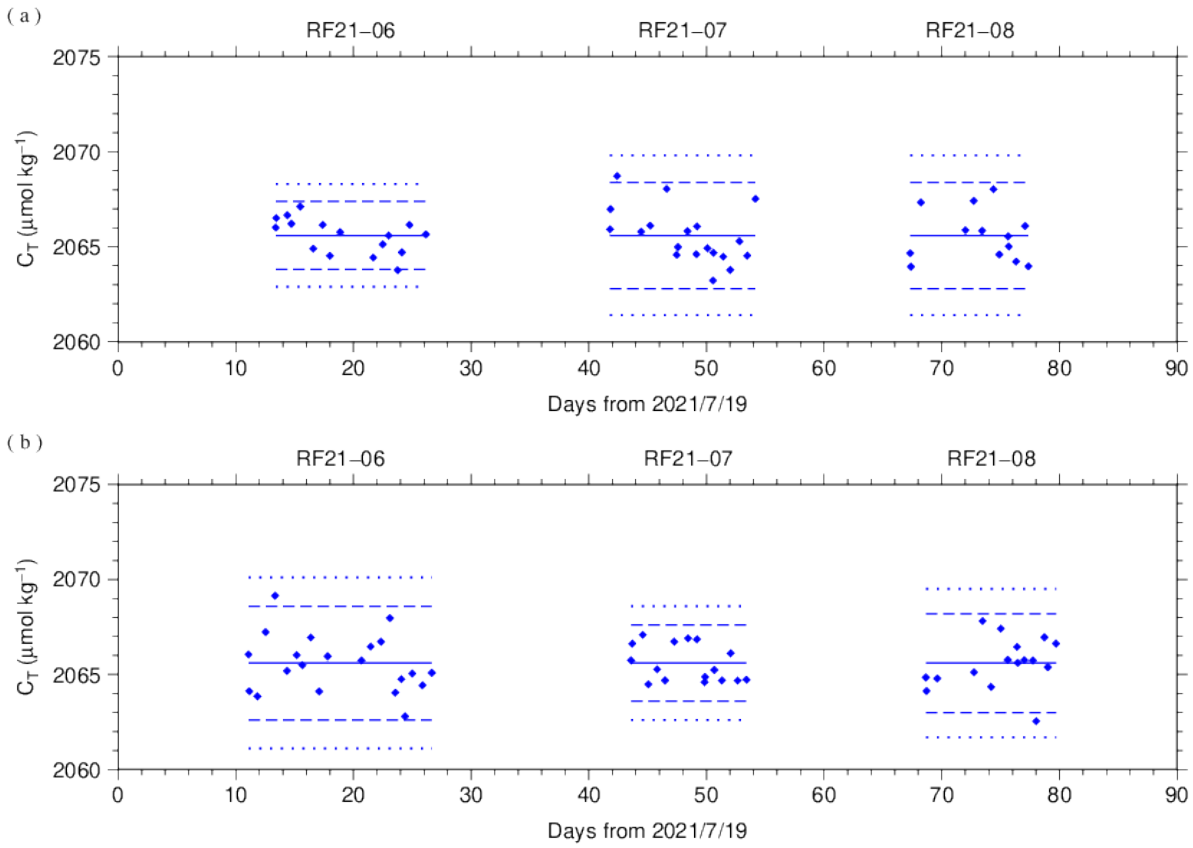

Figure C.6.8. C_T of SSW measured by apparatus (a) A and (b) B. The solid, dashed and dotted lines are the same as in Figure C.6.7.

(6.3) Quality control flag assignment

A quality control flag value was assigned to the DIC measurements (Table C.6.5) using the code defined in the IOCCP Report No.14 (Swift, 2010).

Table C.6.5. Summary of assigned quality control flags.

Flag	Definition	Number of samples
2	Good	1330
3	Questionable	11

4	Bad (Faulty)	3
5	Not reported	0
6	Replicate measurements	119
Total number of samples		1463

Appendix

A1. Methods

(A1.1) Seawater sampling

Seawater samples were collected from 10-liters Niskin bottles mounted on CTD-system and a stainless steel bucket for the surface. Samples for DIC/TA were transferred to Schott Duran® glass bottles (screw top) using sample drawing tubes. Bottles were filled smoothly from the bottom after overflowing double a volume while taking care of not entraining any bubbles, and lid temporarily with inner polyethylene cover and screw cap.

After all sampling finished, 2 mL of sample is removed from each bottle to make a headspace to allow thermal expansion, and then samples were poisoned with 0.2 mL of saturated $HgCl_2$ solution and covered tight again.

(A1.2) Measurement

The unit for DIC measurement in the coupled DIC/TA analyzer consists of a coulometer with a quartz coulometric titration cell, a CO_2 extraction unit and a reference gas injection unit. The CO_2 extraction unit, which is connected to a bottle of 20 % v/v phosphoric acid and a carrier N_2 gas supply, includes a sample pipette (approx. 12 mL) and a CO_2 extraction chamber, two thermoelectric cooling units and switching valves. The coulometric titration cell and the sample pipette are water-jacketed and are connected to a thermostated (25 ° C) water bath. The automated procedures of DIC analysis in seawater were as follows (Ishii et al., 1998):

(a) Approximately 2 mL of 20 % v/v phosphoric acid was injected to an "extraction chamber", *i.e.*, a glass tube with a course glass frit placed near the bottom. Purified N_2 was then allowed to flow through the extraction chamber to purge CO_2 and other volatile acids dissolved in the phosphoric acid.

(b) A portion of sample seawater was delivered from the sample bottle into the sample pipette of CO_2 extraction unit by pressurizing the headspace in the sample bottle. After temperature of the pipette was recorded, the sample seawater was transferred into the extraction chamber and mixed with phosphoric acid to convert all carbonate species to CO_2 (aq).

(c) The acidified sample seawater was then stripped of CO_2 with a stream of purified N_2. After being dehumidified in a series of two thermoelectric cooling units, the evolved CO_2 in the N_2 stream was introduced into the carbon cathode solution in the coulometric titration cell and then CO_2 was electrically titrated.

A2. Working reference material recipe

To produce in-house standard sea water (SSW) used as a working reference material, the surface seawater taken from the western North Pacific, and settled at least a half year in our laboratory. Before bottling, seawater was filtered by membrane filter (0.45 μm-mesh) using magnetic pump and was transferred into a large tank. Then, filtered seawater in the tank was processed in cycle filtration again for 3 hours and was agitated in clean condition air for 6 hours. On the next day, agitated 5 minutes to remove small

bubbles on the tank and transfer to Schott Duran® glass bottles (about 300 mL) as the same method as samples (Appendix A1.1) except for overflowing a half of volume, not double. Created of headspace and poisoned with $HgCl_2$ was as the same as samples, finally, sealed by ground glass stoppers lubricated with Apiezon® grease (L).

References

Dickson, A. G., C. L. Sabine, and J. R. Christian (Eds.) (2007), Guide to best practices for ocean CO_2 measurements. *PICES Special Publication 3*, 191 pp.

DOE (1994), Handbook of methods for the analysis of the various parameters of the carbon dioxide system in sea water; version 2. *A. G. Dickson and C. Goyet (eds), ORNL/CDIAC-74*.

Ishii, M., H. Y. Inoue, H. Matsueda, and E. Tanoue (1998), Close coupling between seasonal biological production and dynamics of dissolved inorganic carbon in the Indian Ocean sector and the western Pacific Ocean sector of the Antarctic Ocean, *Deep Sea Res. Part I*, **45**, 1187–1209, doi:10.1016/S0967-0637(98)00010-7.

Johnson, K. M., A. E. King and J. McN. Sieburth (1985), Coulometric TCO2 analyses for marine studies; an introduction. *Marine Chemistry*, **16**, 61–82.

Johnson, K. M., J. M. Sieburth, P. J. L. Williams and L. Brändström (1987), Coulometric total carbon dioxide analysis for marine studies: Automation and calibration. *Marine Chemistry*, **21**, 117–133.

Swift, J. H. (2010): Reference-quality water sample data, Notes on acquisition, record

keeping, and evaluation. *IOCCP Report No.14, ICPO Pub.* 134, 2010 ver.1.

7. Total Alkalinity (TA)

30 September 2023

(33) Personnel

DEHARA Kohshiro

HAMANA Minoru

NAKAMURA Naoki

(34) Station occupied

A total of 45 stations (RF21-06: 18, RF21-07: 15, RF21-08: 12) were occupied for total alkalinity (TA). Station location and sampling layers of them are shown in Figures C.7.1 and C.7.2, respectively.

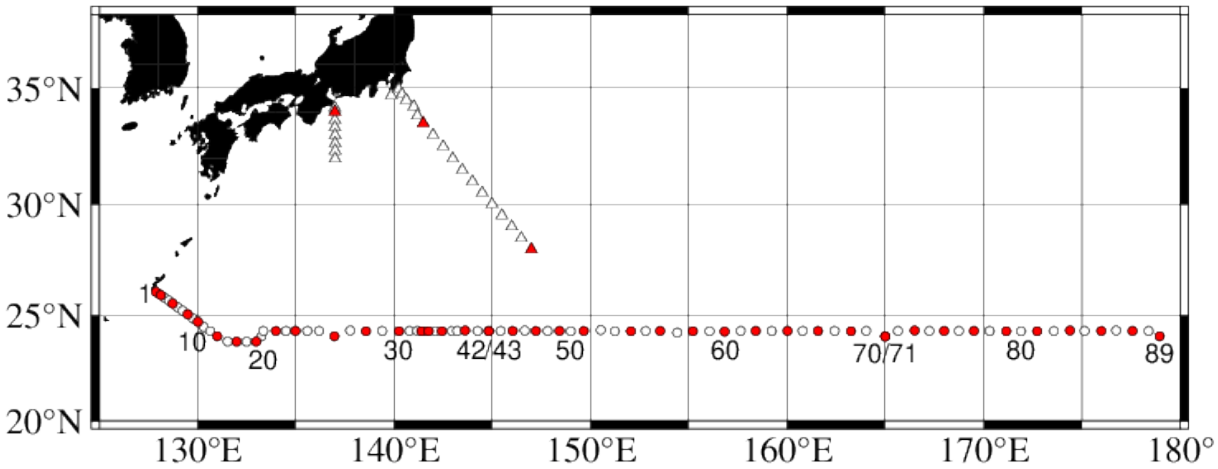

Figure C.7.1. Location of observation stations of TA. Closed and open circles indicate sampling and no-sampling stations, respectively. Triangles show sampling station

which are not reported in the bottle data file, but the data at closed triangles are used for quality control of TA. These data are available from the JMA (https://www.data.jma.go.jp/gmd/kaiyou/db/vessel_obs/data-report/html/ship/ship_e.php?year=2021&season=summer).

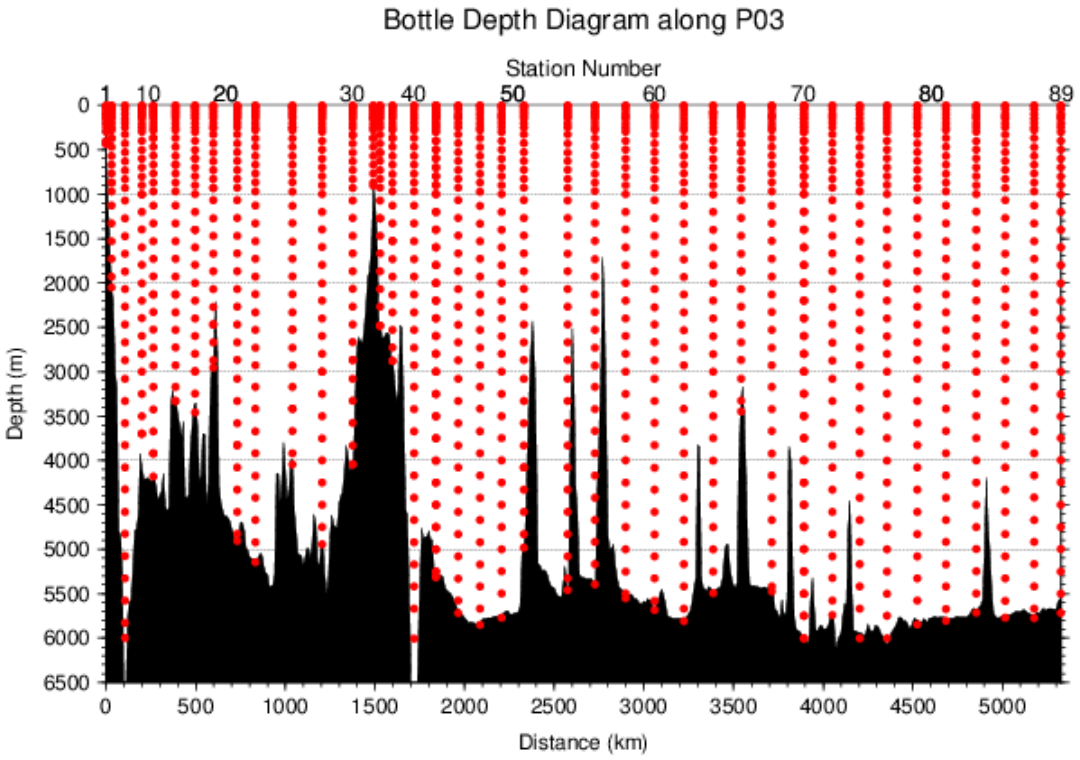

Figure C.7.2. Distance-depth distribution of sampling layers of TA.

(35) Instrument

The measurement of TA was carried out with DIC/TA analyzers (Nihon ANS Co. Ltd., Japan). The methodology that these analyzers use is based on an open titration cell. We used two analyzers concurrently. These analyzers are designated as apparatus A and B.

(36) Sampling and measurement

The procedure of seawater sampling of TA bottles and poisoning with mercury (II) chloride ($HgCl_2$) were based on the Standard Operating Procedure (SOP) described in PICES Special Publication 3 (Dickson et al., 2007). Details are shown in Appendix A1 in C.6.

TA measurement is based on a one-step volumetric addition of hydrochloric acid (HCl) to a known amount of sample seawater with prompt spectrophotometric measurement of excess acid using the sulfonephthalein indicator bromo cresol green sodium salt (BCG) (Breland and Byrne, 1993). We used a mixed solution of HCl, BCG, and sodium chloride (NaCl) as reagent. Details of measurement are shown in Appendix A1.

(37) Calculation

(5.1) Volume of sample seawater

The volumes of pipette V_S using in apparatus A and B was calibrated gravimetrically in our laboratory. Table C.7.1 shows the summary.

Table C.7.1. Summary of sample volumes of seawater V_S for TA measurements.

Apparatus	Vs / mL
A	42.8099
B	41.4764

(5.2) pH_T calculation in spectrophotometric measurement

The data of absorbance A and pipette temperature T (in ° C) were processed to calculate pH_T (in total hydrogen ion scale; details shown in Appendix A1 in C.8) and the concentration of excess acid $[H^+]_T$ (mol kg^{-1}) in the following equations (C7.1)–

(C7.3) (Yao and Byrne, 1998),

$$pH_T = -\log_{10}([H^+]_T)$$

$$= 4.2699 + 0.02578 \cdot (35 - S) + \log\{(R_{25} - 0.00131) / (2.3148 - 0.1299 \cdot R_{25})\}$$

$$- \log(1 - 0.001005 \cdot S)$$

(C7.1)

$$R_{25} = R_T \cdot \{1 + 0.00909 \cdot (25 - T)\} \quad \text{(C7.2)}$$

$$R_T = \left(A_{616}^{SA} - A_{616}^{S} - A_{730}^{SA} + A_{730}^{S}\right)/\left(A_{444}^{SA} - A_{444}^{S} - A_{730}^{SA} + A_{730}^{S}\right). \quad \text{(C7.3)}$$

In the equation (C7.1), R_T is absorbance ratio at temperature T, R_{25} is absorbance ratio at temperature 25 ° C and S is salinity. A_λ^S and A_λ^{SA} denote absorbance of seawater before and after acidification, respectively, at wavelength λ nm.

(5.3) TA calculation

The calculated $[H^+]_T$ was then combined with the volume of sample seawater V_S, the volume of titrant V_A added to the sample, and molarity of hydrochloric acid HCl_A (in mmol L^{-1}) in the titrant to determine to TA concentration A_T (in μmol kg^{-1}) as follows:

$$A_T = (-[H^+]_T \cdot (V_S + V_A) \cdot \rho_{SA} + HCl_A \cdot V_A) / (V_S \cdot \rho_S) \quad \text{(C7.4)}$$

ρ_S and ρ_{SA} denote the density of seawater sample before and after the addition of titrant, respectively. Here we assumed that ρ_{SA} is equal to ρ_S, since the density of titrant has been adjusted to that of seawater by adding NaCl and the volume of titrant (approx. 2.5 mL) is no more than approx. 6 % of seawater sample.

Finally, the value of A_T was multiplied by 1.00067 (= 300.2 / 300.0) to correct dilution effect in A_T induced by addition of $HgCl_2$ solution.

(38) Standardization of HCl reagent

HCl reagents were prepared in our laboratory (Appendix A2) and divided into bottles (HCl batches). The determination of HCl_A was based on measurements of standard sea water (SSW) which was bottled in our laboratory at November 27th, 2019 (Appendix A2 in C.6). The SSWs show good homogeneity among bottles and good temporal stability of A_T at least 12 months. The determination of A_T of SSW was based on pre-cruise measurements at October 26th, 2020 using CRMs provided by Dr. Andrew G. Dickson of the Scripps Institution of Oceanography. The list of lot of the SSW and the batch of the CRMs is shown in Table C.7.2.

Table C.7.2. Assigned A_T and standard deviation of SSW and certified A_T and standard deviation of CRM. Unit of A_T is μmol kg^{-1}. More information about CRM is available at the NOAA web site (https://www.ncei.noaa.gov/access/ocean-carbon-acidification-data-system/oceans/Dickson_CRM/batches.html).

	SSW	CRM
Lot/batch	AH	187
A_T	2266.99±0.64	2204.98±0.37
Salinity	34.538	33.602

The apparent HCl_A of the titrant was determined from assigned SSW using equation (C7.4).

HCl_A was assigned for each HCl batches for each apparatus, as summarized in Table C.7.3 and detailed in Figure C.7.3.

Table C.7.3. Summary of assigned HCl_A for each HCl batches. The reported values are means and standard deviations. Unit is mmol L^{-1}.

Apparatus	Cruise	HCl Batch	HCl_A
A	RF21-06	A_1	50.0806±0.0171 (N=18)
		A_2	50.0986±0.0197 (N=19)
	RF21-07	A_3	50.0556±0.0230 (N=16)
		A_4	50.1493±0.0411 (N=20)
	RF21-08	A_5	50.0384±0.0521 (N=6)
		A_6	50.0386±0.0554 (N=4)
		A_7	49.9667±0.0296 (N=6)
		A_8	49.9409±0.0511 (N=6)
		A_9	49.8942±0.0487 (N=6)
B	RF21-06	B_1	50.0740±0.0341 (N=21)
		B_2	50.1629±0.0304 (N=19)
	RF21-07	B_3	50.1984±0.0211 (N=17)
		B_4	50.2224±0.0241 (N=12)
	RF21-08	B_5	50.1977±0.0215 (N=14)
		B_6	50.1878±0.0207 (N=16)

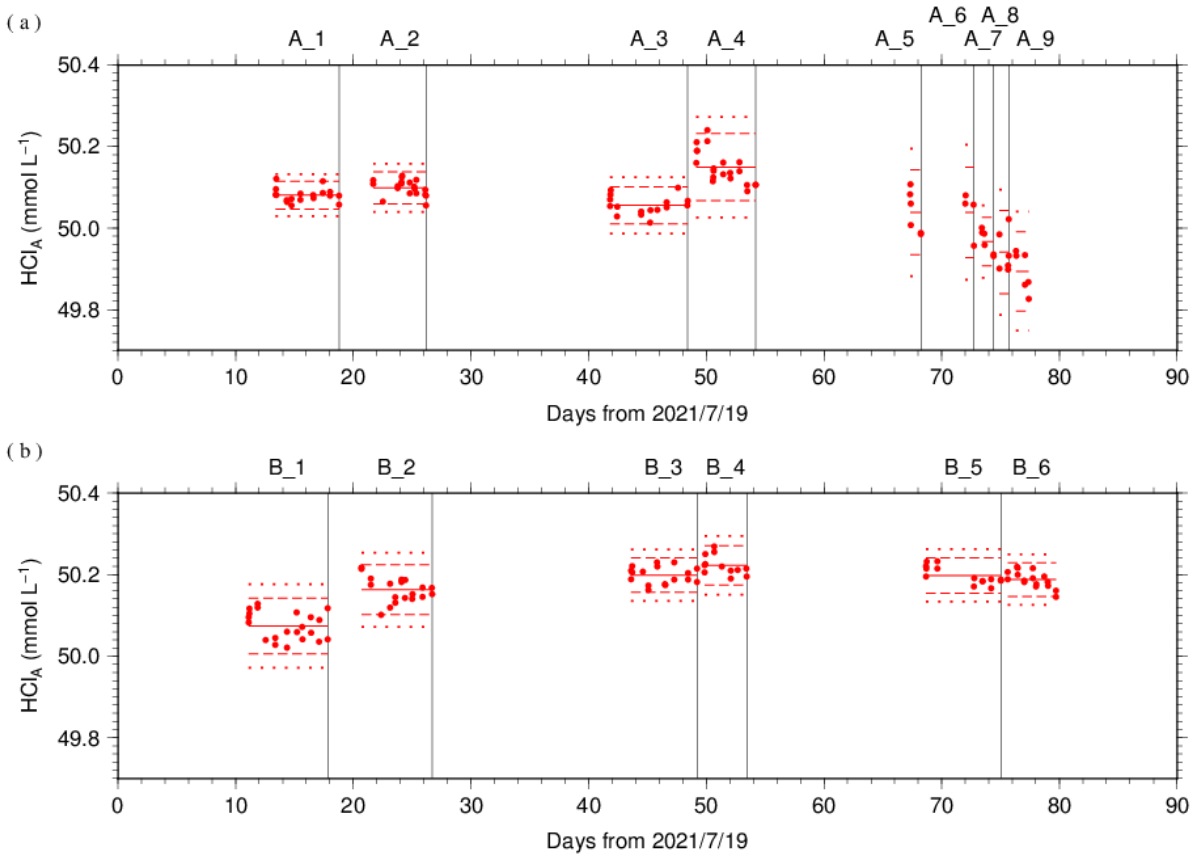

Figure C.7.3. Results of HCl_A measured by apparatus (a) A and (b) B. The HCl batch names are indicated at the top of each graph, and vertical lines denote the day when the HCl batch was switched. The red solid, dashed, and dotted lines denote the mean and the mean ± twice the S.D. and thrice the S.D. for each HCl batches, respectively.

The precisions of HCl_A, defined as the coefficient of variation (= S.D. / mean), were 0.0341–0.1107 % for apparatus A and 0.0412–0.0681 % for apparatus B. They correspond to 0.77–2.51 μmol kg^{-1} and 0.94–1.54 μmol kg^{-1} in A_T of SSW batch AH, respectively.

(39) Quality Control

(7.1) Replicate and duplicate analyses

We took replicate (pair of water samples taken from a single Niskin bottle) and duplicate (pair of water samples taken from different Niskin bottles closed at the same depth) samples of TA throughout the cruise. Table C.7.4 summarizes the results of the measurements with each apparatus. Figures C.7.4–C.7.5 show details of the results. The calculation of the standard deviation from the difference of sets of measurements was based on a procedure (SOP 23) in DOE (1994).

Table C.7.4. Summary of replicate and duplicate measurements. Unit is μmol kg^{-1}.

	Apparatus A	Apparatus B
Measurement	Average magnitude of difference ± S.D.	
Replicate	1.1±1.0 (N=63)	0.9±0.8 (N=70)
Duplicate	0.9±0.8 (N=22)	0.9±0.9 (N=20)

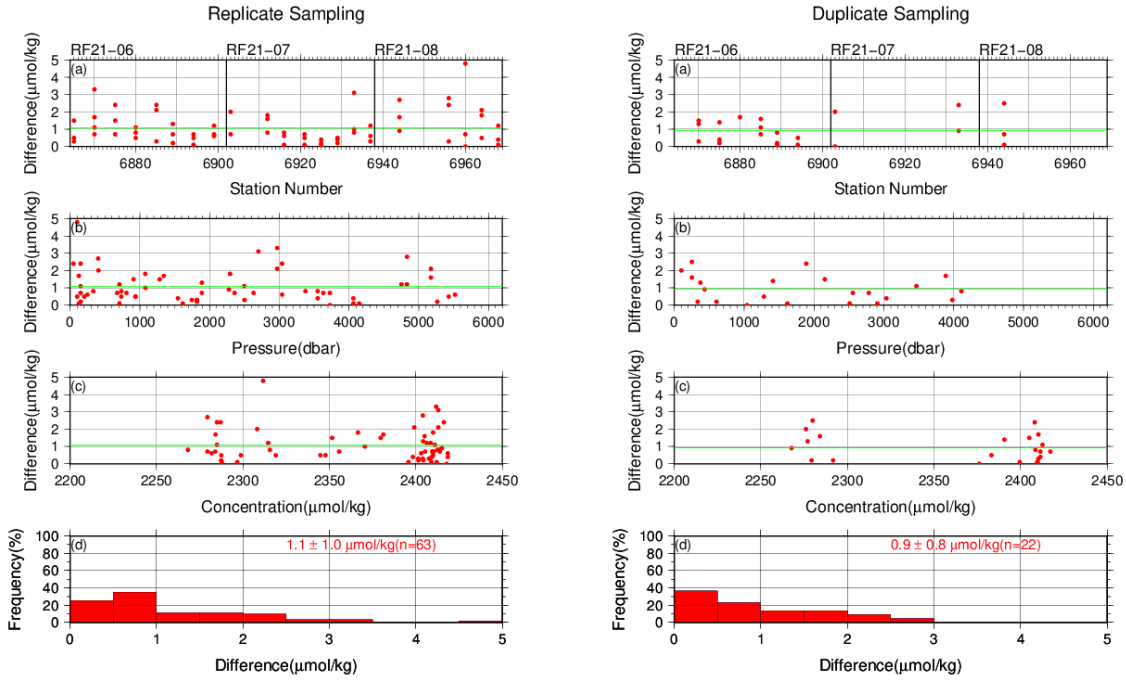

Figure C.7.4. Results of (left) replicate and (right) duplicate measurements during the cruise versus (a) station number, (b) pressure, and (c) A_T determined by apparatus A. The green lines denote the averages of the measurements. The bottom panels (d) show histograms of the measurements.

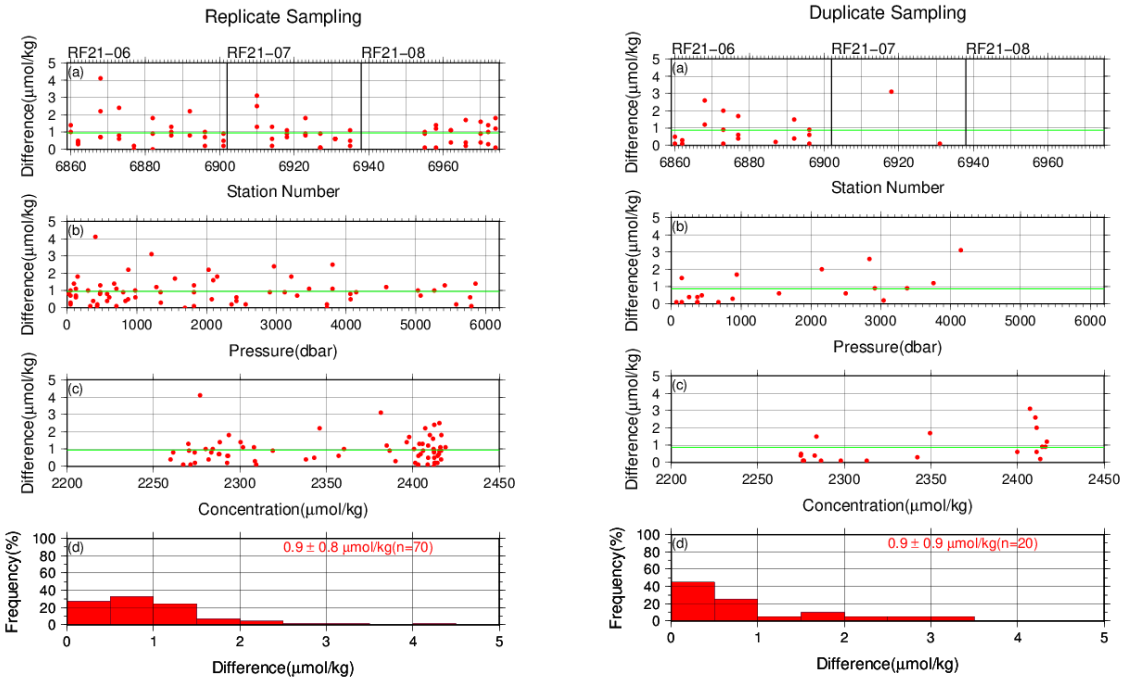

Figure C.7.5. Same as Figure C.7.4, but for apparatus B.

(7.2) Measurements of SSW and CRMs

At analysis of TA samples, we started by measurement of a SSW. If the condition of the measurement was good, measurements of seawater samples were started. As a set of analysis, we measured all seawater samples acquired from a single station. At the end of the sequence of measurements, we measured another SSW bottle to confirm condition of the measurement again. Additionally, we measured a CRM bottle every few stations to confirm a temporal stability of measurement through the cruise. In the cruise, the CRM batch 187 was used (Table C.7.2). SSW and CRM measurements were repeated at 2 and 3 times consecutively from the same bottle, respectively. Table C.7.5 summarizes the differences in the repeated measurements of the SSW and CRM and the mean A_T of the SSW and CRM measurements. Figures C.7.6–C.7.8 show detailed

results.

Table C.7.5. Summary of difference and mean of A_T in the repeated measurements of SSW and CRM. These data are based on good measurements. Unit is μmol kg^{-1}.

Cruise	HCl Batch	Average magnitude of difference ± S.D. (SSW)	Average magnitude of difference ± S.D. (CRM)	Mean Ave. ± S.D. (SSW)	Mean Ave. ± S.D. (CRM)
RF21-06	A_1	0.8±0.7 (N=9)	1.0±0.7 (N=3)	2267.0±0.7 (N=9)	2204.0±1. (N=3)
	A_2	0.6±0.6 (N=9)	0.9±0.7 (N=2)	2266.9±0.8 (N=9)	2204.6±0. (N=2)
RF21-07	A_3	0.8±0.6 (N=7)	0.8±0.6 (N=3)	2267.1±0.9 (N=7)	2204.1±2. (N=3)
	A_4	0.8±0.8 (N=10)	0.7±0.6 (N=3)	2267.0±1.9 (N=10)	2204.7±2. (N=3)
RF21-08	A_5	1.3±1.1 (N=3)	1.4 (N=1)	2267.0±2.6 (N=3)	2206.4 (N=1)

	A_6	2.8±2.4 (N=2)	–	2267.0±2.1 (N=2)	–
	A_7	0.7±0.6 (N=3)	1.9 (N=1)	2267.0±1.5 (N=3)	2208.2 (N=1)
	A_8	2.9±2.4 (N=3)	–	2267.0±1.8 (N=3)	–
	A_9	2.0±1.7 (N=3)	1.3 (N=1)	2267.0±2.2 (N=3)	2207.0 (N=1)
RF21-06	B_1	1.6±1.3 (N=10)	0.6±0.4 (N=3)	2266.9±1.3 (N=10)	2204.9±0. (N=3)
	B_2	1.0±0.9 (N=9)	1.1±0.8 (N=4)	2266.8±1.2 (N=9)	2205.4±1. (N=4)
RF21-07	B_3	0.9±0.8 (N=8)	1.2±0.9 (N=2)	2267.0±0.9 (N=8)	2204.3±0. (N=2)
	B_4	0.9±0.7 (N=5)	1.4±1.1 (N=3)	2266.9±1.2 (N=5)	2205.3±0. (N=3)
RF21-	B_5	0.7±0.6	1.5±1.2	2267.0±1.0	2205.2±1.

08	(N=7)	(N=2)	(N=7)	(N=2)
B_6	0.6±0.5 (N=7)	2.0±1.4 (N=2)	2267.1±0.9 (N=7)	2203.9±1. (N=2)

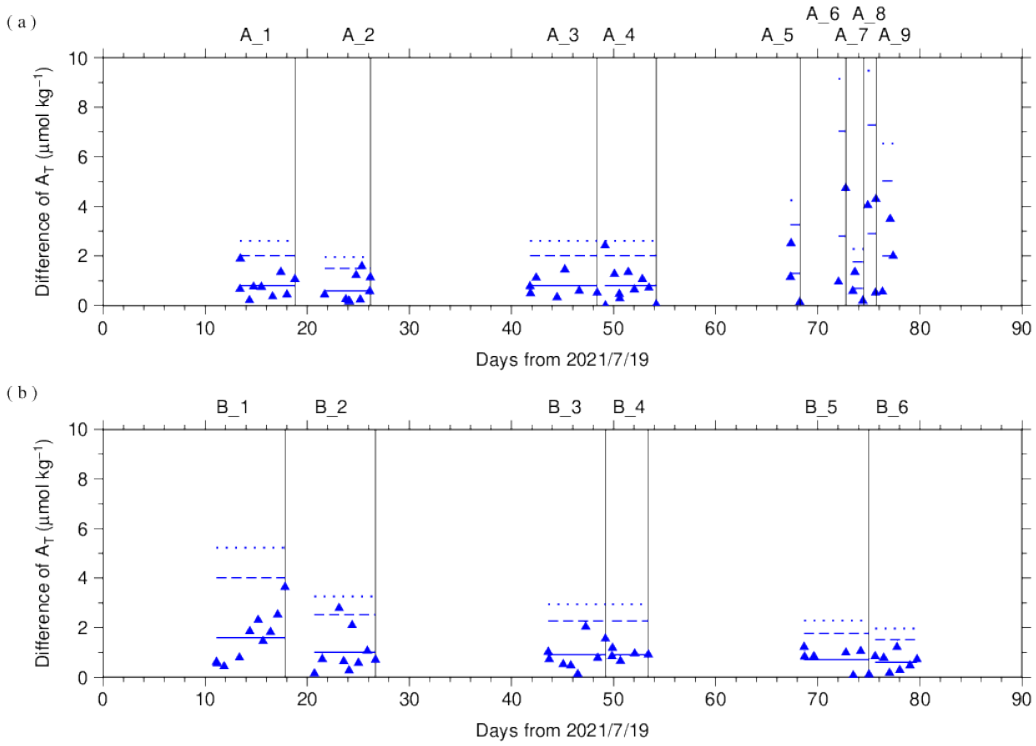

Figure C.7.6. The absolute difference (R) of A_T in repeated measurements of SSW determined by apparatus (a) A and (b) B. The solid line indicates the average of R ($\bar{R}$). The dashed and dotted lines denote the upper warning limit ($2.512\bar{R}$) and upper control limit ($3.267\bar{R}$), respectively (see Dickson et al., 2007). The labels at the top of the graph and vertical lines have the same meaning as in Figure C.7.3.

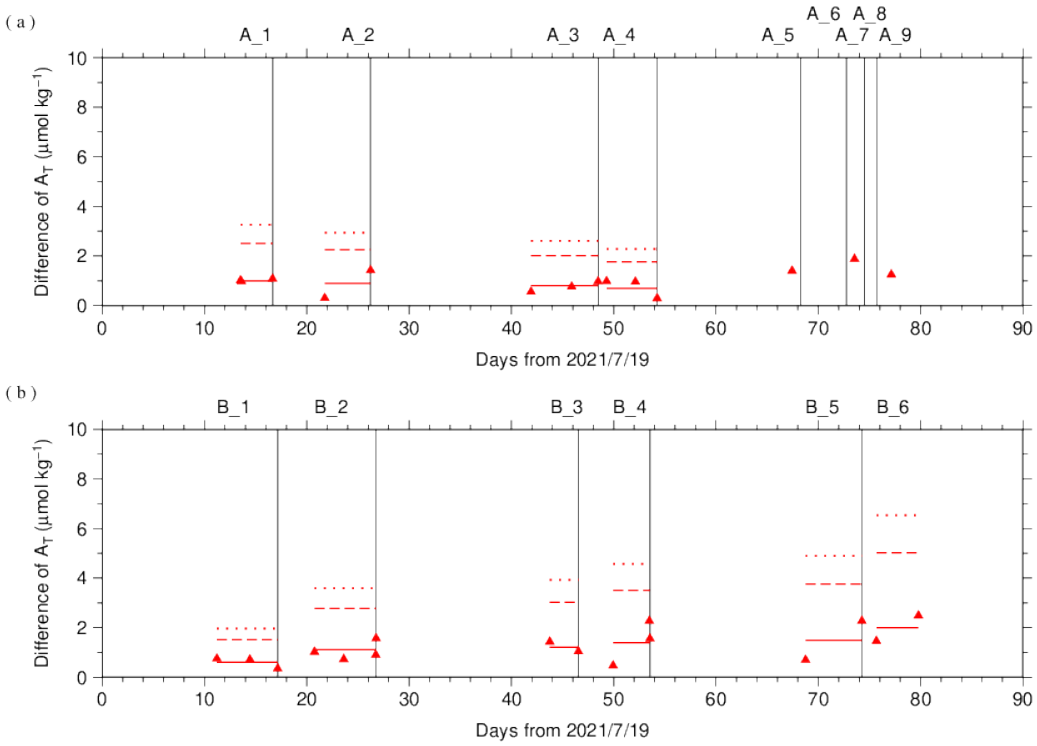

Figure C.7.7. Same as Figure C.7.6, but for CRM.

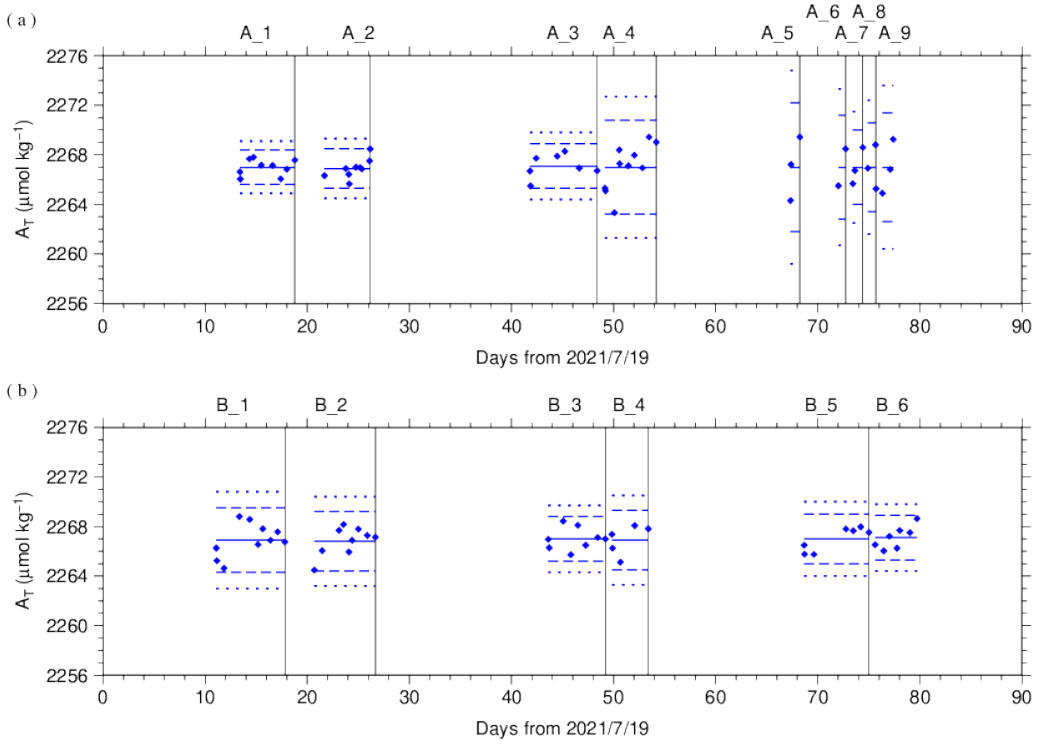

Figure C.7.8. The mean A_T of measurements of SSW. The panels show the results for

apparatus (a) A and (b) B. The solid line indicates the mean of the measurements. The dashed and dotted lines denote the upper/lower warning limit (mean ± 2S.D.) and the upper/lower control limit (mean ± 3S.D.), respectively. The labels at the top of the graph and vertical lines have the same meaning as in Figure C.7.3.

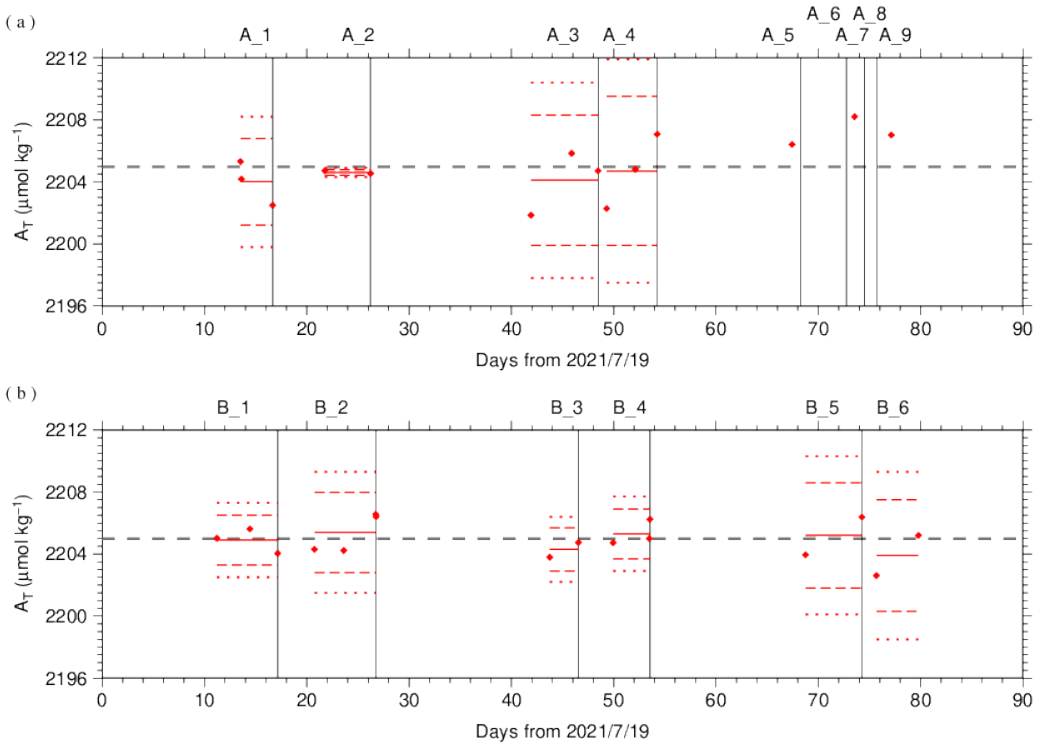

Figure C.7.9. Same as Figure C.7.8, but for CRM. The gray dashed line denotes certified A_T of CRM.

(7.3) Quality control flag assignment

A quality control flag value was assigned to the TA measurements (Table C.7.6) using the code defined in the IOCCP Report No.14 (Swift, 2010).

Table C.7.6. Summary of assigned quality control flags.

Flag	Definition	Number of samples
2	Good	1327
3	Questionable	7
4	Bad (Faulty)	4
5	Not reported	0
6	Replicate measurements	125
Total number of samples		1463

Appendix

A1. Methods

(A1.1) Measurement

The unit for TA measurements in the coupled DIC/TA analyzer consists of sample treatment unit with a calibrated sample pipette and an open titration cell that are water-jacketed and connected to a thermostated water bath (25 °C), an auto syringe connected to reagent bottle of titrant stored at 25 °C, and a double-beam spectrophotometric system with two CCD image sensor spectrometers combined with a high power Xenon lamp. The mixture of 0.05 N HCl and 40 μmol L^{-1} BCG in 0.65 M NaCl solution was used as reagent to automatically titrate the sample as follows:

(a) A portion of sample seawater was delivered into the sample pipette (approx. 42 mL) following sample delivery into the DIC unit for a measurement. After the temperature in the pipette was recorded, the sample was transferred into a cylindrical quartz cell.

(b) An absorption spectrum of sample seawater in the visible light domain was then measured, and the absorbances were recorded at wavelengths of 444 nm, 509 nm, 616 nm, and 730 nm as well as the temperature in the cell.

(c) The titrant that contains HCl was added to the sample seawater by the auto syringe so that pH of sample seawater altered in the range between 3.85 and 4.05.

(d) While the acidified sample was being stirred, the evolved CO_2 was purged with the stream of purified N_2 bubbled into the sample at approx. 200 mL min^{-1} for 5 minutes.

(e) After the bubbled sample steadied down for 1 minute, the absorbance of BCG in the sample was measured in the same way as described in (b), and pH (in total hydrogen ion scale, pH_T) of the acidified seawater was precisely determined spectrophotometrically.

A2. HCl reagents recipes

0.05 N HCl and 40 μmol L^{-1} BCG in 0.65 M NaCl solution

Dissolve 0.30 g of BCG and 190 g of NaCl in roughly 1.5 L of deionized water (DW)

in a 5 L flask, and slowly add 200 mL concentrated HCl. After the powders completely dissolved, dilute with DW to a final volume of 5 L.

References

Breland II, J. A. and R. H. Byrne (1993), Spectrophotometric procedures for determination of sea water alkalinity using bromocresol green, *Deep-Sea Res. I*, 470, 629–641.

Dickson, A. G., C. L. Sabine, and J. R. Christian (Eds.) (2007), Guide to best practices for ocean CO_2 measurements. PICES Special Publication 3, 191 pp.

DOE (1994), Handbook of methods for the analysis of the various parameters of the carbon dioxide system in sea water; version 2. *A. G. Dickson and C. Goyet (eds), ORNL/CDIAC-74*.

Yao, W. and R. H. Byrne (1998), Simplified seawater alkalinity analysis: Use of linear array spectrometers. *Deep-Sea Res. I*, 45, 1383–1392.

Swift, J. H. (2010): Reference-quality water sample data, Notes on acquisition, record keeping, and evaluation. *IOCCP Report No.**14**, ICPO Pub. 134, 2010 ver.1.*

8. pH

30 September 2023

(40) Personnel

DEHARA Kohshiro

HAMANA Minoru

NAKAMURA Naoki

(41) Station occupied

A total of 45 stations (RF21-06: 18, RF21-07: 15, RF21-08: 12) were occupied for pH. Station location and sampling layers of them are shown in Figures C.8.1 and C.8.2, respectively.

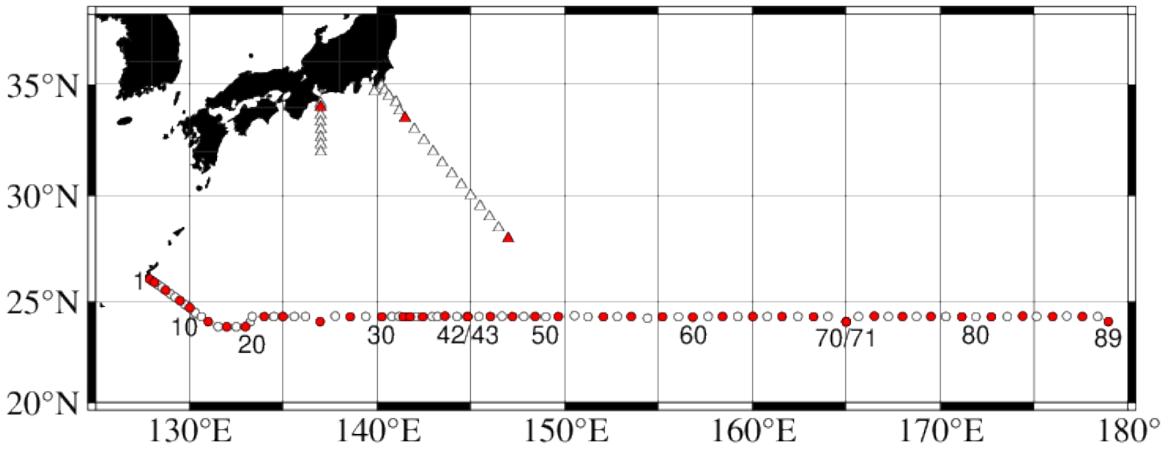

Figure C.8.1. Location of observation stations of pH. Closed and open circles indicate sampling and no-sampling stations, respectively. Triangles show sampling station which are not reported in the bottle data file, but the data at closed triangles are used for quality control of pH. These data are available from the JMA

(https://www.data.jma.go.jp/gmd/kaiyou/db/vessel_obs/data-report/html/ship/ship_e.php?year=2021&season=summer).

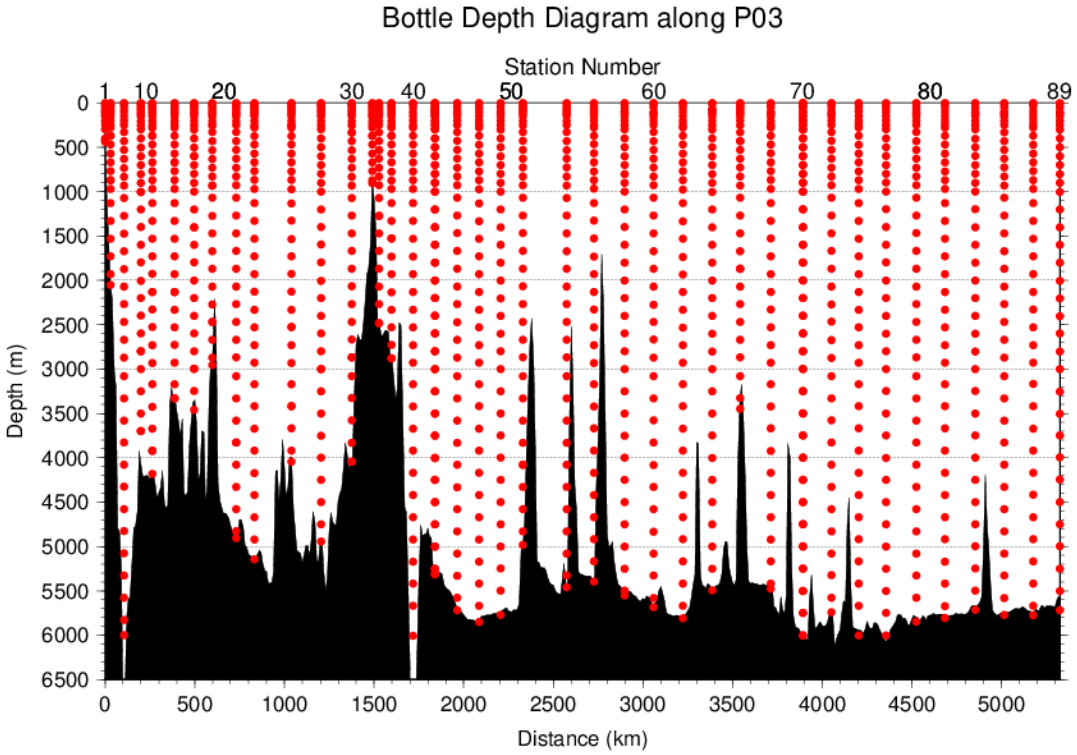

Figure C.8.2. Distance-depth distribution of sampling layers of pH.

(42) Instrument

The measurement of pH was carried out with a pH analyzer (Nihon ANS Co. Ltd, Japan).

(43) Sampling and measurement

Methods of seawater sampling, poisoning, spectrophotometric measurements using the indicator dye *m*-cresol purple (hereafter *m*CP) and calculation of pH_T (on the total

hydrogen ion scale; Appendix A1) were based on Saito et al. (2008). The pH_T is calculated from absorbance ratio (R) with the following equations,

$$pH_T = pK_2 + \log_{10}\{(R - 0.0069)/(2.222 - 0.1331 \cdot R)\} \quad \text{(C8.1)}$$

$$R = \left(A_{578}^{SD} - A_{578}^{S} - A_{730}^{SD} + A_{730}^{S}\right)/\left(A_{434}^{SD} - A_{434}^{S} - A_{730}^{SD} + A_{730}^{S}\right) \quad \text{(C8.2)}$$

where pK_2 is the acid dissociation constant of *m*CP,

$$pK_2 = 1245.69/T + 3.8322 + 0.00211 \cdot (35 - S) \quad \text{(C8.3)}$$

$$(293\ \text{K} \leq T \leq 303\ \text{K},\ 30 \leq S \leq 37).$$

A_λ^S and A_λ^{SD} in equation (C8.2) are absorbance of seawater itself and dye plus seawater, respectively, at wavelength λ (nm). The value of pK_2 in equation (C8.3) is expressed as a function of temperature T (in Kelvin) and salinity S (in psu). Finally, pH_T is reported as the value at temperature of 25 ° C. Details are shown in Appendix A1.

(44) pH perturbation caused by addition of *m*-cresol purple solution

The *m*CP solution using as indicator dye was prepared in our laboratory (Appendix A2) and was subdivided into some bottles (*m*CP batches) that attached to the apparatus. The injection of *m*CP solution perturbs the sample pH_T slightly because the acid-base equilibrium of the seawater is disrupted by the addition of the dye acid-base pair (Dickson et al., 2007).

Before applying R to the equation (C8.1), the measured R in the sample was corrected to that value expected to be unperturbed by the addition of the dye (Dickson et al., 2007; Clayton and Byrne, 1993). The magnitude of the perturbation (ΔR) was

calculated empirically from that by the second addition of the dye and absorbance ratio measurement as follows:

$$\Delta R = R_2 - R_1, \quad \text{(C8.4)}$$

where R_1 and R_2 are the absorbance ratio after the initial addition of dye solution in the sample measurement and after the second addition in the experimental measurement, respectively. Because the value of ΔR depends on the pH_T of sample, we expressed ΔR as a quadratic function of R_1 based on experimental ΔR measurement obtained at this cruise as follows:

$$\Delta R = C_2 \times R_1^2 + C_1 \times R_1 + C_0. \quad \text{(C8.5)}$$

In each measurement for a station, ΔR was measured for about 10 samples from various depths to obtain wide range of R_1 and experimental ΔR data. For each *m*CP batch bottle, coefficients (C_0, C_1 and C_2) were calculated by equation (C8.5), and ΔR was evaluated for each R_1. The coefficients for each *m*CP batch are showed in Table C.8.1. The plots and function curves are illustrated in Figure C.8.3.

Table C.8.1. Summary of coefficients; C_2, C_1 and C_0 in $\Delta R = C_2 \times R_1^2 + C_1 \times R_1 + C_0$.

Stations	*m*CP batch	C_2	C_1	C_0
1–21	1	−1.10745E−03	−1.37833E−02	1.12567E−02
23–42	2	6.11479E−04	−1.49193E−02	1.09467E−02
43–70	3	1.56819E−04	−1.34975E−02	1.24317E−02
71–89	4	−2.92045E−04	−1.36892E−02	1.18006E−02

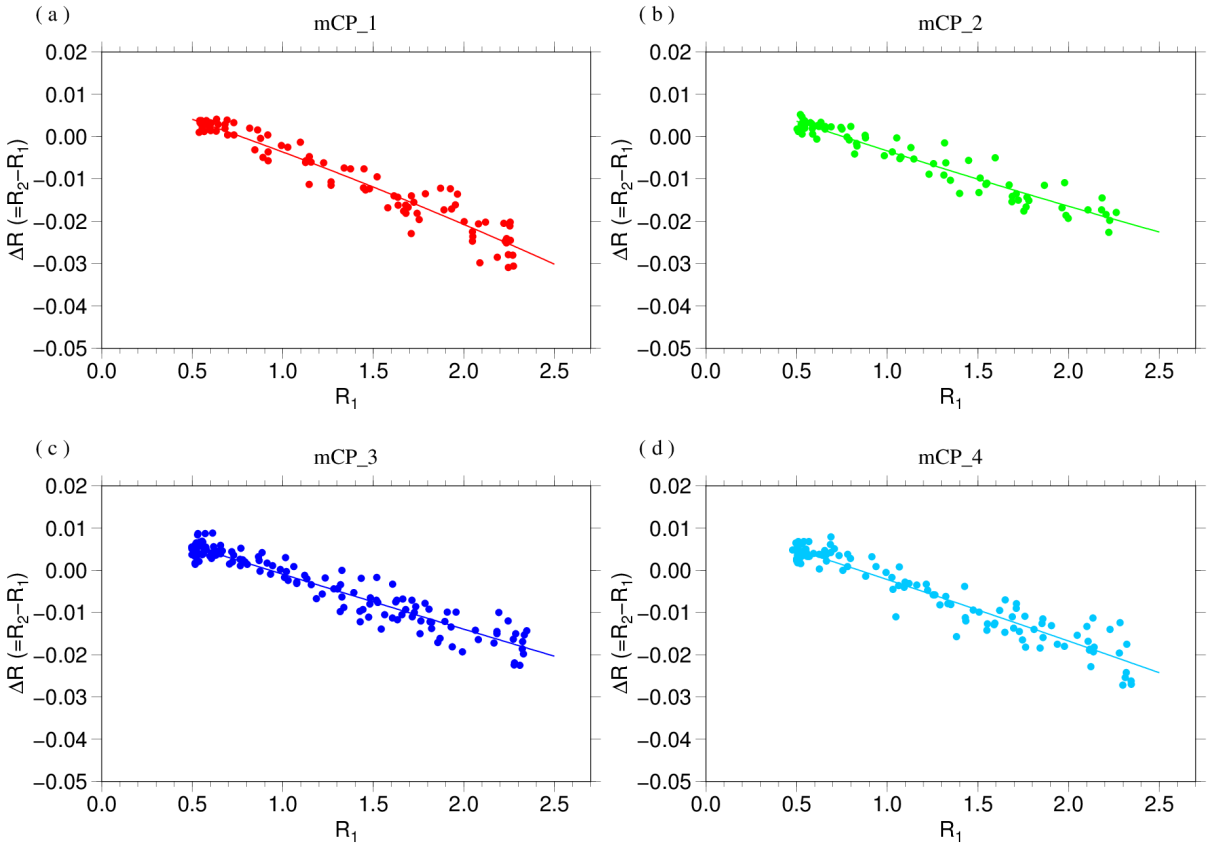

Figure C.8.3. The function curve of the ΔR (= R_2 − R_1) vs R_1 for (a) first, (b) second, (c) third and (d) fourth *m*CP batch of solution shown in Table C.8.1.

(45) Quality Control

(6.1) Replicate and duplicate analyses

We took replicate (pair of water samples taken from a single Niskin bottle) and duplicate (pair of water samples taken from different Niskin bottles closed at the same depth) samples for pH_T determination throughout the cruise. Table C.8.2 summarizes the results of the measurements. Figure C.8.4 shows details of the results. The calculation of the standard deviation from the difference of sets of measurements was based on a procedure (SOP 23) in DOE (1994).

Table C.8.2. Summary of replicate and duplicate measurements of pH_T.

Measurement	Average magnitude of difference ± S.D.
Replicate	0.0015±0.0014 (N=131)
Duplicate	0.0014±0.0014 (N=42)

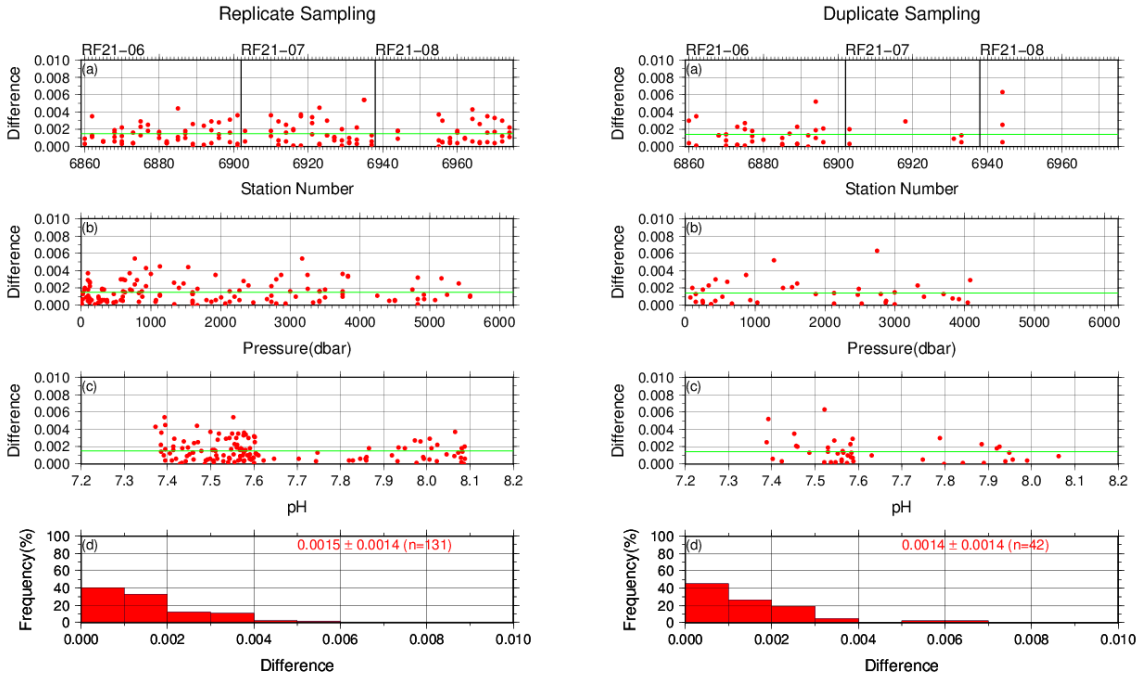

Figure C.8.4. Results of (left) replicate and (right) duplicate measurements during the cruise versus (a) station number, (b) pressure and (c) pH_T. The green lines denote the averages of the measurements. The bottom panels (d) show histograms of the measurements.

(6.2) Measurements of CRM and working reference materials

The precision of the measurements was monitored by using the CRMs and working

reference materials bottled in our laboratory (Appendix A2 in C.6). Although the pH_T value of the CRM was not assigned, it could be calculated from certified parameters of DIC and TA (https://www.ncei.noaa.gov/access/ocean-carbon-acidification-data-system/oceans/Dickson_CRM/batches.html) based on the chemical equilibrium of the carbonate system (Lueker et al., 2000). The pH_T of the CRM (batch 187) was calculated to be 7.8903. Working reference material measurements were carried out first at every station. If the results of the measurements were confirmed to be good, measurements on seawater samples were begun. Sometimes, CRM (batch 187) measurements were done at least once a leg. The measurement for seawater sample and working reference material was made once for a single bottle, and that for CRM was made twice. Table C.8.3 summarizes the means of difference of pH_T between two measurements and pH_T values for a CRM bottle and the means of the pH_T value for a working reference material for each *m*CP batch. Figures C.8.5–C.8.7 show detailed results.

Table C.8.3. Summary of difference and means of the pH_T values for two measurements for a CRM bottle, and mean of pH_T for a working reference material, which was calculated with data with good measurements.

Cruise	*m*CP Batch	Magnitude of difference Ave. ± S.D. (CRM)	Mean Ave. ± S.D. (CRM)	Mean Ave. ± S.D. (Working reference material)
RF21-06	1	0.0017 (N=1)	7.8849 (N=1)	7.8686±0.0027 (N=10)
	2	0.0013±0.0010 (N=3)	7.8794±0.0008 (N=3)	7.8629±0.0012 (N=9)
RF21-07	3	0.0010±0.0007 (N=3)	7.8834±0.0020 (N=3)	7.8655±0.0015 (N=16)
RF21-08	4	0.0014±0.0012 (N=3)	7.8846±0.0030 (N=3)	7.8656±0.0022 (N=14)

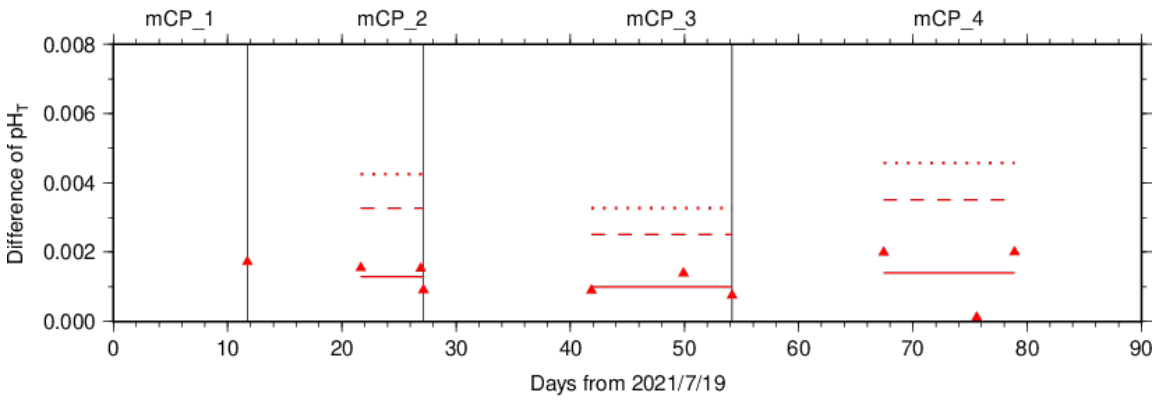

Figure C.8.5. The absolute difference (*R*) of pH_T between two measurements of a CRM

bottle. The *m*CP batch names are shown above the graph, and vertical lines denote the day *m*CP batches were changed. The solid, dashed and dotted lines denote the average range ($\bar{R}$), upper warning limit ($2.512\bar{R}$) and upper control limit ($3.267\bar{R}$) for each *m*CP batch bottle, respectively (see Dickson et al., 2007).

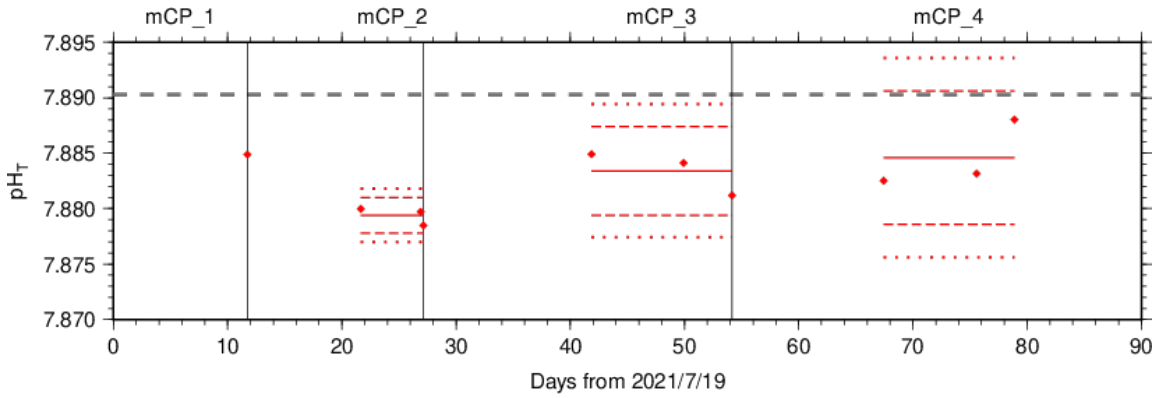

Figure C.8.6. The mean of pH_T values between two measurements of a CRM bottle. The *m*CP batch names are shown above the graph, and vertical lines denote the day when the *m*CP batch was changed. The solid, dashed, and dotted lines denote the mean of measurements, upper/lower warning limit (mean ± 2S.D.), and upper/lower control limit (mean ± 3S.D.) for each *m*CP batch bottle, respectively (see Dickson et al., 2007). The gray dashed line denotes pH_T of CRM calculated from certified parameters.

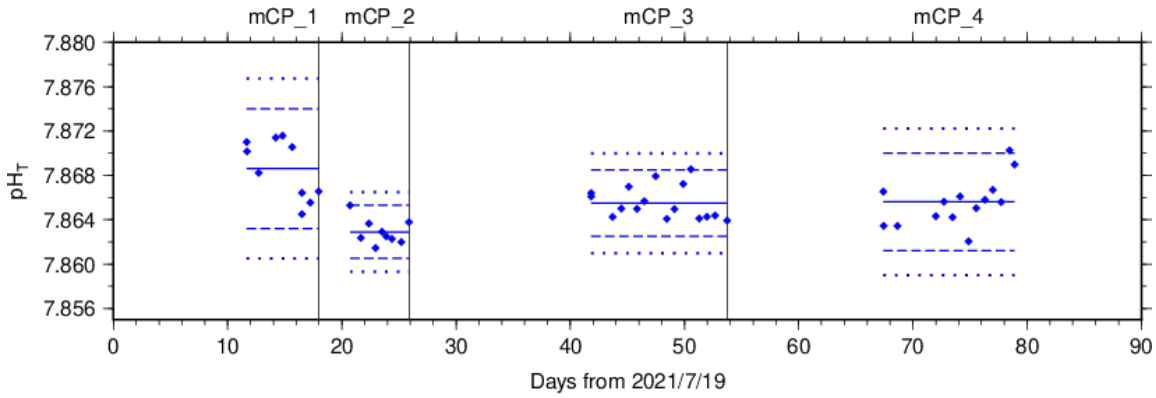

Figure C.8.7. Same as C.8.6, but for working reference material.

(6.3) Quality control flag assignment

A quality control flag value was assigned to the pH measurements (Table C.8.4) using the code defined in the IOCCP Report No.14 (Swift, 2010).

Table C.8.4. Summary of assigned quality control flags.

Flag	Definition	Number of samples
2	Good	1313
3	Questionable	20
4	Bad (Faulty)	7
5	Not reported	0
6	Replicate measurements	123
Total number of samples		1463

(6.4) Comparison at cross-stations during the cruise

There were cross-stations during the cruise located at 24°-15′ N/144°-50′ E (Stn.42 in RF21-06 and Stn.43 in RF21-07) and 24°N/165°E (Stn.70 in RF21-07 and Stn.71 in RF21-08). At these points, hydrocast sampling for pH_T was conducted two times at interval of 18 days (Stn.42 and Stn.43) and 18 days (Stn.70 and Stn.71), respectively. These profiles are shown in Figure C.8.8.

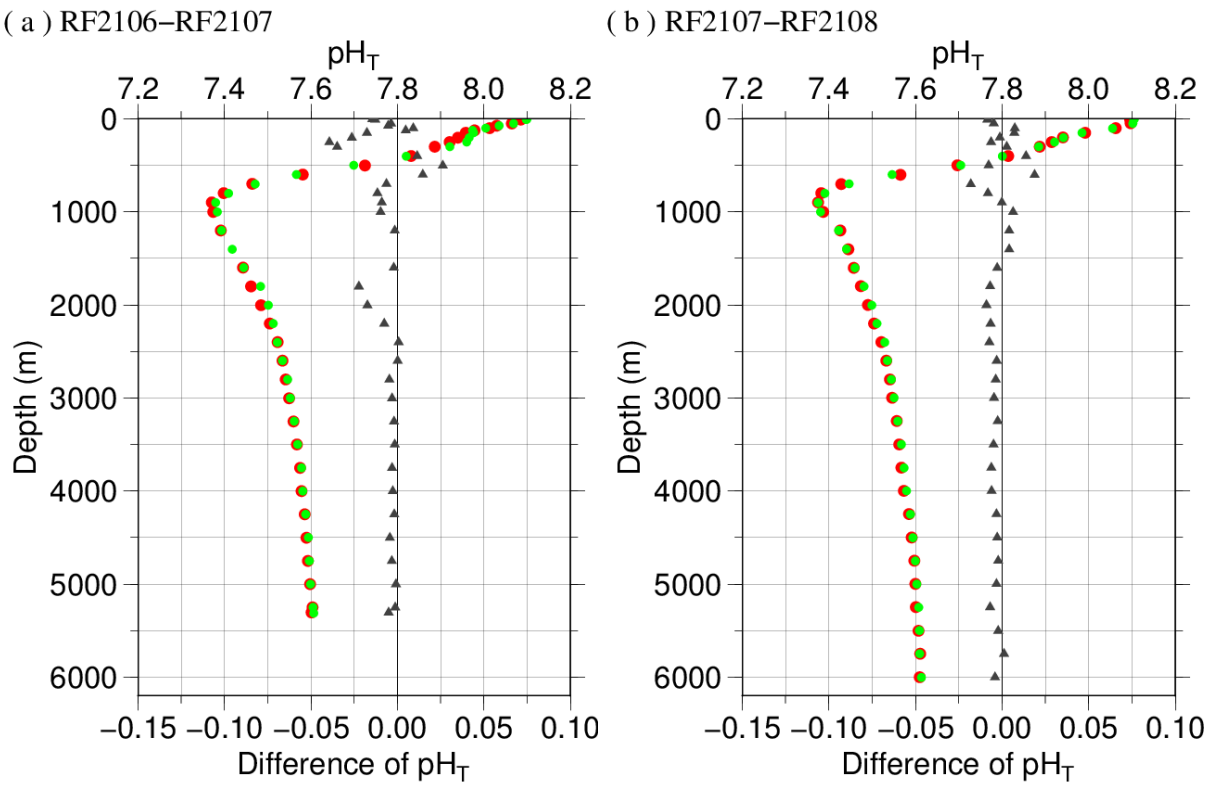

Figure C.8.8. Comparison of pH_T observed at same location in different legs of the cruise: (a) 24°-15′ N/144°-50′ E (RF21-06 and RF21-07) and (b) 24°N/165°E (RF21-07 and RF21-08). The red and green circles denote former (Stns.42 and 70) and latter (Stns.43 and 71) stations, respectively. Triangles denote the difference in pH_T measured at same depth in different legs.

(6.5) Comparison at cross-stations of WHP cruises

We compared pH_T data of this cruise and other WHP cruises by JMA and Japan Agency for Marine-Earth Science and Technology (JAMSTEC) at cross points. Summary of the comparisons are shown in Figure C.8.9(a) for cross point with WHP-P9 line (around 24°N/137°E), Figure C.8.9(b) for cross point with WHP-P10 line (around

24˚N/149˚E) and Figure C.8.9(c) for cross point with WHP-P13 line (around 24˚N/165˚E). Data of other cruises are downloaded from the CCHDO web site (https://cchdo.ucsd.edu).

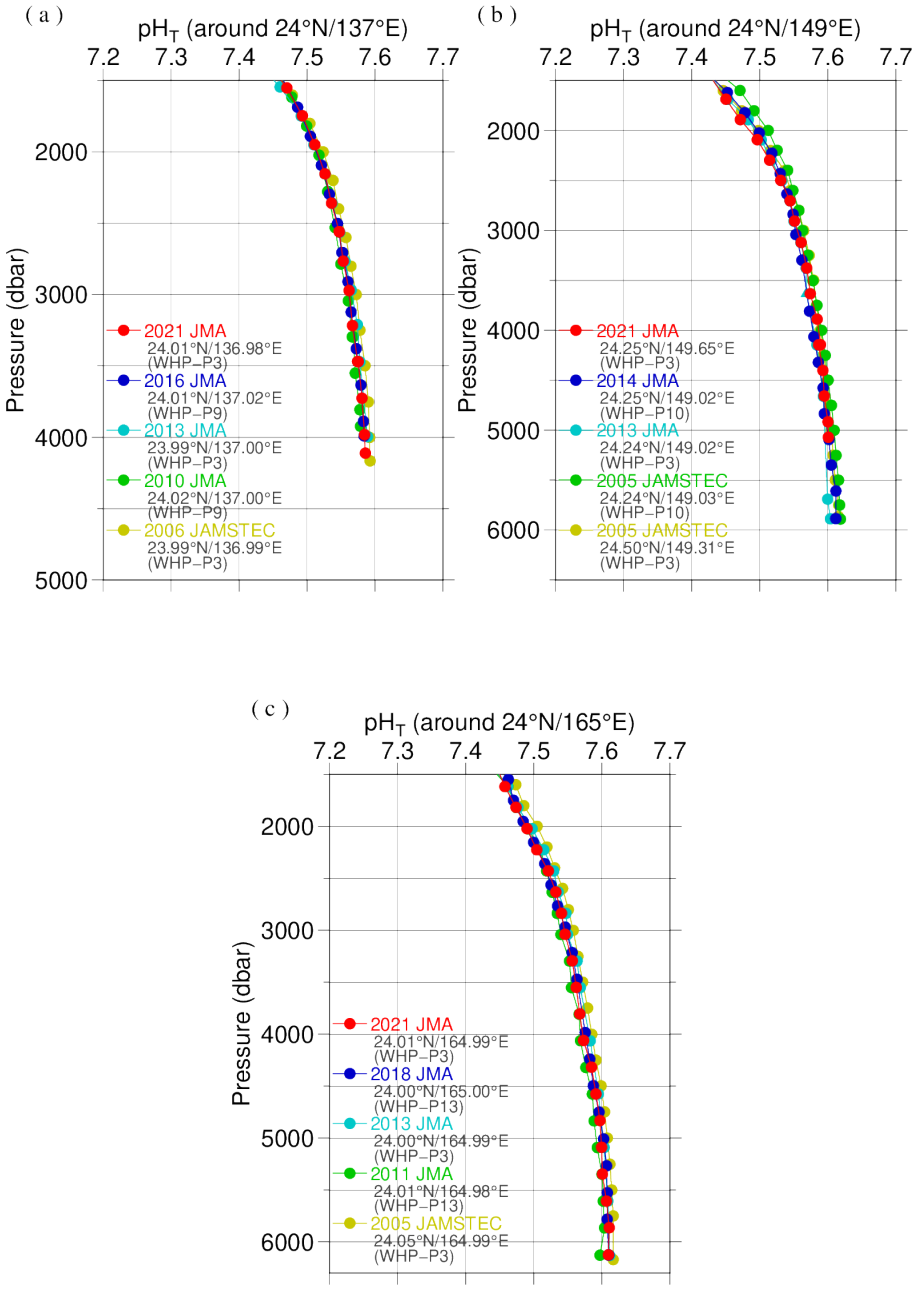

Figure C.8.9. Comparison of pH$_T$ profiles at (a) 24˚N/137˚E (cross point with WHP-

P9 line), (b) 24°N/149°E (cross point with WHP-P10 line) and (c) 24°N/165°E (cross point with WHP-P13 line). Circles and triangles denote good and questionable values, respectively. The red ones show this cruise.

Appendix

A1. Methods

(A1.1) Seawater sampling

Seawater samples were collected from 10-liters Niskin bottles mounted on CTD-system and a stainless steel bucket for the surface. Samples for pH were transferred to Schott Duran® glass bottles using sample drawing tubes. Bottles were filled smoothly from the bottom after overflowing double a volume while taking care of not entraining any bubbles, and lid temporarily with ground glass stoppers.

After all sampling finished, 2 mL of sample is removed from each bottle to make a headspace to allow thermal expansion. Although the procedure is differed from Standard Operating Procedure (SOP) described in PICES Special Publication 3, SOP-2 (Dickson, 2007), poisoned with 0.2 mL of saturated $HgCl_2$ solution to prevent change in pH_T caused by biological activity. Finally, samples were sealed with ground glass stoppers lubricated with Apiezon® grease (L).

(A1.2) Measurement

Custom-made pH analyzer (2009 model; Nihon ANS) was prepared and operated in the cruise. The analyzer comprised of a sample dispensing unit, a pre-treatment unit combined with an automated syringe, and two (sample and reference) spectrophotometers combined with a high power xenon light source. Spectrophotometric cell was made of quartz tube that has figure of “U”. This cell was covered with stainless bellows tube to keep the external surface dry and for total light

to reflect in the tube. The temperature of the cell was regulated to 25.0 ± 0.1 ° C by means of immersing the cell into the thermostat bath, where the both ends of bellows tube located above the water surface of the bath. Spectrophotometer, cell and light source were connected with optical fiber.

The analysis procedure was as follows:

a) Seawater was ejected from a sample loop.

b) A portion of sample was introduced into a sample loop including spectrophotometric cell. The spectrophotometric cell was flushed two times with sample in order to remove air bubbles.

c) An absorption spectrum of seawater in the visible light range was measured. Absorbance at wavelengths of 434 nm, 488 nm, 578 nm and 730 nm as well as cell temperature were recorded. To eject air bubbles from the cell, the sample was moved four times and the absorbance was recorded at each stop.

d) 10 μl of indicator *m*CP was injected to the loop.

e) Circulating 2 minutes 40 seconds through the loop tube, seawater sample and indicator dye was mixed together.

f) Absorbance of *m*CP plus seawater was measured in the same way described above (c).

(A1.3) Calculation

In order to state clearly the scale of pH, we mention "pH_T" that is defined by equation (C8.A1.3.1),

$$pH_T = -\log_{10}([H^+]_T/C^0) \qquad \text{(C8.A1.3.1)}$$

where $[H^+]_T$ denotes the concentration of hydrogen ion expressed in the total hydrogen ion scale. $[H^+]_T = [H^+]_F\left(1 + [SO_4]_T/K_{HSO_4^-}\right)$, where $[H^+]_F$ is the concentration of free hydrogen ion, $[SO_4]_T$ is the total concentration of sulphate ion and $K_{HSO_4^-}$ is acid dissociation constant of hydrogen sulphate ion (Dickson, 1990). C^0 is the standard value of concentration (1 mole per kilogram of seawater, mol kg^{-1}). The pH_T was reported as the value at temperature of 25 ° C in "total hydrogen ion scale".

pH_T was calculated from the measured absorbance (A) based on the following equations (C8.A1.3.2) and (C8.A1.3.3), which are the same as (C8.1) and (C8.2), respectively.

$$\begin{aligned} pH_T &= pK_2 + \log_{10}([I^{2-}]/[HI^-]) \\ &= pK_2 + \log_{10}\{(R - 0.0069)/(2.222 - 0.1331 \cdot R)\} \end{aligned} \qquad \text{(C8.A1.3.2)}$$

$$R = \left(A_{578}^{SD} - A_{578}^{S} - A_{730}^{SD} + A_{730}^{S}\right)/\left(A_{434}^{SD} - A_{434}^{S} - A_{730}^{SD} + A_{730}^{S}\right) \qquad \text{(C8.A1.3.3)}$$

where pK_2 is the acid dissociation constant of *m*CP. $[I^{2-}]$ / $[HI^-]$ is the ratio of *m*CP base form (I^{2-}) concentration over acid form (HI^-) concentration which is calculated from the corrected absorbance ratio (R) shown in the section 8(5) and the ratios of

extinction coefficients (Clayton and Byrne, 1993). A_λ^S and A_λ^{SD} in equation (C8.A1.3.3) are absorbance of seawater itself and dye plus seawater, respectively, at wavelength λ (nm). The value of pK_2 ($= -\log_{10}(K_2/k^0)$, $k^0 = 1$ mol kg^{-1}) had also been expressed as a function of temperature T (in Kelvin) and salinity S (in psu) by Clayton and Byrne (1993), but the calculated value has been subsequently corrected by 0.0047 on the basis of a reported pH_T value accounting for "tris" buffer (DelValls and Dickson, 1998):

$$\begin{aligned} pK_2 &= pK_2(\text{Clayton \& Byrne, 1993}) + 0.0047 \\ &= 1245.69/T + 3.8322 + 0.00211 \cdot (35 - S). \end{aligned} \quad \text{(C8.A1.3.4)}$$

(293 K ≤ T ≤ 303 K, 30 ≤ S ≤ 37)

Finally, pH_T determined at a temperature t ($pH_T(t)$, with t in ° C) was corrected to the pH_T at 25.00 ° C ($pH_T(25)$) with the following equation (Saito et al., 2008).

$$\begin{aligned} &(pH_T(t) - pH_T(25))/(t - 25.00) \\ &= (2.00170 - 0.735594 \cdot pH_T(25) + 0.0896112 \cdot pH_T(25)^2 - \\ &0.00364656 \cdot pH_T(25)^3). \end{aligned} \quad \text{(C8.A1.3.5)}$$

A2. pH indicator

Indicator *m*-cresol purple (*m*CP) solution

Add 0.67 g *m*CP to 500 mL deionized water (DW) in a borosilicate glass flask. Pour DW slowly into flask to weight of 1 kg (*m*CP + DW), and mix well to dissolve *m*CP.

Regulate the pH (free hydrogen ion scale) of indicator solution to 7.9±0.1 by small amount of diluted NaOH solution (approx. 0.25 mol L^{-1}) if the pH was out of the range. The pH of indicator solution was monitored using glass electrode pH meter. The reagent had not been refining.

References

Clayton T.D. and R.H. Byrne 1993. Spectrophotometric seawater pH measurements: total hydrogen ion concentration scale calibration of m-cresol purple and at-sea results. *Deep-Sea Res. I*, **40**, 2115–2129.

DelValls, T. A and A. G. Dickson, 1998. The pH of buffers based on 2-amino-2-hydroxymethyl-1,3-propanediol ('tris') in synthetic sea water. *Deep-Sea Res. I*, **45**, 1541-1554.

Dickson, A.G. 1990. Standard potential of the reaction: AgCl(s) + 1/2 H2(g) = Ag(s) + HCl(aq), and the standard acidity constant of the ion HSO_4^- in synthetic sea water from 273.15 to 318.15 K. *J. Chem. Thermodynamics*, **22**, 113–127.

Dickson, A.G., Sabine, C.L. and Christian, J.R. (Eds.) 2007. Guide to best practices for ocean CO_2 measurements. *PICES Special Publication* 3, 191 pp.

Lueker, T.J, A.G. Dickson and C.D. Keeling, 2000. Ocean pCO_2 calculated from dissolved inorganic carbon, alkalinity, and equations for K_1 and K_2: validation based on laboratory measurements of CO_2 in gas and seawater at equilibrium. *Marine Chem.*, **70**, 105-119.

Saito, S., M. Ishii, T. Midorikawa and H.Y. Inoue 2008. Precise Spectrophotometric Measurement of Seawater pH_T with an Automated Apparatus using a Flow Cell in a Closed Circuit. *Technical Reports of Meteorological Research Institute*, **57**, 1–28.

Swift, J. H. (2010): Reference-quality water sample data, Notes on acquisition, record keeping, and evaluation. *IOCCP Report No.**14**, ICPO Pub. 134, 2010 ver.1*

9. Lowered Acoustic Doppler Current Profiler

25 November 2021

(1) Personnel

CHIBA Yasuomi (JMA)

WADA Koichi (JMA)

(2) Instrument and measurement

Direct flow measurement from sea surface to sea bed was carried out using a Lowered Acoustic Doppler Current Profiler (LADCP). The instrument, RDI Workhorse Monitor 300 kHz (S/N 16468, 14108; Teledyne RD Instruments, USA), was attached on the CTD frame, orientating downward. The CPU firmware version was 50.41.

One ping raw data were recorded. Settings for the collecting data were as listed in Table C.9.1. A total of 76 operations were made with the CTD observations. The performance of the LADCP (S/N 16468) was good between Stn.1 (RF6860) and Stn.57 (RF6924). After Stn.58 (RF6925), data from Stn.58 (RF6925) to Stn.70 (RF6937) is missing due to a bulkhead connector failure. Using LADCP (S/N 14108) from stn.71 (RF6956), it was good.

Table C9.1. Setting for the correcting data.

Bin length	8 m

Bin number	25
Error Threshold	2000 mm/s
Ping interval	1.0 sec

(3) Data process and result

Vertical profiles of absolute velocity are obtained by the inversion method (*Visbeck*, 2002). Both the up and down casts were used for the calculation. Because the first bin from LADCP is influenced by the turbulence generated by CTD frame, the weighted mean coefficient for the calculation was set to 0.1. The GPS navigation data were used in the calculation of the reference velocities and the bottom-track data were used for the correction of the reference velocities. Shipboard ADCP (SADCP) data averaged for 5 minutes were also included in the calculation. The CTD data were used for the sound speed and depth calculation. IGRF (International Geomagnetic Reference Field) 11th generation data were used for calculating magnetic deviation to correct the direction of velocity. In the calculation processing, we used Matlab routines (version 8b: 5 April 2004) provided by M. Visbeck and G. Krahmann. Because the uncertainty of velocity observed by SADCP is about 10 cm/s, we regard the error velocity from LADCP upper 1000 dbar as about 10 cm/s. Figures C.9.1 and C.9.2 show the results of the zonal velocity (eastward is positive) and the meridional velocity (northward is positive), respectively. Figure C.9.3 shows measurement errors of velocity estimated by the inversion method.

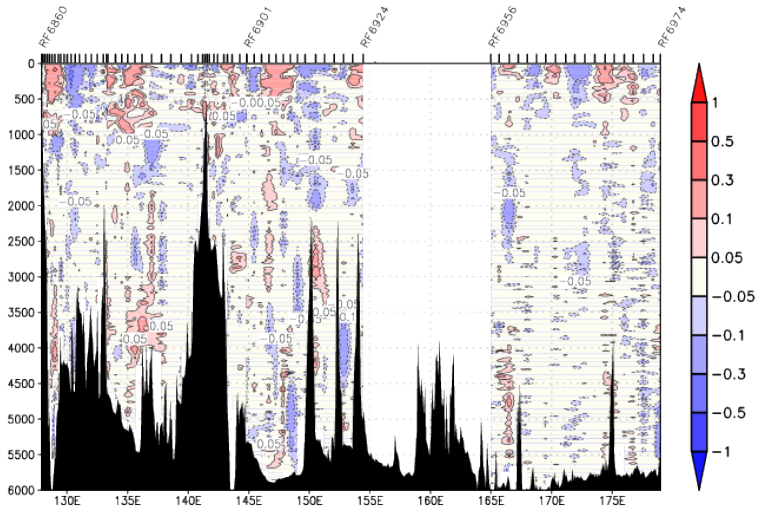

Figure C.9.1. The cross-section of zonal velocity (m/s, eastward is positive). Blanks are missing data from stn.58 to stn.71.

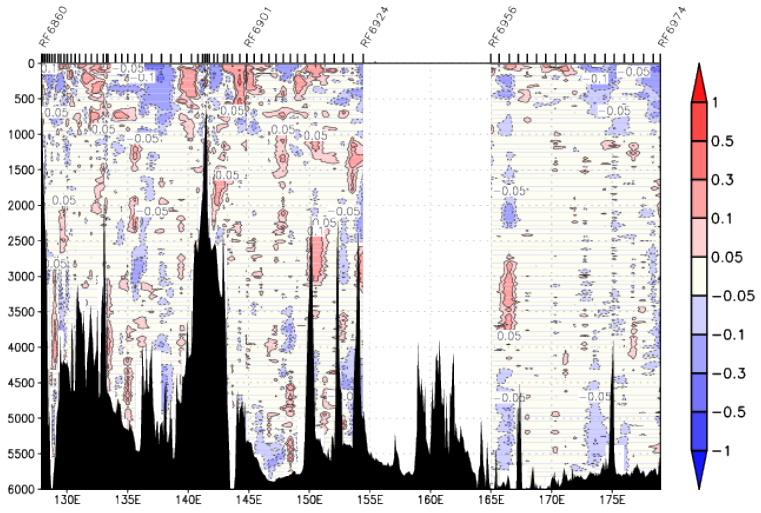

Figure C.9.2 The cross-section of meridional velocity (m/s, northward is positive). Blanks are missing data from stn.58 to stn.71.

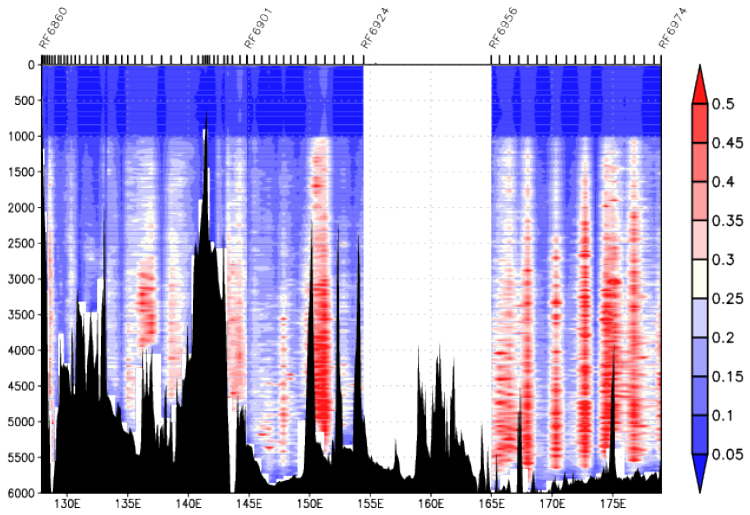

Figure C.9.3. Cross-section of measurement error in velocity (m/s) estimated by the inversion method. Blanks are missing data from stn.58 to stn.71.

Reference

Visbeck, M. (2002): Deep velocity profiling using Lowered Acoustic Doppler Current Profilers: Bottom track and inverse solutions. *J. Atmos. Oceanic Technol.*, ***19***, 794-807.

10. Chlorofluorocarbon (CFC-11 and CFC-12) (to be submitted in the next update)